

SYNTHESIS, ELECTROCHEMICAL CHARACTERIZATION AND ORGANIC
SOLAR CELL APPLICATIONS OF SELENOPHENE CONTAINING
CONJUGATED POLYMERS

A THESIS SUBMITTED TO
THE GRADUATE SCHOOL OF NATURAL AND APPLIED SCIENCES
OF
MIDDLE EAST TECHNICAL UNIVERSITY

BY

MUSTAFA YAŞA

IN PARTIAL FULLFILMENT OF THE REQUIREMENTS
FOR
THE DEGREE OF MASTER OF SCIENCE
IN
POLYMER SCIENCE AND TECHNOLOGY

AUGUST 2017

Approval of the thesis:

**SYNTHESIS, ELECTROCHEMICAL CHARACTERIZATION AND
ORGANIC SOLAR CELL APPLICATIONS OF SELENOPHENE
CONTAINING CONJUGATED POLYMERS**

submitted by **MUSTAFA YAŞA** in partial fulfillment of the requirements for the degree of **Master of Science in Polymer Science and Technology Program, Middle East Technical University** by,

Prof. Dr. Gülbin Dural Ünver

Dean, Graduate School of **Natural and Applied Sciences**

Prof. Dr. Necati Özkan

Head of Program, **Polymer Science and Technology**

Prof. Dr. Levent Toppare

Supervisor, **Department of Chemistry, METU**

Examining Committee Members

Prof. Dr. Ali Çırpan

Chemistry Dept., METU

Prof. Dr. Levent Toppare

Chemistry Dept., METU

Assoc. Prof. Dr. Yasemin Arslan Udum

Advanced Technologies Dept., Gazi University

Assist. Prof. Dr. Görkem Günbaş

Chemistry Dept., METU

Assoc. Prof. Dr. Emren Nalbant Esentürk

Chemistry Dept., METU

Date: 11.08.2017

I hereby declare that all information in this document has been obtained and presented in accordance with academic rules and ethical conduct. I also declare that, as required by these rules and conduct, I have fully cited and referenced all material and results that are not original to this work.

Name, Last Name: Mustafa
Yaşa

Signature:

ABSTRACT

SYNTHESIS, ELECTROCHEMICAL CHARACTERIZATION AND ORGANIC SOLAR CELL APPLICATIONS OF SELENOPHENE CONTAINING CONJUGATED POLYMERS

Yaşa, Mustafa

M.S., Polymer Science and Technology Program

Supervisor: Prof. Dr. Levent Toppare

August 2017, 86 pages

Donor-Acceptor (D-A) type conjugated polymers are very popular for potential applications such as organic light emitting diodes, solar cells, electrochromic devices and organic field effect transistors. In literature, cyclopentadithiophene and its derivatives are commonly used electron donor units for organic solar cells. The incorporation of selenium atom into polymer backbone results in low band gap polymers as compared to sulfur and oxygen counterparts. In this study, selenophene containing conjugated polymers were synthesized via Suzuki and Stille polycondensation reactions. Polymers were used as active layers for organic solar cells. Electrochemical and spectroelectrochemical characterizations and also organic solar cell application of these polymers were performed. For the structural analysis, Nuclear Magnetic Resonance Spectroscopy (NMR) and Gel Permeation Chromatography (GPC) techniques were used. Cyclic voltammetry (CV) were used to determine electrochemical properties of the polymers. The I-V characteristics of cells were investigated under AM 1.5 G illuminations. The effects of thermal and solvent annealing on morphology were also determined.

Keywords: Conjugated polymers, selenophene, quinoxaline, organic solar cell

ÖZ

SELENOFEN İÇEREN POLİMERLERİN SENTEZİ, ELEKTROKİMYASAL KARAKTERİZASYONLARI VE GÜNEŞ GÖZESİ ÇALIŞMALARI

Yaşa, Mustafa
Yüksek Lisans, Polimer Bilim ve Teknolojisi Programı

Tez Yöneticisi: Prof. Dr. Levent Toppare

Ağustos 2017, 86 sayfa

Organik ışık yayan diyot, güneş gözesi, elektrokromik cihaz ve alan etkili organik transistör gibi uygulamalardan ötürü donör-akseptör (D-A) tipi konjüge polimerler oldukça popülerdir. Literatürde, siklopentadiyofen ve türevleri güneş gözesi için sıklıkla kullanılan elektron donör ünitelerindedir. Tiyofen ve oksijen türevleri ile kıyaslandığında, selenyum atomunun polimer iskeleti üzerine takılması daha düşük bant aralıklarına sahip polimerler elde etmeyi sağlar. Bu çalışmada, selenofen içeren konjüge polimerler Suzuki ve Stille kenetlenme reaksiyonları kullanılarak sentezlenmiştir. Polimerler organik güneş gözesi için aktif tabaka olarak kullanılmıştır. Polimerlerin elektrokimyasal, spektroeletrokimyasal karakterizasyonları ve organik güneş pili uygulamaları yapılmıştır. Yapısal tayin için, Nükleer Magnetik Rezonans (NMR) ve Jel Geçirgenlik Kromatografisi (GPC) teknikleri kullanılmıştır. Polimerlerin elektrokimyasal özelliklerinin tayini için dönüşümlü voltametri kullanılmıştır. Güneş gözelerinin akım-voltaj karakteristiği AM 1.5G aydınlatması altında incelenmiştir. Termal ve çözelti tavlama yöntemlerinin morfolojiye etkisine bakılmıştır.

Anahtar Kelimeler: Konjüge polimerler, Selenofen, Kinokzalin, Organik Güneş Gözesi

to my family

ACKNOWLEDGMENTS

I would first like to thank my supervisor Prof. Dr. Levent Toppare for his precious guidance and providing me a great working environment full of great people. He is the reason why I decided to have degree on polymer science. He was a role model for me and always will be.

I would like to thank Assist. Prof. Dr. Görkem Günbaş. He always made me feel as a member of his research group and helped me cope with organic syntheses whenever I needed.

I would like to thank Assoc. Prof. Dr. Yasemin Arslan Udum and Dr. Şerife Özdemir Hacıoğlu for their help in electrochemical characterizations of the polymers and for clearing off all the questions of mine about electrochemistry.

I would like to thank Gönül Hızalan for her help in photovoltaic studies and for teaching me a lot of things in organic solar cells when she was my mentor.

I would like to thank Seza Göker for her precious help and advices for synthetic procedures and for being a great friend and listener. She always kept me motivated while working in the lab. We have never seen black kittens passing through the lab but had déjà vu a lot.

I want to express my gratitude to Ebru Işık and Çağla İstanbulluoğlu for their great friendship and funny times we spent together during coffee breaks.

I would like to thank Alim Yolalmaz and Nurzhan Beksultanova for their friendship. They always found a way to cheer me up.

I would like to thank the gamer gang; Ali Ekber Karabağ, Tolga Yaman, Samet Aytekin, Şevki Can Cevher, Majid Akbar, and Gencay Çelik for creating such an environment to have fun at the end of tiring weeks.

I would like to thank Ali Toksoy who contributed a lot to my decision for chasing science. If he had not given that encyclopedia years ago, I would not find a way to get motivated for science.

I would like to thank my family for always supporting my decisions and being there for me.

Finally, I would like to thank TÜBİTAK for granting 2210-C scholarship.

TABLE OF CONTENTS

ABSTRACT	v
ÖZ.....	vii
ACKNOWLEDGMENTS.....	x
TABLE OF CONTENTS	xii
LIST OF TABLES	xvi
LIST OF FIGURES.....	xvii
LIST OF ABBREVIATIONS	xx
CHAPTERS	
1. INTRODUCTION.....	1
1.1. The theory of conducting polymers.....	1
1.2. Conjugated polymers.....	2
1.2.1. Conductivity characteristics of Conjugated Polymers.....	3
1.3. Applications of Conjugated Polymers: Polymer Electronics	5
1.3.1. Conjugated Polymers-Based Batteries	5
Polypyrrole (PPy)	6
Polyaniline (PANI).....	6
Polyacetylene (PA).....	6
1.3.2. Light Emitting Applications	7
1.3.3. Solar Cells.....	8
1.3.3.1. Basic Principles	10
1.3.3.1.1. Light Absorption and Collection.....	10
1.3.3.1.2. Exciton Generation and Diffusion.....	11
1.3.3.1.3. Exciton Dissociation	11

1.3.3.1.4. Charge Transport and Collection	11
1.3.3.2. Device Preparation	12
1.3.3.3. Characterization	13
1.3.3.3.1. Open-Circuit Voltage	13
1.3.3.3.2. Short-Circuit Current Density	14
1.3.3.3.3. Fill Factor	14
1.4. Design and Engineering of Conjugated Polymers.....	15
1.4.1. Electrochemical Polymerization.....	16
1.4.2. Oxidative Polymerization.....	17
1.4.3. Stille Coupling	17
1.4.4. Suzuki Coupling	19
1.4.5. Sonogashira Coupling.....	20
1.4.6. Heck Reaction.....	21
1.5. Motivation	22
1.5.1. Incorporation of Selenophene as a π -bridging unit and Benzo[1,2-b:4,5-b']dithiophene with quinoxaline unit.....	24
2. EXPERIMENTAL	27
2.1. Materials	27
2.2 Methods and Equipment.....	27
2.3. Synthesis.....	28
2.3.1. Monomer Syntheses	28
2.3.1.1. 4,7-Dibromobenzo[c][1,2,5]thiadiazole	28
2.3.1.2. 3,6-Dibromobenzene-1,2-diamine.....	29
2.3.1.4. Synthesis of 1,2-bis(3,4-bis(octyloxy)phenyl)ethane-1,2-dione	31
2.3.1.5. Synthesis of 2,3-Bis(3,4-bis(octyloxy)phenyl)-5,8-dibromoquinoxaline .	32
2.3.1.6. Synthesis of Tributyl(selenophen-2-yl)stannane.....	33

2.3.1.7. Synthesis 2,3-Bis(3,4-bis(octyloxy)phenyl)-5,8-di(selenophen-2-yl)quinoxaline.....	34
2.3.1.8. Synthesis of 2,3-Bis(3,4-bis(octyloxy)phenyl)-5,8-bis(5-bromoselenophen-2-yl) quinoxaline.....	35
2.3.2. Polymer Syntheses.....	36
2.3.2.1. Synthesis of Poly[5-(5-(4,8-bis(2-ethylhexyl)benzo[1,2-b:4,5-b']dithiophen-2-yl)selenophen-2-yl)-2,3-bis(3,4-bis(octyloxy)phenyl)-8-(selenophen-2-yl)quinoxaline]-PBDTSeQ	36
2.3.2.2. Synthesis of Poly[3-(5-(2,3-bis(3,4-bis(octyloxy)phenyl)-8-(selenophen-2-yl)quinoxalin-5-yl)selenophen-2-yl)-9-(heptadecan-9-yl)-9H-carbazole]-PSeQCz	37
2.3.2.3. Synthesis of Poly[2,3-bis(3,4-bis(octyloxy)phenyl)-5-(5-(9,9-dioctyl-9H-fluoren-3-yl)selenophen-2-yl)-8-(selenophen-2-yl)quinoxaline]-PFiSeQ	38
2.4. Characterization of the polymers.....	39
2.4.1. Gel Permeation Chromatography (GPC).....	39
2.4.2. Electrochemical Characterizations	39
2.4.2.1. Cyclic Voltammetry	39
2.4.2.2. Spectroelectrochemical Studies	41
2.4.2.3. Kinetic Studies.....	41
3. RESULTS AND DISCUSSIONS	43
3.1. Electrochemical Characterizations	43
3.1.1. Cyclic Voltammetry studies of the polymers	43
3.2. Spectroelectrochemical Characterizations.....	48
3.2.1. Spectroelectrochemical studies of the polymers	48
3.3. Kinetic Studies.....	53
3.3.1. Kinetic Studies of the polymers.....	54
3.4. Bulk Heterojunction Solar Cell Studies.....	56

4. CONCLUSIONS.....	59
REFERENCES.....	61
APPENDIX.....	71

LIST OF TABLES

TABLES

Table 1. Electrochemical properties of the polymers.....	48
Table 2. Calorimetric values of PSeQCz	49
Table 3. Calorimetric values of PFiSeQ.....	51
Table 4. Calorimetric values of PBDTSeQ.....	52
Table 5. Spectroelectrochemical properties of the polymers	53
Table 6. Kintetic studies of the polymers.....	56
Table 7. Photovoltaic properties of PBDTSeQ:PCBM-based OPV	57
Table 8. Photovoltaic properties of PFiSeQ:PCBM-based OPV	58

LIST OF FIGURES

FIGURES

Figure 1. 1. Structure of Polyacetylene, PA.....	2
Figure 1. 2. Structures of some conventional conjugated polymers	3
Figure 1. 3. Conductivity scale of conjugated polymers.....	4
Figure 1. 4. Structure of bilayer organic solar cell.....	9
Figure 1. 5. Working principle of a bulk heterojunction organic solar cell.....	10
Figure 1. 6. Architecture of bulk heterojunction (BHJ) solar cell	12
Figure 1. 7. Typical current density-voltage (J-V) curve.....	15
Figure 1. 8. Oxidative Chemical Polymerization of benzene	17
Figure 1. 9. General mechanism of Stille Coupling.....	18
Figure 1. 10. Stille Coupling Polymerization	19
Figure 1. 11. Suzuki Coupling Polymerization.....	19
Figure 1. 12. General mechanism of Suzuki Coupling	20
Figure 1. 13. General mechanism Sonogashira Coupling.....	21
Figure 1. 14. Heck Reaction.....	21
Figure 1. 15. Aromatic and resonance forms of poly (p-phenylene) and poly (thiophene)	23
Figure 1. 16. Optimized band gap through donor-acceptor interaction	23
Figure 1. 17. BDT based conjugated polymers incorporated with thiophene and quinoxaline units	25
Figure 1. 18. Fluorene and carbazole based polymer incorporated with thiophene and quinoxaline units	26
Figure 2. 1. Synthetic route of 4,7- dibromobenzo[c][1,2,5]thiadiazole.....	28
Figure 2. 2. Synthetic route of 3,6-dibromobenzene-1,2-diamine	29
Figure 2. 3. Synthetic route of 1,2-bis(octyloxy)benzene.....	30
Figure 2. 4. Synthetic route of 1,2-bis(3,4-bis(octyloxy)phenyl)ethane-1,2-dione ...	31

Figure 2. 5. Synthetic route of 2,3-bis(3,4-bis(octyloxy)phenyl)-5,8-dibromoquinoxaline	32
Figure 2. 6. Synthetic route of tributyl(selenophen-2-yl)stannane.....	33
Figure 2. 7. Synthetic route of 2,3-bis(3,4-bis(octyloxy)phenyl)-5,8-di(selenophen-2-yl)quinoxaline.....	34
Figure 2. 8. Synthetic route of 2,3-bis(3,4-bis(octyloxy)phenyl)-5,8-bis(5-bromoselenophen-2-yl) quinoxaline	35
Figure 2. 9. Synthetic route of PBDTSeQ.....	36
Figure 2. 10. Synthetic route of PSeQCz	37
Figure 2. 11. Synthetic route of PFISeQ	38
Figure 2. 12. Waveform of potential in CV as a function of time	40
Figure 2. 13. Cyclic voltammogram.....	40
Figure 3. 1. Single scan cyclic voltammogram of PSeQCz in 0.1 M TBAPF ₆ /ACN solution.....	44
Figure 3. 6. Scan rate dependence of PBDTSeQ	47
Figure 3. 7. Electronic absorption spectra of PSeQCz in 0.1 M TBAPF ₆ /ACN solution and colors at different potentials	49
Figure 3. 8. Electronic absorption spectra of PFISeQ in 0.1 M TBAPF ₆ /ACN solution and colors at different potentials	50
Figure 3. 9. Electronic absorption spectra of PBDTSeQ in 0.1 M TBAPF ₆ /ACN solution and colors at different potentials	51
Figure 3. 10. Optical transmittance changes of PSeQCz at 595 nm and 1075 nm	54
Figure 3. 11. Optical transmittance changes of PFISeQ at 680 nm	55
Figure 3. 12. Optical transmittance changes of PBDTSeQ at 445 nm and 615 nm...	55
Figure 3.13. J-V curve of of PBDTSeQ:PCBM-based OPV.....	57
Figure 3.14. J-V curve of PFISeQ:PCBM-based OPV.....	58
Figure A 1. ¹ H-NMR spectrum of 4,7- dibromobenzo[c][1,2,5]thiadiazole	71
Figure A 2. ¹³ C-NMR spectrum of 4,7- dibromobenzo[c][1,2,5]thiadiazole.....	72
Figure A 3. ¹ H-NMR spectrum of 3,6-dibromobenzene-1,2-diamine	73
Figure A 4. ¹³ C-NMR spectrum of 3,6-dibromobenzene-1,2-diamine	74

Figure A 5. ¹ H-NMR spectrum of 1,2-bis(octyloxy)benzene	75
Figure A 6. ¹³ C-NMR spectrum of 1,2-bis(octyloxy)benzene	76
Figure A 7. ¹ H-NMR spectrum of 1,2-bis(3,4-bis(octyloxy)phenyl)ethane-1,2-dione	77
Figure A 8. ¹³ C-NMR spectrum of 1,2-bis(3,4-bis(octyloxy)phenyl)ethane-1,2-dione	78
Figure A 9. ¹ H-NMR spectrum of 2,3-bis(3,4-bis(octyloxy)phenyl)-5,8- dibromoquinoxaline	79
Figure A 10. ¹³ C-NMR spectrum of 2,3-bis(3,4-bis(octyloxy)phenyl)-5,8- dibromoquinoxaline	80
Figure A 11. ¹ H-NMR spectrum of tributyl(selenophen-2-yl)stannane.....	81
Figure A 12. ¹³ C-NMR spectrum of tributyl(selenophen-2-yl)stannane	82
Figure A 13. ¹ H-NMR spectrum of 2,3-bis(3,4-bis(octyloxy)phenyl)-5,8- di(selenophen-2-yl)quinoxaline	83
Figure A 14. ¹³ C-NMR spectrum of 2,3-bis(3,4-bis(octyloxy)phenyl)-5,8- di(selenophen-2-yl)quinoxaline	84
Figure A 15. ¹ H-NMR spectrum of 2,3-bis(3,4-bis(octyloxy)phenyl)-5,8-bis(5- bromoselenophen-2-yl) quinoxaline	85
Figure A 16. ¹³ C-NMR spectrum of 2,3-bis(3,4-bis(octyloxy)phenyl)-5,8-bis(5- bromoselenophen-2-yl) quinoxaline	86

LIST OF ABBREVIATIONS

D-A	Donor-Acceptor
NMR	Nuclear Magnetic Resonance Spectroscopy
GPC	Gel Permeation Chromatography
CV	Cyclic Voltammetry
AM	Air Mass
PPV	Poly (phenylene vinylene)
LED	Light Emitting Diode
PP	Poly (phenylene)
PANI	Poly (aniline)
PPy	Poly (pyrrole)
PT	Poly (thiophene)
PEDOT	Poly(3,4-ethylenedioxythiophene)
HOMO	Highest Occupied Molecular Orbital
LUMO	Lowest Occupied Molecular Orbital
EAP	Electroactive Polymer
PA	Poly (acetylene)
OLED	Organic Light Emitting Diode
CuPc	Copper Phthalocyanine
OPV	Organic Photovoltaic

BHJ	Bulk Heterojunction
ITO	Indium Tin oxide
PSS	Polystyrene Sulfonate
PC₇₀BM	[6,6]-phenyl-C70-butyric acid methyl ester
V_{oc}	Open Circuit Voltage
J_{sc}	Short-circuit Current Density
FF	Fill Factor
ACN	Acetonitrile
Et₄NBF₄	Tetraethylammonium tetrafluoroborate
NHE	Normal Hydrogen Electrode
DCM	Dichloromethane
TLC	Thin Layer Chromatography
EtOH	Ethanol
THF	Tetrahydrofuran
CHCl₃	Chloroform
NBS	N-Bromosuccinimide
PDI	Polydispersity Index
M_n	Number Average Molecular Weight
M_w	Weight Average Molecular Weight
PS	Poly (styrene)
TBAPF₆	Tetrabutylammonium hexafluorophosphate

ICE	Commission Internationale de l'Eclairage
UV	Ultraviolet
Vis	Visible
E_g^{op}	Optical Band Gap
E_g^{ec}	Electronic Band Gap
P_{max}	Maximum Power
P_{in}	Input Power

CHAPTER 1

INTRODUCTION

Energy demand of the world is increasing day by day and this increases the interest in renewable energy sources. Sun is one of the most important renewable energy sources. Considering the fact that the energy absorbed by earth from the sun is higher than the annual demand, utilizing of this energy will meet the most of the need.

1.1. The theory of conducting polymers

Conducting polymers are organic materials that can conduct electricity. The history of conducting polymers goes back to 1830s with the discovery of oxidized forms of polyaniline. Between 1830 and 1840, studies for the structural determination of indigo via dry distillation resulted in the discovery of aniline [1]. Oxidation of this molecule led to a green colored product which got the place in terminology as polyaniline. Polyaniline is known as one of the most important conducting polymers due to its usage in sensors, electrodes and batteries and it is environmentally stable and the conductivity is tunable. The preparation is succeeded by the oxidation of aniline salt. Advanced studies of polyaniline started in 1980s. In 1985 MacDiarmid reported that polyaniline was doped to replicate metallic conductivity via addition of protons to the polymer using 1M HCl solution [2]. The product obtained had π delocalization in the polymer backbone and was stable in ambient atmosphere permanently. Attractiveness of semiconductor materials led to design of more interesting materials having conjugated systems and the chance of structural modification.

1.2. Conjugated polymers

Conjugated polymers, without any doubt, have been recognized as one of the most important materials for plastic electronics. The advantages of them over other semiconductors are the possibility of solution processing, change via structural modification, low cost and light weight. The very first synthetic conjugated polymer was polythiazyl which was superconducting at 0.26 K and an insoluble powder/film having a range of conductivity between 10 and 1700 S.cm⁻¹. The polymer is commonly synthesized as dark golden/yellowish crystals or as films that has a metallic appearance. Due to its metallic character and superconducting characteristics, this conjugated polymer has taken a great attention [3,4]. The interest in conjugated polymers has increased significantly after the discovery of the fact that the electrical conductivity of conjugated polymers can be increased upon oxidation [5]. In 1977, Heeger and co-workers discovered that the conductivity of polyacetylene, one of the simplest linear conjugated polymers (Figure 1.1), could be increased by seven orders of magnitude upon oxidizing polyacetylene with halogens like chlorine, iodine or bromine and with arsenic pentafluoride [6]. This breakthrough discovery proved that plastics can be modified to conduct electricity and brought Alan Heeger, Hideki Shirakawa and Alan MacDiarmid the Nobel Prize in chemistry 2000 for the discovery and development of conjugated polymers.

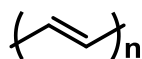


Figure 1. 1. Structure of Polyacetylene, PA

In 1990, Burroughes and co-workers had discovered the electroluminescence in poly (*p*-phenylene vinylene), PPV. It was reported that the polymer can be implemented

as active layer in the preparation of light emitting diodes (LEDs) and displays [7]. With these abovementioned big discoveries, the age of plastic electronics has started and led to the design of new conjugated polymers (Figure 1.2) which have a large range of applications in energy materials, sensors and other electronics.

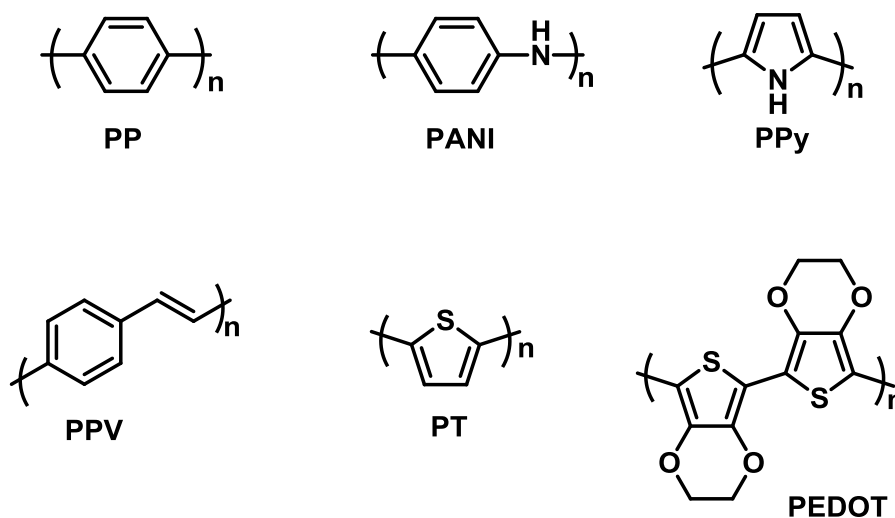


Figure 1. 2. Structures of some conventional conjugated polymers

1.2.1. Conductivity characteristics of Conjugated Polymers

That polymers can be provided with metallic characteristics, without any doubt, was a breakthrough, since for a long time, polymeric materials were known as insulating materials. Conjugated polymers lie between crystalline and amorphous materials resulting in a different charge transfer mechanism in material compared to that of crystalline derivative materials. Conjugated polymers are intrinsically conductive, conducting without any doping process. Presence of conjugated double bonds along the polymer backbone cause electrical conductivity in polymers providing a path for electron transfer through the polymer backbone. That the polymer consists of alternating single and double bonds is known as conjugation.

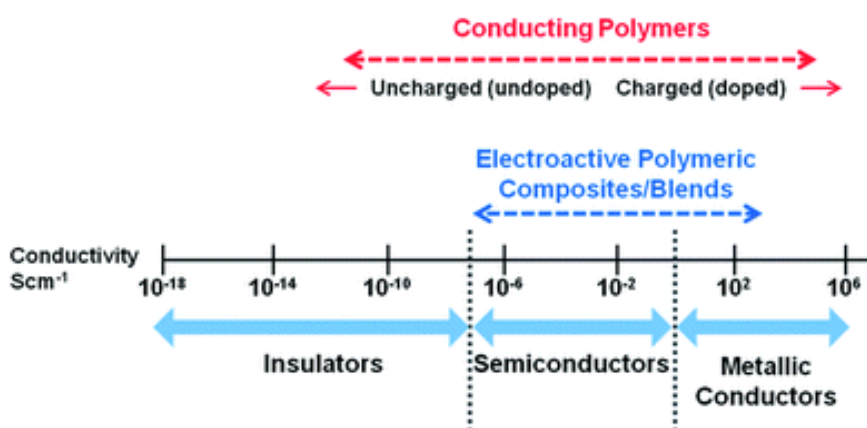


Figure 1. 3. Conductivity scale of conjugated polymers [8]

In conjugated polymers, carbon atom in a double bond has an sp^2 hybridization. This carbon leaves a p_z orbital for a π bond. Thus the electrons in this π bond get delocalized by conjugation through neighboring π bonds. Formation of those π bonds gives rise to charge carrier mobility. The last band filled with π electrons is known as Highest Occupied Molecular Orbital (HOMO). Above this band there is a gap which extends to empty π orbital known as Lowest Unoccupied Orbital (LUMO). This energy gap between HOMO and LUMO is called band gap. In metallic conductors, the band is partially filled and this specific property is the main reason resulting in conductivity of this type of materials. Electrical insulators have a completely filled valence band and a completely empty conduction band and these results in a large band gap. However, semiconductors possess filled and unfilled bands, valence band and conduction band, respectively [9].

In conjugated polymers, energy positions of the HOMO and LUMO levels and the magnitude of the band gap are the most important parameters to identify the optoelectronic properties. The band gap of a conjugated polymer can be measured from π - π^* transition in the UV-Vis spectrum of the polymer film (optical band gap) or from redox potentials via electrochemistry through doping the polymer both p-doping and n-doping (electronic band gap) [10]. The optical band gap of conjugated polymers is determined by the following formula:

$$E_g = \frac{1240}{\lambda_{\text{edge}}} \text{ (eV)}$$

and the electronic band gap is measured by the following formula:

$$E_g = \text{HOMO} - \text{LUMO} \text{ (eV)}$$

For the conjugated polymers utilized in photovoltaics, having low band gap is a crucial parameter for the absorption of incident light [11–13].

1.3. Applications of Conjugated Polymers: Polymer Electronics

For many years, polymers have been used as insulators until the discovery that polymers can be provided with conductivity and conductivity can be increased substantially upon doping process. Applications of conjugated polymers have been limited until 2000s. Synthesizing new polymeric materials with better conductivity and processability gave a new impulse to the field.

1.3.1. Conjugated Polymers-Based Batteries

Requirement for power is growing rapidly and current technologies cannot meet the need. This problem draws attention to alternative technologies like electrically active polymers for batteries. Since conjugated polymers can be processed both via reduction and oxidation, they are potential candidates for alternative batteries. Utilization of electroactive polymers (EAPs) in batteries provides reduced cost, weight and environmental impacts. Besides, EAPs can be manipulated to end up with specific properties, such as conductivity, storage capacity, reversibility, voltage range, porosity, and chemical and environmental stability. Electroactive polymers

exhibit high conductivities, flexible morphologies, chemical stability, low cost and ease of processing as well as they show electronic and ionic conductivity during charge and discharge. These properties EAPs drew great attention to research on them [14–16]. The most used conjugated polymers for battery applications are polypyrrole, polyaniline, and polyacetylene [17,18].

Polypyrrole (PPy)

PPy is one of the most utilized conjugated polymers in battery applications, mostly used as cathode. Lundström utilized PPy as both cathode and anode in an acetonitrile-based electrolyte [19]. The study reveals the preparation of secondary batteries with large coulombic efficiencies.

Polyaniline (PANI)

PANI is generally used as cathode in battery applications. It is perfectly stable, highly electroactive, has a high doping level, and high capacitance [16]. PANI works in both aqueous and non-aqueous cells. It can be manipulated by forming poly (n-methyl aniline) to make the polymer more stable against chemical degradation. In this new polymer, hydrogen sites are blocked by methyl groups and the polymer becomes more redox active.

Polyacetylene (PA)

PA is used as both cathode and anode in conjugated polymer based batteries since it has both p- and n-dopable properties. Since polyacetylene is prepared generally by

Ziegler-Natta catalyst, trace amount of Ti and Al are faced as well as other metal residues. These traces cause decrease in stability. Formation of PA proceeds as fibrils and powder which both are insoluble. In order to utilize polyacetylene as working electrode it has to be doped [14].

1.3.2. Light Emitting Applications

History of organic light emitting materials goes back to 1960s. Pope *et. al.* reported the luminescence in anthracene. In 1980s, tang and VanSlyke reported the research on organic materials, revealing new light-emitting materials with organic fluorescent dyes. In 1990, Friend *et. al.* reported the research concerning PPV (poly (phenylene vinylene)), the first conjugated polymer used for an organic light emitting diode, as active material in a single-layer Organic Light Emitting Diode (OLED) to overcome the disadvantages of expensive and inconvenient inorganic materials [7,20–22]. OLEDs encompass two types of devices; polymer light emitting diodes and small molecule light emitting diodes.

An OLED structure is composed of an organic layer between a metal contact (being cathode, generally aluminum or silver) and a transparent electrode (being anode, usually ITO: indium-tin oxide). Providing the device with an electrical current, an electric field is created and electrons and holes are injected from cathode and anode, respectively (injection of electrons into the LUMO of the molecule by the cathode and injection of the holes to the HOMO of the molecule by the anode). The cathode material provides the active layer with electrons and the anode is responsible for removing these electrons from the active layer. The particles meet each other at a certain point in the active layer to form excitons and then decay to produce light by the relaxation of energy state. The light depends on the structure of the molecule/conjugated polymer. The energy gap is highly affect the wavelength of the

emission [23,24]. First commercial OLEDs were implemented in mp3 players, mobile phones, small screens of housewares etc.

1.3.3. Solar Cells

Energy demand of the humanity is continuously increasing and fossil fuels are running out and cause global warming due to massive amount of carbon dioxide accumulated in the earth's atmosphere. These figure out the fact that studies on the development of renewable energy must be concentrated. One of the renewable energy sources is the sun and the energy sun radiates in one day is more than the energy needed for the world just for a year. Solar energy is an inexhaustible energy source to fulfill this demand. Intensive studies on the solar energy encompass solar cell technology. Solar cells harvest light from the sun and turn this solar energy into electrical energy. The problem of this technology is the stability and efficiency. Inorganic solar cells are the mostly commercially used solar cells due to their high efficiency compared to the organic analogues. Yet, research on organic solar cells is challenging and intensive due to being environmentally friendly, inexpensive and ease of process. The first organic solar cell was reported by Tang (1986) with an efficiency of 1%. The cell had a bilayer structure; a donor unit (p-type semiconductor) and an acceptor (n-type semiconductor) unit. As the hole transporting material he used copper phthalocyanine (CuPc) and as electron transporting layer he used perylene derivatives to construct a bilayer organic solar cell [25]. Organic photovoltaics (OPVs) are prepared by employing solution processing methods like spin-coating, dip-coating, ink-jet printing, screen-printing and doctor-blade coating [26–28]. A typical organic solar cell consists of a blend of donor and acceptor units. This blend provides an interface through the photoactive layer and it is known as bulk heterojunction (BHJ). At the very beginning of development of organic solar cells, architecture of the devices was based on bilayer model as illustrated in Figure 1.7.

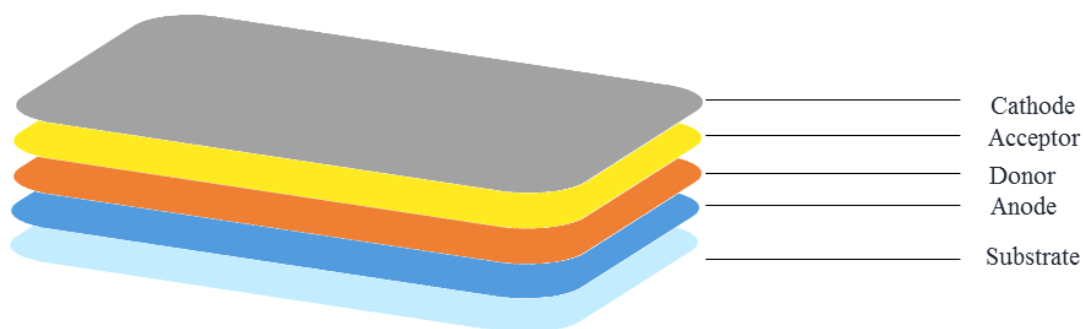


Figure 1. 4. Structure of bilayer organic solar cell

Since the excitons have a limited life time their diffusion lengths are quite short (5-14 nm). Before diffusion to the acceptor unit, excitons are generated in the donor decay to the ground state [10]. This drawback results in the loss of absorbed photons by the photoactive layer and low quantum efficiency. This small area of the interface located between donor and acceptor affects the performance of bilayer heterojunction organic photovoltaics. To overcome this obstacle, Yu *et. al.* reported the concept of bulk heterojunction [29]. Blending donor and acceptor semiconductors together provides a network with a large donor-acceptor interface area in bulk heterojunction. Considering the morphology, it prevents the charge recombination and any absorbing parts of the blend are in few nanometers between the donor and the acceptor. This results in a higher quantum efficiency of charge separation and efficient charge collection.

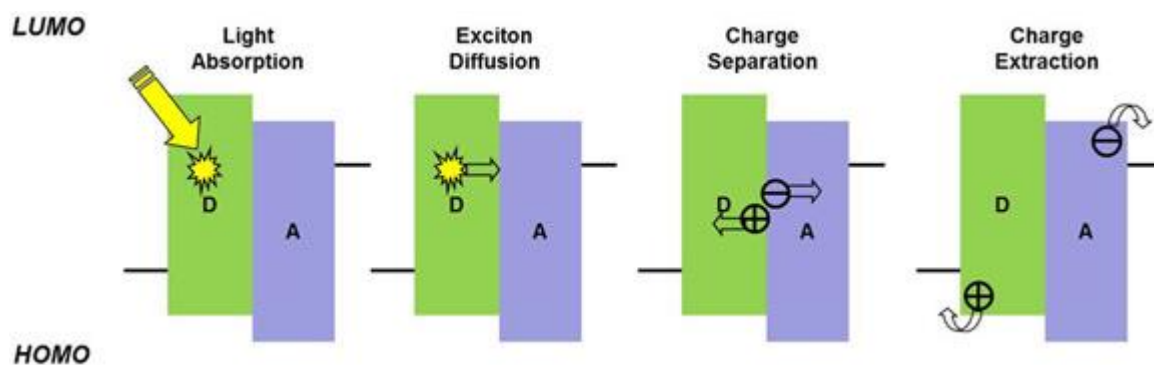


Figure 1. 5. Working principle of a bulk heterojunction organic solar cell

1.3.3.1. Basic Principles

Working principle of an organic solar cell involves following steps; light absorption and collection, exciton generation and diffusion, exciton dissociation, charge transport and charge collection.

1.3.3.1.1. Light Absorption and Collection

The absorption spectrum of the photoactive layer should match the solar emission spectrum for an efficient collection of light. The photoactive layer should sufficiently be thick to absorb the entire incident light. For organic materials, this matching corresponds to the energy gap between the energies of highest occupied molecular orbital (HOMO) and the lowest unoccupied molecular orbital (LUMO).

$$E_g = HOMO - LUMO$$

1.3.3.1.2. Exciton Generation and Diffusion

In organic photovoltaic devices generation of charges is the key step. Following the light absorption, charges are generated via photo induced electron transfer reaction. In this reaction an electron is transferred from the p-type semiconductor to the n-type semiconductor. Pairs of electrons and holes, excitons, are generated in the active layer by bonding through coulombic attraction. Exciton is the combination of an excited and a neutral state. Charge separation (separation of exciton: electron / hole pair) proceeds via the binding energy. Generated excitons diffuse to the interface of the p-type and n-type material (donor and acceptor) with respect to their lifetime.

1.3.3.1.3. Exciton Dissociation

Exciton dissociation requires an ionization potential energy which is lower than the binding energies of excitons and requires a higher electron affinity. Providing these conditions, excitons are separated into electrons and holes.

1.3.3.1.4. Charge Transport and Collection

Following the dissociation process, the free electron-hole pairs are transported in the active layer, from donor to acceptor. The transportation proceeds via hopping mechanism. Finally, the charges are transported to the opposite electrodes and collected. Defects on the active layer might cause the recombination and trapping of the charges. This causes loss of charge, resulting in low power conversion efficiency in the device.

1.3.3.2. Device Preparation

In the preparation of organic solar cell devices solution processability is the key method and for the preparation of the film on the surface vacuum techniques is employed. Since polymers thermally decompose and their molar mass are extremely high, solution process at low temperatures is a necessity for polymer-based organic photovoltaics [30]. Coating techniques such as spin-coating, doctor blading, screen printing, and ink-jet printing are employed in the preparation of films. The Figure 1.9 is the schematic representation of a typical bulk heterojunction organic cell.

In a typical bulk heterojunction organic solar cell, the photoactive layer, involving donor and acceptor materials, is sandwiched between two different electrodes possessing different work functions, which are indium tin oxide (ITO) employed as the anode and a metal as the cathode electrode which is generally aluminum.

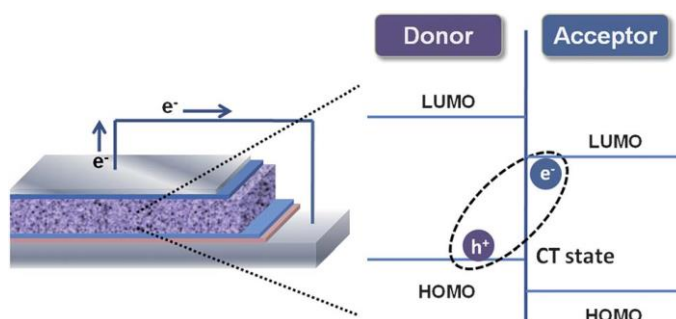


Figure 1. 6. Architecture of bulk heterojunction (BHJ) solar cell [31]

The substrate can be both a stiff or a flexible material which is an insulator, as well. The surface of substrate is coated with the anodic material (ITO) which is a transparent electrode. Onto ITO layer is coated polyethylenedioxythiophene: polystyrenesulfonate (PEDOT: PSS), a water dispersed polymer blend, for hole collection and reducing the roughness of the anode layer. This coating is followed by

the spin casting of the photoactive layer, polymer: PCBM. Buckminster fullerene derivative possess a substituent that prevents extensive crystallization following the mixing and improves the miscibility. At the top of these layers, the cathode electrode is thermally deposited. In this state-of-the-art design of bulk heterojunction solar cells, anodic material has a variable work function of 4.5 eV-4.75 eV, relying on the method of cleaning applied to the surface of ITO. Aluminum has a high work function of 4.3 eV and to reduce this a layer of LiF is thermally deposited between PCBM and aluminum [32].

1.3.3.3. Characterization

Efficiency in organic solar cell corresponds to the power generated by the device with respect to the absorbed light, and it is designated as power conversion efficiency. Massive research on developing new combination of organic semiconductors aims to improve power conversion efficiency of organic solar cells considering three main parameters; the open-circuit voltage (V_{OC}), the short-circuit current density (J_{SC}), and the fill factor (FF).

1.3.3.3.1. Open-Circuit Voltage

V_{OC} is the maximum potential obtained from the solar cell while there is no applied current. It is with respect to the difference between highest occupied molecular orbital (HOMO) of the *p-type* semiconductor (donor) and the lowest occupied molecular orbital (LUMO) of the *n-type* semiconductor (acceptor).

1.3.3.3.2. Short-Circuit Current Density

It is the maximum current density at zero applied potential under illumination. Short-circuit current is highly dependent on absorption capacity of the photoactive material, dissociation and collection of charges.

1.3.3.3.3. Fill Factor

Fill factor is the ratio maximum power generated by the solar cell to the external circuit and the potential power as the following;

$$FF = \frac{P_{max}}{V_{OC} * J_{SC}} = \frac{V_{max} * J_{max}}{V_{OC} * J_{SC}}$$

Above mentioned parameters are extracted to characterize the device performance from a typical current density-voltage (J - V) curve which is obtained from the device under illumination. This is supplied by AM 1.5 G (Air Mass), having a power of 100 mW/cm², solar spectrum based on the path that incident light follows. A typical current density-voltage curve is presented in Figure 1.10. The power conversion efficiency is calculated from the following formula generated from the combination of those parameters.

$$PCE = \frac{P_{max}}{P_{in}} = \frac{FF * V_{OC} * J_{max}}{P_{in}}$$

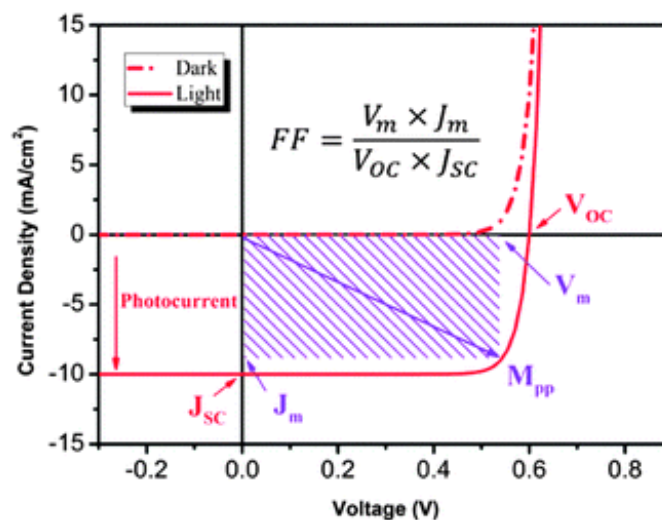


Figure 1. 7. Typical current density-voltage (J-V) curve [33]

1.4. Design and Engineering of Conjugated Polymers

Polymeric materials to be used in the applications of solar energy need to possess two important structural parameters; π -conjugated backbone and functional groups. π -conjugated backbone includes unsaturated units and provides the localizing of π orbital along the chain resulting in charge transport and absorption of light. One of the advantages of conjugated polymers is solubility and ease of processing. Therefore, functional groups that have solubilizing properties are advantageous for processing and manufacturing. Interaction and conjugation among these units are the keys that control both the electronic and structural properties of the polymer, such as optical absorption, redox characteristics and energy levels which at the end determine the band gap [5,34]. Many synthetic pathways for conjugated polymers are available in the literature to obtain desired polymers with respect to the application area. The most popular ones are electrochemical polymerization, oxidative chemical polymerization, Stille Coupling, Suzuki Coupling, Sonogashira Coupling and Heck Reaction.

1.4.1. Electrochemical Polymerization

Intrinsically conducting polymers can be easily prepared by electrochemical oxidation of monomers on electrode surfaces as films. In electrochemical polymer reactions, the conjugated polymer is electrochemically doped [35,36]. First significant studies on electropolymerization were conducted in 1970s. In 1979, Diaz *et. al.* reported the synthesis of poly(pyrrole) and poly(aniline) on platinum electrode [37,38]. The polymers were synthesized galvanostatically in a two-electrode cell medium which contains a solution of 0.1 M tetraethylammonium tetrafluoroborate (Et_4NBF_4) and 0.06 M pyrrole in hydrous 99% acetonitrile (ACN). It was observed that the films strongly adhered to the platinum surface and with this study they succeeded to synthesize a highly stable and flexible poly (pyrrole) films. In the process of electrochemical polymerization, the monomer first is dissolved in an appropriate solvent. To the solution, the desired doping salt is added and the monomer is oxidized on the surface of electrode via application of an anodic potential.

Hundreds of papers were reported revealing electrochemically syntheses of many intrinsically conjugated polymers [39–41]. In electrochemically polymerization of monomers, the monomer is first dissolved in an appropriate solvent. The desired anionic salt is introduced and the monomer is oxidized at the surface of electrode via an anodic potential applied. One of the crucial factors in electrochemical polymerization is the stability of both solvent and electrolyte at the oxidation potential of the monomer since they together provide a conductive medium. That is why the selection of the solvent and the electrode for the stability is particularly important.

Electrochemical polymerization of conjugated monomers has advantages over alternative polymerization techniques. In electrochemical process, there is no need for chemical reagents like oxidants, in conventional chemical procedures it is

obtained as powder. The insolubility of the polymer is a drawback of electrochemical polymerization [42].

1.4.2. Oxidative Polymerization

Oxidative polymerization is utilized to prepare polymers from aromatic compounds like pyrrole, aniline, thiophene and furan derivatives. The oxidation is achieved upon usage of an anhydrous inorganic catalyst like FeCl_3 and AlCl_3 (Lewis acids) as polymerization catalysts [43,44]. This method is the simplest one to prepare high molecular weight conjugated polymers. FeCl_3 is highly utilized in the preparation of polymers composed of heterocyclic monomers. The process is solution based and product formation proceeds by precipitation in bulk as insoluble crystals.

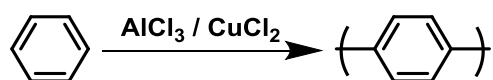


Figure 1. 8. Oxidative Chemical Polymerization of benzene

1.4.3. Stille Coupling

Being discovered by John Kenneth Stille and David Milstein in 1977, Stille Coupling is a versatile reaction between halides/pseudo halides and stannanes to form new C-C bonds [45]. Stille coupling is one of the most efficient and widely used techniques in the preparation of alternating conjugated polymers consisting of two or more distinct monomers. Tolerating different functional groups and mild reaction conditions are the major advantages of Stille coupling. Since halides can be altered on the molecule before utilizing them in Stille coupling, the polymers can be designed with different

functional moieties with desired properties [46]. The reaction is stereospecific and regioselective. The yields of Stille coupling are generally high. Utilizing Stille Coupling represents versatile tolerances with its mild reaction conditions and solubility of monomers due to wide range of functional groups.

Stille reaction which is mediated by Pd (0) proceeds via cross-coupling of organohalides with organostannanes. The figure illustrates the general mechanism of Stille reaction which involves an oxidation step, a transmetalation step and a reductive elimination step. In the reaction Pd (II) can also be used as catalyst but the system is Pd (0) mediated. That is why Pd (0) being the active catalyst will be utilized upon reduction from Pd (II).

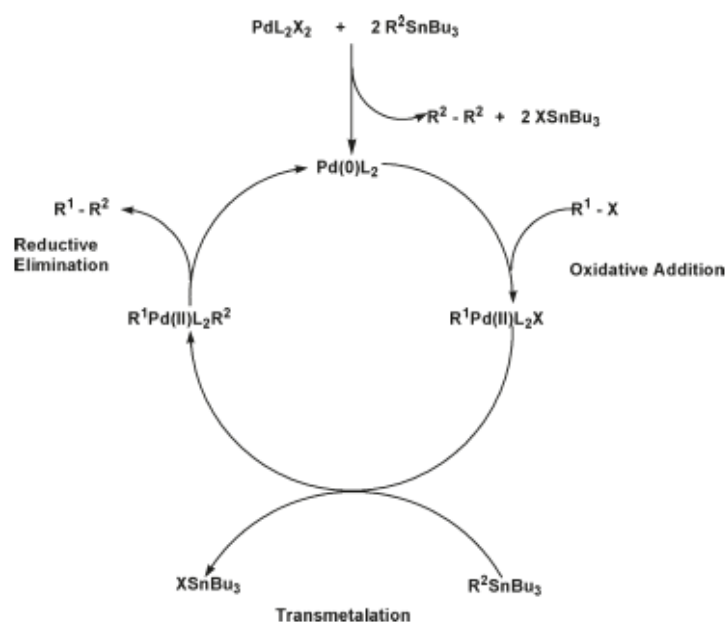


Figure 1. 9. General mechanism of Stille Coupling [46]

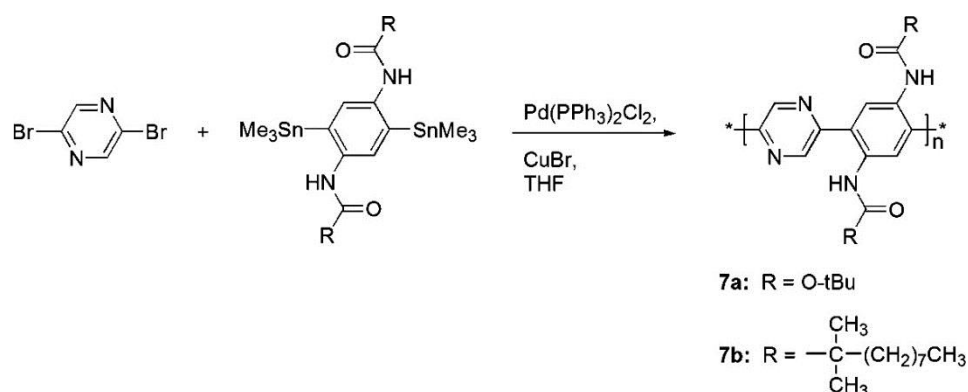


Figure 1. 10. Stille Coupling Polymerization [46]

1.4.4. Suzuki Coupling

Suzuki reaction is the coupling of an aryl/vinyl boronic acid to an aryl/vinyl halide catalyzed by Pd (0). The organoboron compound can be borane ester or borane, as well as boronic acid. Being reported by Akira Suzuki in 1979, Suzuki coupling is a stereospecific palladium-catalyzed organic reaction. Palladium-catalyzed polycondensation Suzuki coupling proceeds in a chain-growth polymerization step that is initiated by an initiator derived from the catalyst [47,48]. Suzuki coupling provides with the ease of reaction conditions, use of aqueous solvents and substrate supports. Reactants are commercially available and the byproducts of boron can be easily removed following the completion of the reaction.

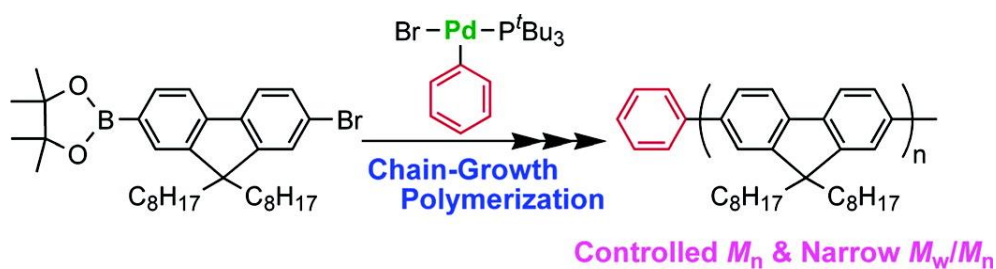


Figure 1. 11. Suzuki Coupling Polymerization [48]

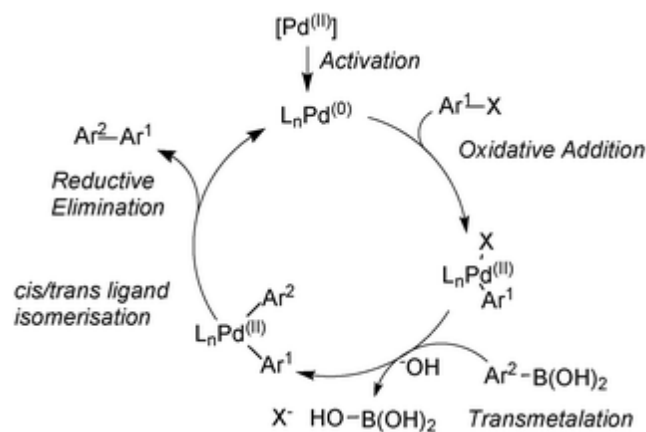


Figure 1. 12. General mechanism of Suzuki Coupling [49]

1.4.5. Sonogashira Coupling

First reported in 1975 by Kenkichi Sonogashira and Nobue Hagihara, palladium-catalyzed Sonogashira coupling reaction is one of the widely used methods for the preparation of conjugated enynes and arylacetylenes. Being regioselective, Sonogashira reaction provides the generation of diverse building blocks and heterocycles. The reaction proceeds with the presence of two different catalysts, a halide salt of copper (I) and a zero valent palladium complex, Pd (0) [50–52].

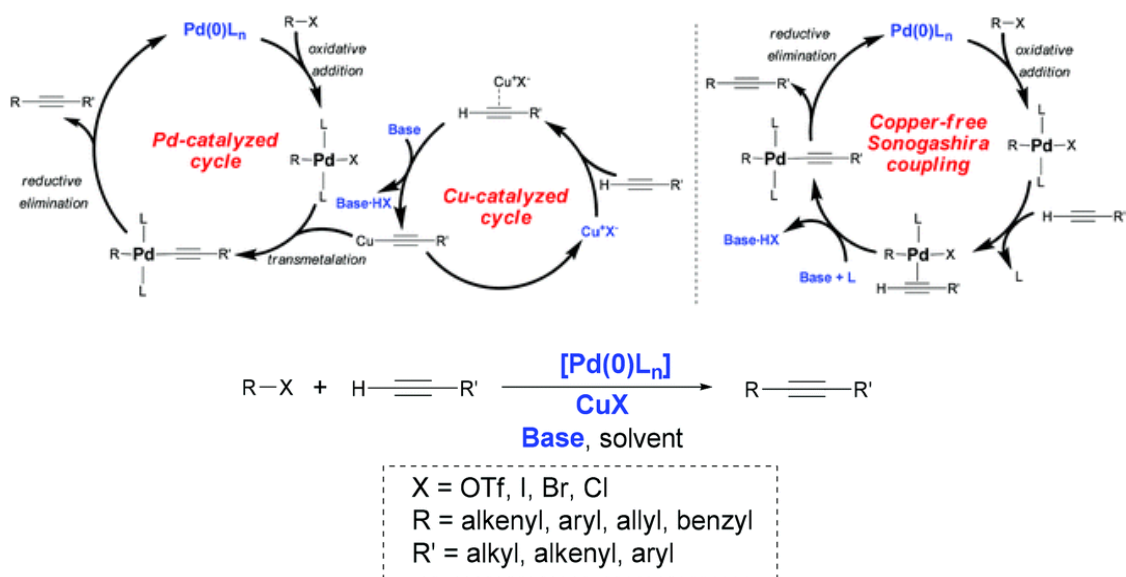
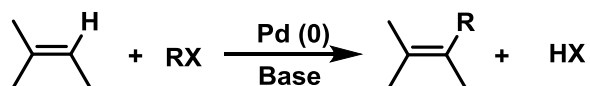


Figure 1. 13. General mechanism Sonogashira Coupling [52]

1.4.6. Heck Reaction

Now known as Heck Reaction, it was discovered by Mizoroki and Heck independently at the beginning of 1970s [53–55]. The reaction is palladium-catalyzed and utilized to couple aryl halides or vinyl halides to alkenes for new formation of C-C bonds in the presence of a base. Synthetically the reaction is attractive due to mild reaction conditions, high stereoselectivity, low toxicity and costs of reagents.



R: arly, vinyl

X: I, Br, COCl, OTf, etc.

Figure 1. 14. Heck Reaction

1.5. Motivation

In this study, donor-acceptor (D-A) type conjugated polymers were synthesized following the design. Selenophene was incorporated as pi-bridge while benzodithiophene and quinoxaline were used as donor and acceptor units, respectively. The synthesized polymers were used as photoactive layers in solar cell devices after electrochemical and spectroelectrochemical characterizations.

Conjugated polymers have a large range of applications like light emitting diodes, biosensors, batteries, capacitors, and solar cells due to flexibility, electronic properties, low cost, manipulation of structure, and ease of processing. Improvement of polymer solar cells' efficiency highly depends on the band gap of the polymers which should have narrow optical band gap, desired optoelectronic properties, and tunable energy levels. Reduced band gap is obtained by the minimization of the mismatch between solar emission spectrum and light absorption of organic solar cell [56–59]. Engineering of the band gap can give desired conjugated polymers with desired properties, like electrical and optical properties. Preparation of low band-gap polymers is highly dependent on two approaches, stabilization of quinoid resonance structure and donor-acceptor approach. Conjugated polymers have two resonance structures; aromatic and quinoid. Having a smaller band gap, the quinoid structure is less stable compared to aromatic structure. Adaptation of quinoid structure is succeeded via destruction of aromaticity resulting in the loss of stabilization energy. π -electrons located on the conjugated backbone delocalize and double bonds transform into single bonds and at the same time single bonds transform into double bonds. Resonance structures formed due to those transformations are favorable. Providing the quinoid form with an aromatic unit by fusing makes it more stable. Stabilization is achieved by forming large aromatic resonance stabilization energy resulted from alternating aromatic and quinoid units.

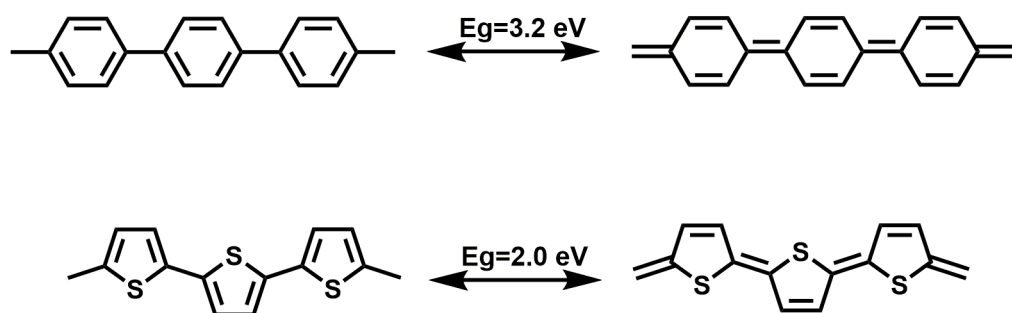


Figure 1. 15. Aromatic and resonance forms of poly (p-phenylene) and poly (thiophene)

Donor-Acceptor (D-A) interaction is another approach in preparation of low band gap conjugated polymers. The concept is to employ alternating electron donating and electron withdrawing units in the backbone of the conjugated polymer to reduce the band gap. Such conjugated polymers are called as “D-A-D” polymers. First example of this approach revealed by Havinga *et. al.* in 1993. The study proved that reducing band gap is succeeded by introducing alternating donor and acceptor units in the backbone [60].

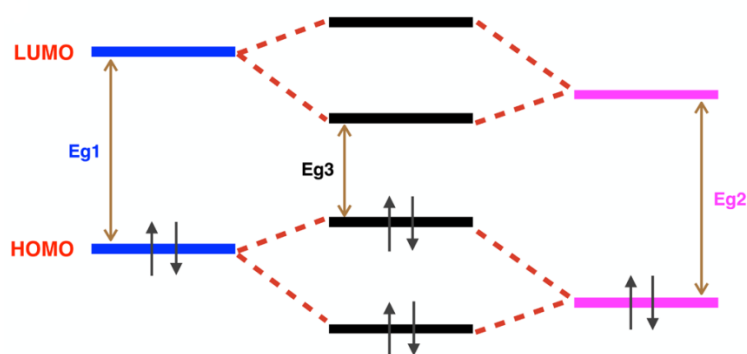


Figure 1. 16. Optimized band gap through donor-acceptor interaction [58]

1.5.1. Incorporation of Selenophene as a π -bridging unit and Benzo[1,2-b:4,5-b']dithiophene with quinoxaline unit

Selenophene is highly used in conjugated polymers as a substitute of thiophene. Due to its larger size, selenophene causes a decrease in overlap with it has more quinoidal character compared to its analogous thiophene. Its ionization potential is lower than that of thiophene, thus incorporation of selenium atom decreases LUMO level of polymers. This, results in a reduced band gap in conjugated polymers compared to thiophene derivatives. Replacing sulfur atom in thiophene structure with selenium results in enhanced charge transport characteristics such as charge mobility. Incorporation of selenophene leads to red shift of the absorbance. Despite of those, lone pairs of selenophene atoms are more mobile than of thiophene atoms since less participating in aromaticity, resulting in the improvement of the chain interaction among chains [61–66].

Benzodithiophene (BDT) is one of the most attractive donor units for conjugated polymers. Due to its planar and fused structure, BDT is ideal for π - π stacking. Introduction of alkylthienyl unit into BDT results in improved photovoltaic properties in terms of coplanarity and extended absorption band [67]. Since the structure of BDT is planar, intramolecular rotation is restricted and π -orbital overlap is maximized in the polymer backbone. Hopping mechanism is improved due to face to face π -stacking. Incorporation of BDT can also make the polymer backbone rigid and coplanar. As a result of this π -conjugation increases and the band gap decreases [68–71]. In literature, there are many studies revealing BDT, thiophene and quinoxaline based conjugated polymers. Ye *et al.* reported power conversion efficiency of a device based on PBDTDTQx-T which includes both BDT and quinoxaline units bearing thiophene as π bridging unit. The device showed a PCE of 5 % with an optical band gap of 1.67 eV [72]. Two other studies reported a PCE of 2.66 % and 1.1 % of devices based on thiophene, quinoxaline and BDT with optical band gaps of 1.68 eV 1.73 eV, respectively [73,74].

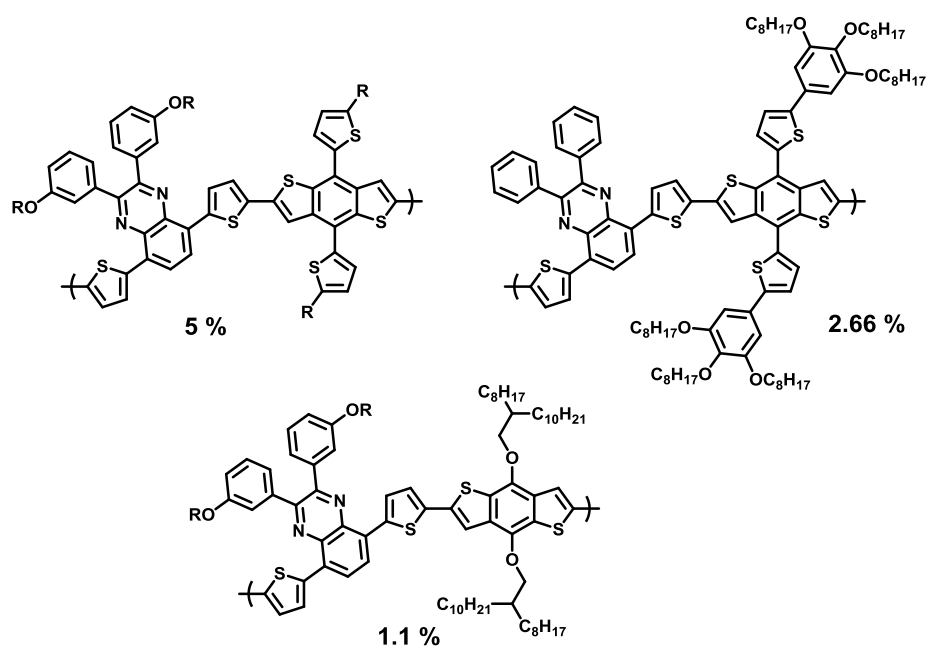


Figure 1. 17. BDT based conjugated polymers incorporated with thiophene and quinoxaline units

1.5.3. 9H-fluorene and 9H-carbazole

Fluorene bearing conjugated polymers have low HOMO energy levels resulting in higher open circuit voltage. Introducing alkyl chains to fluorene unit improves solubility and extends conjugation. Incorporation of carbazole with selenophene in the polymer backbone results in extraordinary photochemical stabilities. Modification of carbazole with an alkyl chain introduced to nitrogen atom enhances the solubility of polymer derivatives. Although carbazole bearing conjugated polymers demonstrate excellent properties for photovoltaics, but they are generally have low molecular weights [10]. Figure shows some results of devices based on fluorene and carbazole units incorporated with thiophene and quinoxaline units.

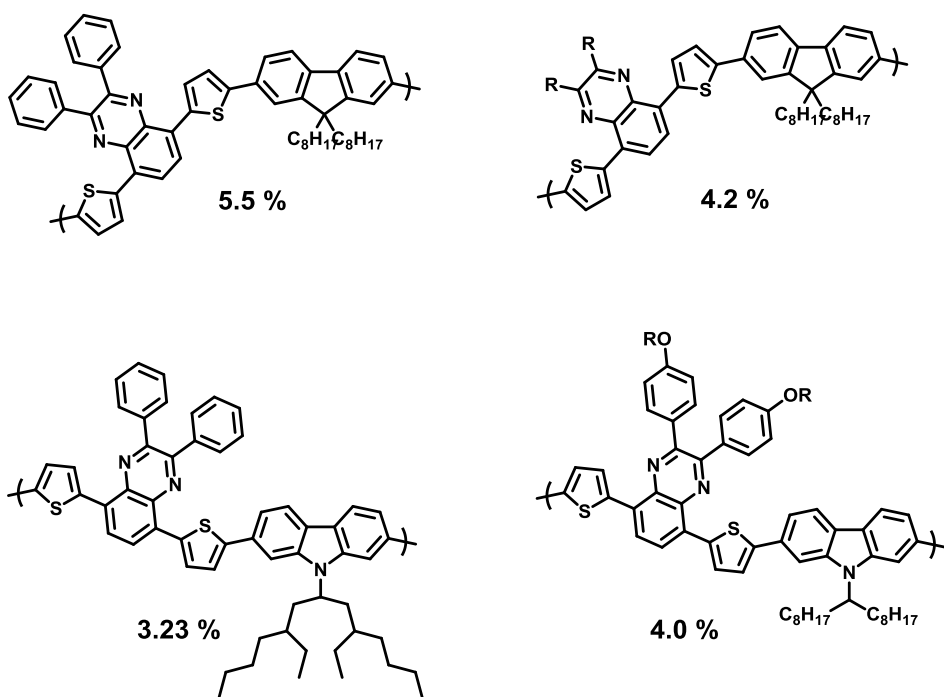


Figure 1. 18. Fluorene and carbazole based polymer incorporated with thiophene and quinoxaline units [75–78]

CHAPTER 2

EXPERIMENTAL

2.1. Materials

All chemicals were purchased from Sigma & Aldrich except 4,8-bis[5-(2-ethylhexyl)thiophen-2-yl]-2,6-bis(trimethylstannyl)benzo[1,2-b:4,5-b']dithiophene and selenophene which were purchased from TCI Chemicals.

2.2 Methods and Equipment

Except for syntheses of 4,7-dibromobenzo[c][1,2,5]thiadiazole, 3,6-dibromobenzene-1,2-diamine, 2,3-bis(3,4-bis(octyloxy)phenyl)-5,8-bis(5-bromoselenophen-2-yl)quinoxaline and 2,3-bis(3,4-bis(octyloxy)phenyl)-5,8-bis(5-bromofuran-2-yl)quinoxaline, all reactions were conducted under argon atmosphere to provide inert atmosphere. Products were purified by column chromatography employing Silica Gel 60 (Merck, 0.063-0.200mm/70-230 mesh ASTM). In order to determine the structures and purity of synthesized molecules and polymers, a Bruker Avance DPX 400 NMR Spectrometer was implemented to obtain ^1H and ^{13}C NMR spectra. As a reference, CDCl_3 was used for each sample and chemical shifts were recorded in ppm with respect to tetramethylsilane internal reference.

To investigate the redox properties of synthesized polymers cyclic voltammetry (CV) was implemented. A three-electrode system was used to perform cyclic voltammetry. Silver and platinum wires were used as reference and counter electrodes, respectively. Indium tin oxide (ITO) casted glass substrate was used as the working electrode in an electrolyte containing 0.1 M tetrabutylammonium

hexafluorophosphate in acetonitrile. Highest Occupied Molecular Orbital (HOMO) and Lowest Occupied Molecular Orbital (LUMO) levels were determined with respect to Normal Hydrogen Electrode (NHE), -4.75 eV in vacuum. Spectroelectrochemical studies of polymers were performed with an Agilent G1103A UV-VIS Spectrophotometer. Kinetic studies for investigation of electrochromic switching times and percent transmittance were performed by a Solartron 1285 Potentiostat.

Organic solar cell fabrication and characterization were carried out in an MBRAUN 200B Glove Box System filled with nitrogen ($\text{H}_2\text{O} < 0.1$ ppm, $\text{O}_2 < 0.1$ ppm). Current-Voltage (J - V) characteristics were examined under illumination of an ATLAS Materials Testing Solar Simulator.

2.3. Synthesis

2.3.1. Monomer Syntheses

2.3.1.1. 4,7-Dibromobenzo[*c*][1,2,5]thiadiazole

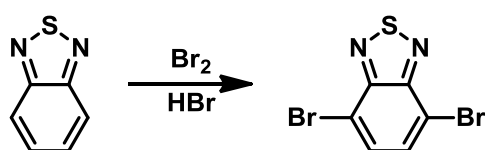


Figure 2. 1. Synthetic route of 4,7- dibromobenzo[*c*][1,2,5]thiadiazole [79]

Benzo[*c*][1,2,5]thiadiazole (5.0 gr, 37 mmol) was introduced into a three-necked flask charged with a stirring bar. HBr (90 mL) was added and the solution was heated. At 100 °C, HBr and Br_2 (40 mL and 4 mL, 77 mmol) were added drop wise.

After addition of HBr/Br₂, the temperature was set to 135 °C and the mixture was stirred overnight. The flask was kept in ice bath for 2 hours. The mixture was washed with NaHSO₃, dissolved in dichloromethane (DCM) and extracted with water. DCM was removed under reduced pressure and diethyl ether was added to crude product to remove mono brominated benzothiadiazole. 9.7 gr was obtained. Yield: 90%.

¹H NMR (400 MHz, CDCl₃): δ: 7.73 (s, 2H)

¹³C NMR (100 MHz, CDCl₃): δ: 152.95, 132.27, 114.09.

2.3.1.2. 3,6-Dibromobenzene-1,2-diamine

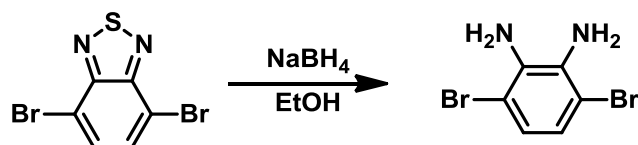


Figure 2. 2. Synthetic route of 3,6-dibromobenzene-1,2-diamine [79]

4, 7-Dibromobenzo[c][1,2,5]thiadiazole (1.0 g, 3.4 mmol) was dissolved in ethanol (25 mL) in a 1L erlenmeyer charged with a stirring bar. The solution was cooled to 0°C. NaBH₄ (5.0 g, 132 mmol) which was taken under argon atmosphere was added portion wise to the solution. The mixture was left to stir overnight at room temperature. The solvent was removed under reduced pressure for 3-4 hours. Water was added to the mixture and product was extracted with diethyl ether. Collected organic phases were washed with distilled water twice. Solvent was removed by rotary evaporation. A white solid was obtained. Yield: 750 mg, 83 %.

^1H NMR (400 MHz, CDCl_3): δ : 6.85 (d, 2H), 3.89 (s, 4H)

^{13}C NMR (100 MHz, CDCl_3): δ : 133.74, 123.28, 109.71.

2.3.1.3. Synthesis of 1,2-bis(octyloxy)benzene

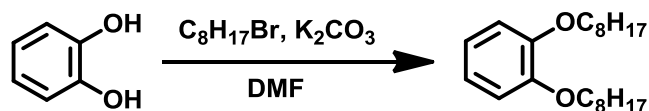


Figure 2. 3. Synthetic route of 1,2-bis(octyloxy)benzene [80]

A two-necked, 100 mL flask was charged with a stirring bar. Pyrocatechol (4.0 g, 36 mmol) was introduced and the flask was taken under argon atmosphere. Dry DMF (35 mL) was added after 1 hour and the solution was heated. 30 minutes later K_2CO_3 (13 g, 94 mmol) was added. At 100 °C, 1-bromooctane (14 g, 73 mmol) was introduced. Thin Layer Chromatography (TLC) controlled reaction was stirred overnight at reflux temperature. The solvent was removed under reduced pressure and the mixture was dissolved in dichloromethane and washed with water and brine, respectively. Dichloromethane was removed under reduced pressure and the product was purified by recrystallization in methanol. A grey solid was obtained. Yield: 9.9 g, 81 %.

^1H NMR (400, CDCl_3): δ : 6.89 (s, 4H), 3.99 (t, $J=6.65$ Hz, 4H), 1.81 (p, $J=6.85$ Hz, 4H), 1.47 (m, 4H), 1.28-1.37 (m, 16H), 0.88 (t, $J=6.41$ Hz, 6H)

^{13}C NMR (100 MHz, CDCl_3): δ : 149.125, 120.99, 114.12, 69.27, 31.85, 29.41, 26.06, 22.69, 14.11.

2.3.1.4. Synthesis of 1,2-bis(3,4-bis(octyloxy)phenyl)ethane-1,2-dione

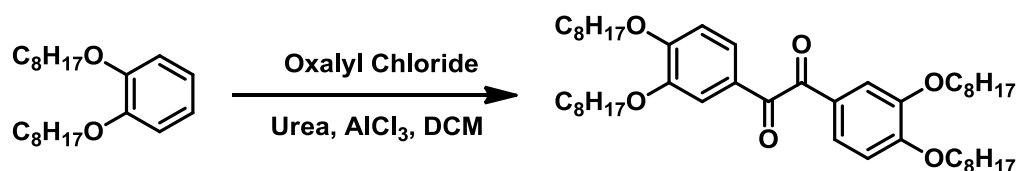


Figure 2. 4. Synthetic route of 1,2-bis(3,4-bis(octyloxy)phenyl)ethane-1,2-dione [80]

A two-necked, 100 mL flask was charged with a stirring bar. Alkoxy benzene (1,85g, 5.5 mmol), urea (0.3 g, 5.2 mmol) and $AlCl_3$ (1.1 g, 8.4 mmol) were introduced. The mixture was cooled to $0^\circ C$. Dichloromethane (15 mL) was added. Oxalylchloride (0.3 mL, 3.4 mmol) was added drop wise. The mixture was left to stir overnight. The mixture was poured into cold water and extracted with dichloromethane. Collected organic phase was extracted with $NaHCO_3$, dried over Na_2SO_4 and concentrated by rotary evaporation. Yield: 990 mg, 50 %.

1H NMR (400, $CDCl_3$): δ : 7.56 (d, $J= 1.86$ Hz, 2H), 7.43 (dd, $J=1.86$ Hz, 8.36, 2H), 6.86 (d, $J= 11.54$ Hz, 2H), 4.05 (t, $J= 5.25$ Hz, 8H), 1.84 (m, 8H), 1.45 (m, 8H), 1.31-1.28 (m, 32H), 0.88 (m, 12H)

^{13}C NMR (100 MHz, $CDCl_3$): δ : 193.82, 165.73, 154.98, 149.27, 126.12, 121.00, 114.14, 69.29, 31.84, 29.30, 29.08, 26.07, 22.68, 14.10.

2.3.1.5. Synthesis of 2,3-Bis(3,4-bis(octyloxy)phenyl)-5,8-dibromoquinoxaline

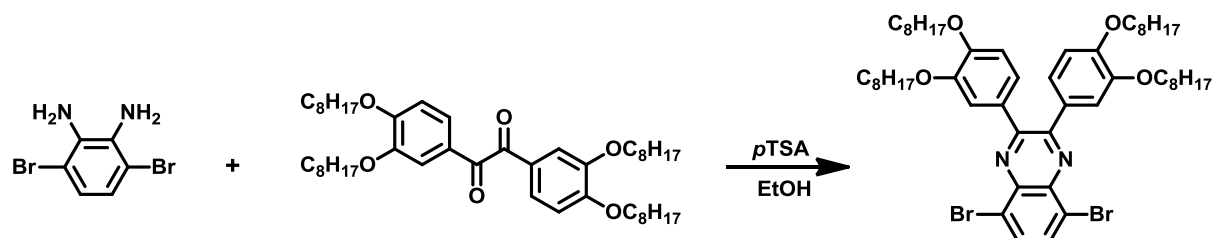


Figure 2. 5. Synthetic route of 2,3-bis(3,4-bis(octyloxy)phenyl)-5,8-dibromoquinoxaline [81]

A 100 mL, two-necked flask was charged with a stirring bar. 3,6-Dibromobenzene-1,2-diamine (0.22 g, 0.85 mmol) and 1,2-bis(3,4-bis(octyloxy)phenyl)ethane-1,2-dione (0.62 g, 0.85 mmol) were introduced. The mixture was taken under argon atmosphere. *p*-Toluene sulfonic acid was added in catalytic amount. Ethanol (EtOH) (10 mL) was added and the mixture was refluxed overnight, then it was cooled to 0°C. Obtained precipitate was filtrated and washed with EtOH. Yield: 0.57 g, 66 %.

^1H NMR (400 MHz, CDCl_3): δ : 7.85 (s, 2H), 7.56 (d, $J=1.97$ Hz, 2H), 7.43 (dd, $J=2.02, 8.44$ Hz, 2H), 6.85 (d, $J=2.11$ Hz, 2H), 3.86 (t, $J=6.67$, 8H), 1.74 (m, 8H), 1.47 (m, 8H), 1.31-1.29 (m, 32H), 0.89 (m, 12H)

^{13}C NMR (100 MHz, CDCl_3): δ : 151.50, 148.57, 146.62, 136.85, 130.4, 128.49, 121.31, 113.54, 110.90, 67.11, 29.73, 27.31-26.99, 23.90, 20.56, 11.96.

2.3.1.6. Synthesis of Tributyl(selenophen-2-yl)stannane



Figure 2. 6. Synthetic route of tributyl(selenophen-2-yl)stannane [82]

A two-necked, 50 mL flask was charged with a stirring bar and taken under argon atmosphere. Selenophene (5.0 g, 38 mmol) was introduced. Tetrahydrofuran (THF) (70 mL, dried) was added 30 minutes later. The solution was cooled to -78 °C. N-butyl lithium (15 mL, 38 mmol in 2.5 M hexane) was added drop wise. The system was maintained at -78 °C for one hour. Tributyltin chloride (11 mL, 41 mmol) was added drop wise. The mixture was maintained at -78 °C for four hours. Then, the mixture was left to stir overnight. After removing the solvent by rotary evaporation, dichloromethane was poured into the mixture and washed with NaHCO₃, water and brine. Combined organic layers were dried over anhydrous Na₂SO₄ and concentrated under reduced pressure. Yield: 14 g, 95 %.

¹H NMR (400 MHz, CDCl₃) δ: 8.36 (d, *J*=4.87 Hz, 1H), 7.53 (m, 1H), 7.5 (dd, *J*=2.44, 9.44 Hz, 1H), 1.59 (m, 6H), 1.35 (m, 6H), 1.12 (m, 6H), 0.92 (t, *J*=7.33 Hz, 9H)

¹³C NMR (100 MHz, CDCl₃): δ: 143.60, 137.91, 135.30, 130.55, 29.00, 27.30, 13.67, 11.13.

2.3.1.7. Synthesis 2,3-Bis(3,4-bis(octyloxy)phenyl)-5,8-di(selenophen-2-yl)quinoxaline

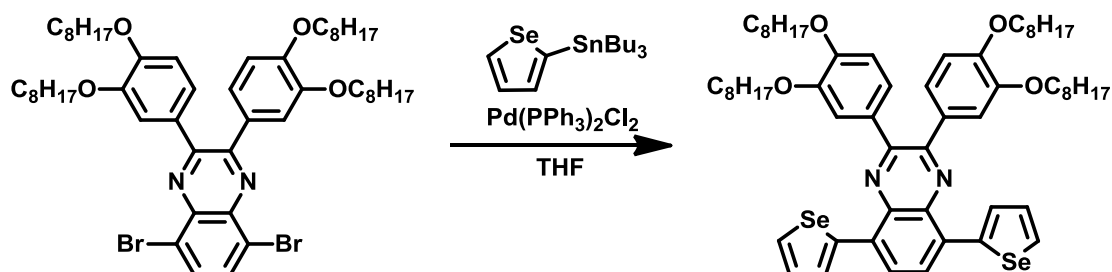


Figure 2. 7. Synthetic route of 2,3-bis(3,4-bis(octyloxy)phenyl)-5,8-di(selenophen-2-yl)quinoxaline [83]

A 100 mL, two-necked was charged with a stirring bar. 2,3-Bis(3,4-bis(octyloxy)phenyl)-5,8-dibromoquinoxaline (0.4 g, 0.4 mmol) was introduced and the flask was taken under Ar atmosphere. 20 minutes later dry THF (35 mL) was added. PdCl₂(PPh₃)₂ (45 mg) was added and the mixture was heated. At 60 °C, tributyl(selenophen-2-yl) stannane (0.88 mg, 2.1 mmol) was added and the temperature was set to 100°C. The mixture was stirred for several 18 hours. The mixture was cooled to room temperature and concentrated under reduced pressure. Obtained red mixture was subjected to column chromatography (hexane and chloroform, 1:1) to afford a red solid. Yield: 0.36 g, 95 %.

¹H NMR (400 MHz, CDCl₃) δ: 8.22 (2H, s), 8.19 (d, *J*=5.78 Hz, 2H), 8.05 (d, *J*=3.24 Hz, 2H), 7.45 (dd, *J*=4.00, 5.77 Hz, 2H), 7.36 (d, *J*=2.02 Hz, 2H), 7.23 (d, *J*=8.31 Hz, 2H), 6.86 (d, *J*=8.40 Hz, 2H), 4.04 (t, *J*=6.65 Hz, 4H), 3.93 (t, *J*=6.72 Hz, 4H), 1.86 (m, 4H), 1.78 (m, 4H), 1.40-1.25 (m, 40H), 0.9 (q, *J*=6.60 Hz, 12H)

¹³C NMR (100 MHz, CDCl₃): δ: 163.03, 159.15, 151.69, 110.32, 102.37, 85.34, 31.86, 29.37, 26.08, 22.69, 22.23, 14.12.

2.3.1.8. Synthesis of 2,3-Bis(3,4-bis(octyloxy)phenyl)-5,8-bis(5-bromoselenophen-2-yl) quinoxaline

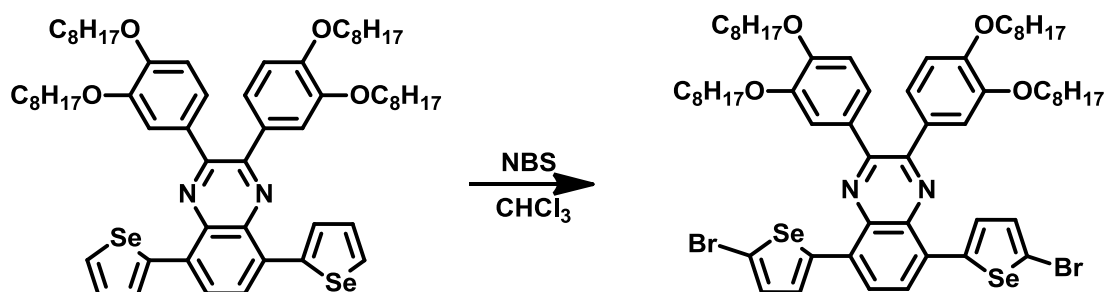


Figure 2. 8. Synthetic route of 2,3-bis(3,4-bis(octyloxy)phenyl)-5,8-bis(5-bromoselenophen-2-yl) quinoxaline [82]

2,3-Bis(3,4-bis(octyloxy)phenyl)-5,8 di(selenophen-2-yl) quinoxaline (0.46 g, 0.43 mmol) was dissolved in chloroform (CHCl₃) in a 100 mL flask charged with a stirring bar. N-bromosuccinimide (NBS) (0.15 g, 0.86 mmol) was added in three portion. The mixture was left to stir overnight at ambient temperature. Mixture was poured into 65 mL distilled water. Organic phase was extracted with CHCl₃, dried over Na₂SO₄ and concentrated under reduced pressure. Through recrystallization with EtOH, a reddish solid was obtained. Yield: 0.46 g, 89 %.

¹H NMR (400 MHz, CDCl₃) δ : 8.15 (s, 2H), 7.73 (d, $J=4.38$ Hz, 2H), 7.41 (s, 2H), 7.36 (d, $J=4.35$ Hz, 2H), 7.07 (dd, $J=2.03, 8.32$ Hz, 2H), 6.82 (d, $J=8.42$ Hz, 2H), 4.02 (q, $J=6.70$ Hz, 8H), 1.85 (m, 8H), 1.50 (m, 8H), 1.25-1.36 (m, 32H), 0.9 (t, $J=6.71$ Hz, 12H)

¹³C NMR (100 MHz, CDCl₃): δ : 150.11, 148.11, 146.73, 140.43, 133.55, 129.73, 129.26, 128.26, 123.56, 121.38, 120.79, 113.77, 110.35, 67.31, 29.70, 27.20, 24.00, 20.55, 11.94.

2.3.2. Polymer Syntheses

2.3.2.1. Synthesis of Poly[5-(5-(4,8-bis(2-ethylhexyl)benzo[1,2-b:4,5-b']dithiophen-2-yl)selenophen-2-yl)-2,3-bis(3,4-bis(octyloxy)phenyl)-8-(selenophen-2-yl)quinoxaline]-PBDTSeQ

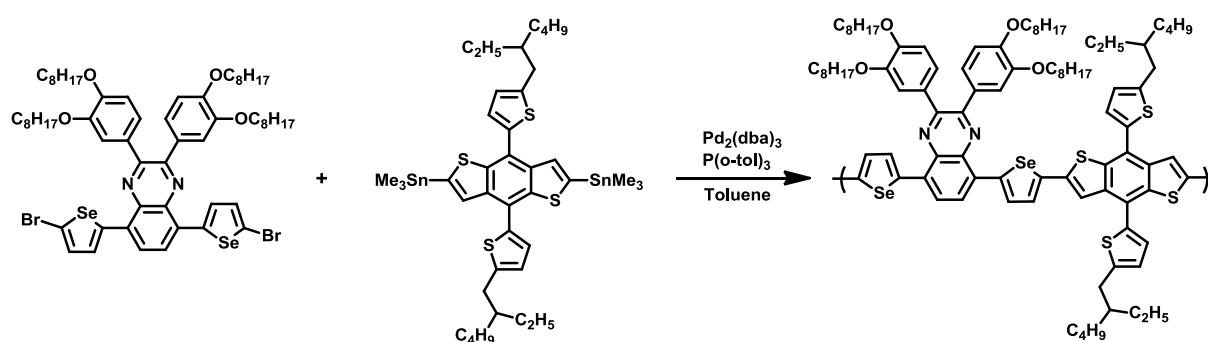


Figure 2. 9. Synthetic route of PBDTSeQ [82]

A 100 mL, two-necked was charged with a stirring bar and taken under Ar atmosphere. 30 minutes later 2,3-bis(3,4-bis(octyloxy)phenyl)-5,8-bis(5-bromoselenophen-2-yl)quinoxaline (0.13 g, 0.11 mmol), 4,8-bis[5-(2-ethylhexyl)thiophen-2-yl]-2,6-bis(trimethylstannyl)benzo[1,2-b:4,5-b']dithiophene (0.10 g, 0.11 mmol) and Pd(PPh₃)₄ (10 mg) were introduced. Dry toluene (11 mL) was added and the mixture was stirred at reflux temperature. 21 hours later, chlorobenzene (0.2 mL) was added. 7 hours later after addition of chlorobenzene, tributyl(furan-2-yl)stannane (0.4 mL) was added. The mixture was cooled to ambient temperature. Solvent was removed under reduced pressure. Cold methanol was added and the mixture was kept in the fridge overnight. Sodium diethyldithiocarbamate trihydrate (10 mg) was added and stirred for 1h. The mixture was filtered through a Soxhlet thimble and the thimble was put in a Soxhlet extractor to purify with acetone, hexane and chloroform, respectively. Polymer was collected via CHCl₃ fraction. Solvent was removed under reduced pressure and polymer was

precipitated in cold methanol and dried to afford dark blue crystals (160 mg). Yield: 89 %.

M_n : 16000 Da, M_w : 22000 Da, PDI: 1.57

2.3.2.2. Synthesis of Poly[3-(5-(2,3-bis(3,4-bis(octyloxy)phenyl)-8-(selenophen-2-yl)quinoxalin-5-yl)selenophen-2-yl)-9-(heptadecan-9-yl)-9H-carbazole]-PSeQCz

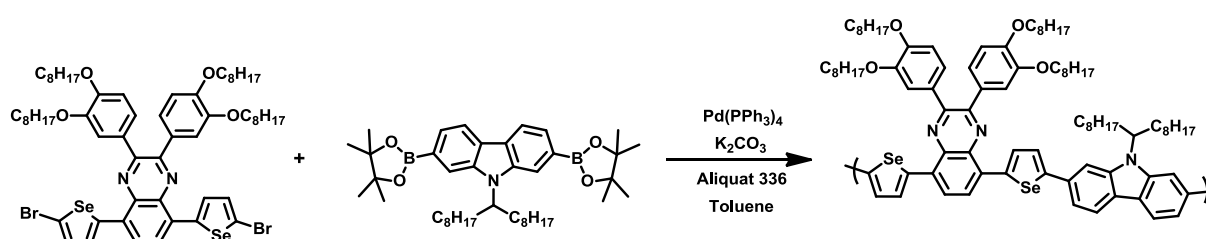


Figure 2. 10. Synthetic route of PSeQCz [84]

A 50 mL flask was charged with a stirring bar and taken under Ar atmosphere. 1 h later 2,3-bis(3,4-bis(octyloxy)phenyl)-5,8-bis(5-bromoselenophen-2-yl)quinoxaline (0.23 g, 0.19 mmol), 9-(heptadecan-9-yl)-2,7-bis(4,4,5,5-tetramethyl-1,3,2-dioxaborolan-2-yl)-9H-carbazole (0.125 g, 0.19 mmol) and Pd(PPh₃)₄ (10 mg) were introduced. 2M K₂CO₃ (0.38 mL) were added. Aliquat 336 (1-2 drops) was introduced in toluene (10 mL). Reaction mixture was left to stir at reflux temperature. 48 h later chlorobenzene (0.2 mL) was added. 60 h later 0.4 mL tributyl(furan-2-yl)stannane was added. Reaction mixture was cooled to ambient temperature. Solvent was removed under reduced pressure. The crude product was extracted with CHCl₃/H₂O three times and dried over MgSO₄ and the solvent was removed under reduced pressure. Cold methanol was added to the product and it was kept in the fridge overnight. 10 mg Pd scavenger (sodium diethyldithiocarbamate trihydrate) was added. The mixture was filtered through a Soxhlet thimble and

extracted via Soxhlet extractor with acetone (5h), hexane (3h) and chloroform (1.5 h) respectively. Polymer was obtained from hexane fraction. Hexane was removed under reduced pressure and the polymer was added cold methanol to obtain dark crystals (198 mg). Yield: 72 %.

M_n : 4670 Da, M_w : 5520 Da, PDI: 1.18

2.3.2.3. Synthesis of Poly[2,3-bis(3,4-bis(octyloxy)phenyl)-5-(5-(9,9-dioctyl-9H-fluoren-3-yl)selenophen-2-yl)-8-(selenophen-2-yl)quinoxaline]-PFISEQ

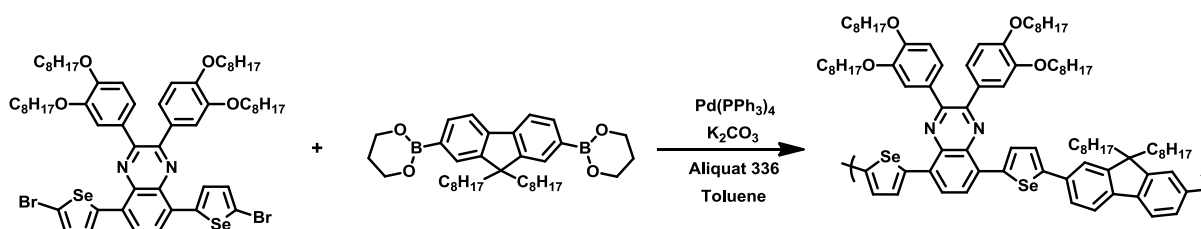


Figure 2. 11. Synthetic route of PFISEQ [84]

A 50 mL flask was charged with a stirring bar and taken under Ar atmosphere. 1 h later 2,3-bis(3,4-bis(octyloxy)phenyl)-5,8-bis(5-bromoselenophen-2-yl)quinoxaline (0.21 g, 0.17 mmol), 2,2'-(9,9-dioctyl-9H-fluorene-2,7-diyl)bis(1,3,2-dioxaborinane) (0.097 g, 0.173 mmol) and Pd(PPh₃)₄ (10 mg) were introduced. 2M K₂CO₃ (0.35 mL) were added. Aliquat 336 (1-2 drops) was introduced in toluene (10 mL). Reaction mixture was left to stir at reflux temperature. 48 h later chlorobenzene (0.2 mL) was added. 60 h later 0.4 mL tributyl(furan-2-yl)stannane was added. Reaction mixture was cooled to ambient temperature. Solvent was removed under reduced pressure. The crude product was extracted with CHCl₃/H₂O three times and dried over MgSO₄ and the solvent was removed under reduced pressure. Cold methanol was added to the product and it was kept in the fridge overnight. 10 mg Pd scavenger (sodium diethyldithiocarbamate trihydrate) was added. The mixture was filtered

through a Soxhlet thimble and extracted via Soxhlet extractor with acetone (5h), hexane (3h) and chloroform (1.5 h) respectively. Polymer was obtained from hexane fraction. Hexane was removed under reduced pressure and the polymer was added cold methanol to obtain dark crystals (195 mg). Yield: 80 %.

M_n : 7204 Da, M_w : 9643 Da, PDI: 1.33

2.4. Characterization of the polymers

2.4.1. Gel Permeation Chromatography (GPC)

GPC is a method for determination of average molecular weight of polymers. It is able to separate high molecular weight and low molecular weight polymers providing both molecular weight distribution and polydispersity index (PDI) in a single analysis [60,85,86]. The method was performed using a SHIMADZU CTO-10AS VP calibrated with a universal standard polystyrene (PS) sample. In order to run the analysis, polymers (5 mg) were dissolved in chloroform (2.0 mL) and the solution is injected to the device. At the end of the analysis, number average molecular weight (M_n), weight average molecular weight (M_z) and polydispersity index were obtained.

2.4.2. Electrochemical Characterizations

2.4.2.1. Cyclic Voltammetry

Cyclic voltammetry is a method of analyzing electroactive materials. In this case, HOMO and LUMO levels of electroactive polymers were calculated. It is generally the first experiment performed in electrochemical studies of polymers. Reduction and oxidation peaks of polymers with respect to the applied potential are obtained in

this process. The potential of a stationary working electrode is linearly scanned in a form of triangular wave. The potential applied on the working electrode is controlled versus a reference electrode. The resulting current due to the applied potential is measured [87].

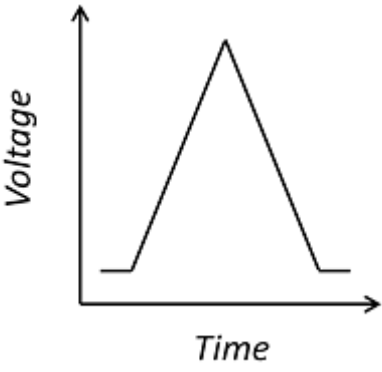


Figure 2. 12. Waveform of potential in CV as a function of time

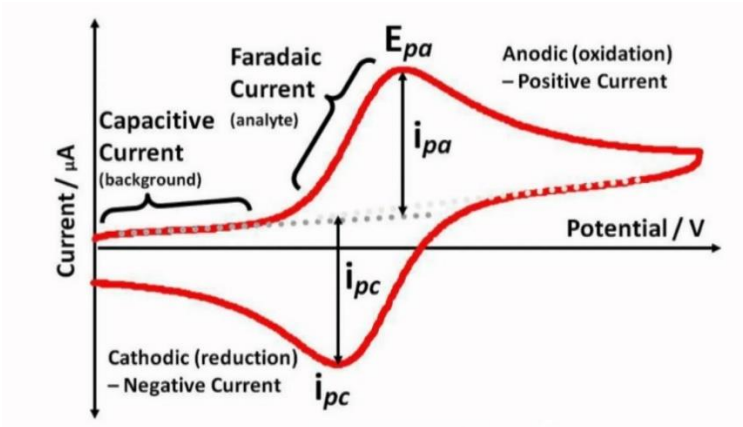


Figure 2. 13. Cyclic voltammogram

In a cyclic voltammogram, i_{pa} stands for anodic peak current which is in fact the maximum current obtained in reduction. And E_{pa} stands for anodic peak potential, and in this case, which is in fact is the maximum potential obtained in reduction. The same case is valid for the lower part of the voltammogram. i_{pc} and E_{pc} are cathodic peak current and cathodic peak potential, respectively. Cyclic voltammetry is performed in a three-electrode system, including a working, a counter and a reference electrode. Employing cyclic voltammetry, reduction and oxidation properties of synthesized polymers were investigated.

2.4.2.2. Spectroelectrochemical Studies

It is a technique that combines electrochemical and spectroscopic performances in a single system providing optical band gap, polaron and bipolaron bands, and the maximum wavelength where the absorbance is maximum by investigating changes in electronic transitions between HOMO and LUMO levels of the polymers.

Upon oxidation of the polymers with a step wisely increasing potential, spectral changes are obtained by a UV-VIS-NIR spectrophotometer. Similarly, this technique is employed in a three electrode system as is the case for cyclic voltammetry.

2.4.2.3. Kinetic Studies

For the investigation of electrochromic switching times and percent transmittance changes, kinetic studies were performed. The technique provides those characteristics at λ_{max} of the polymers, as a function of time. The potential is applied between neutral and oxidized states, repeatedly. The technique includes both spectroscopy and square wave voltammetry [79].

CHAPTER 3

RESULTS AND DISCUSSIONS

3.1. Electrochemical Characterizations

Examination of reduction and oxidation behaviors and determination of HOMO and LUMO levels of the polymer were performed by cyclic voltammetry (CV). Upon dissolving 3 mg polymer in 1 mL of chloroform, the solution was spray coated on a glass substrate coated with indium tin oxide (ITO). The system is a three electrode system. ITO was employed as the working electrode while a platinum and a silver wire were used as counter and reference electrodes, respectively. Electrodes were placed in a cell containing a solution of 0.1 M tetrabutylammonium hexafluorophosphate in acetonitrile (TBAPF₆/ACN). The voltammograms of the polymer were obtained by cycling at a scan rate of 100 mV/s.

3.1.1. Cyclic Voltammetry studies of the polymers

Performances of cyclic voltammetry showed that PSeQCz is ambipolar i.e., showing both p-dopable and n-dopable characteristics. In anodic region, oxidation potential was determined as 1.17 V while the reduction potential was 0.82 V. During the potential application in the cathodic region, two redox peaks were observed. The redox couples were observed at -1.78V / -1.37 V, and at -2.23 V / -1.84 V, respectively. The voltammogram of PSeQCz is represented in Figure 3.1.

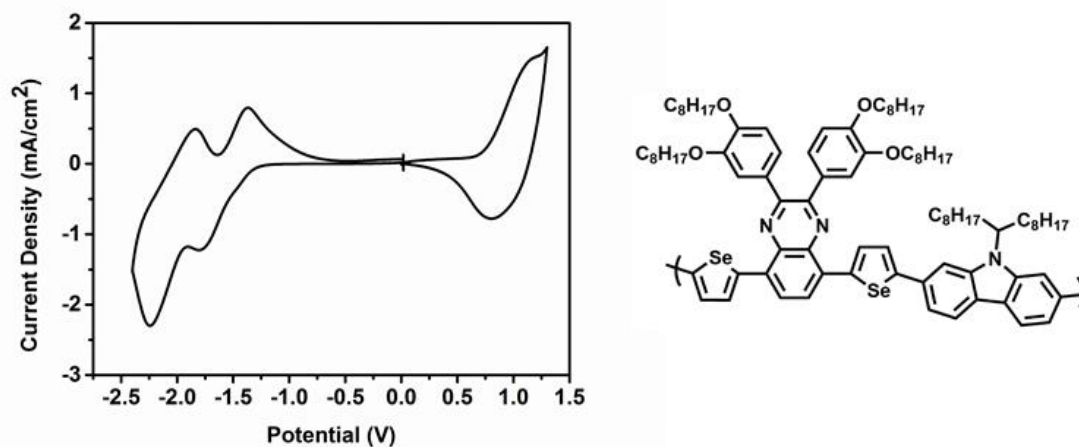


Figure 3. 1. Single scan cyclic voltammogram of PSeQCz in 0.1 M TBAPF₆/ACN solution

HOMO (Highest Occupied Molecular Orbital) and LUMO (Lowest Occupied Molecular Orbital) for PSeQCz were determined using onset oxidation and onset reduction potentials, respectively. Onset redox potentials were obtained from an intersection of the baseline and the tangent to the redox peaks. The following formulas provide energy levels versus vacuum.

$$E_{HOMO} = -(E_{onset,ox} + 4.75) \text{ (eV)}$$

$$E_{LUMO} = -(E_{onset,red} + 4.75) \text{ (eV)}$$

Electronic band gap of PSeQCz was determined from the following equation;

$$E_g^{ec} = HOMO - LUMO \text{ (eV)}$$

From CV studies of PSeQCz, HOMO and LUMO were calculated as -5.45 eV and -3.37 eV, respectively. Inserting those values into the equation, the electronic band gap was determined as 2.08 eV.

Cyclic voltammetry studies of PFiSeQ depicted that the polymer is ambipolar i.e., showing both p-dopable and n-dopable characteristics. In anodic region, during the potential application, oxidation potential was determined as 1.20 V while the reduction potential was 0.69 V. In the cathodic region, two redox peaks were observed. The redox couples were observed at -1.62V / -1.08 V, and at -2.00 V / -1.57 V, respectively. CV voltammogram of PFiSeQ is represented in Figure 3.2.

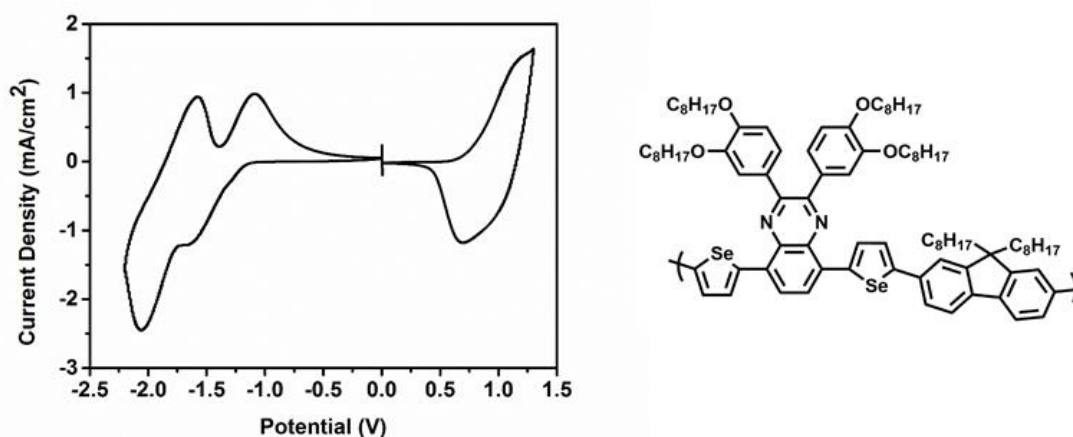


Figure 3. 2. Single scan cyclic voltammogram of PFiSeQ in 0.1 M TBAPF₆/ACN solution

From CV studies of PFiSeQ, HOMO and LUMO were calculated as -5.48 eV and -3.55 eV, respectively. Inserting those values into the equation, the electronic band gap was determined as 1.93 eV.

CV studies showed that PBDTSeQ is ambipolar, showing both p-dopable and n-dopable characteristics. In anodic region, oxidation potential was determined as 1.51 V while the reduction potential was 0.71 V. During the potential application in the cathodic region, two redox peaks were observed. The redox couples were observed at -1.36 V / -1.32 V, and at -2.00 V / -1.51 V, respectively. CV voltammogram of PBDTSeQ is represented in Figure 3.3.

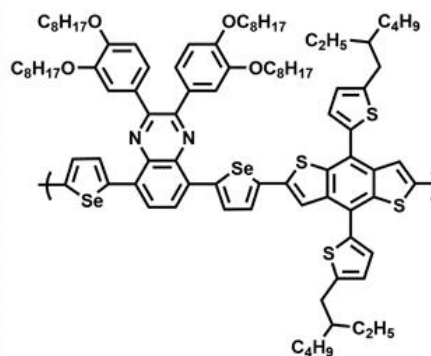
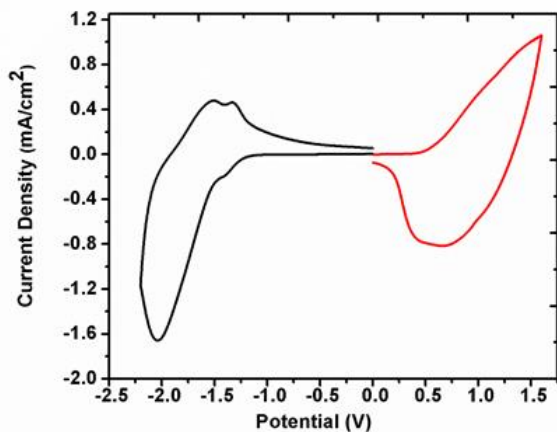


Figure 3. 3. Single scan cyclic voltammogram of PBDTSeQ in 0.1 M TBAPF₆/ACN solution

Investigation of the scan rate dependence was also performed via cyclic voltammetry. Scan rate dependence test proves whether the mass transfer is diffusion controlled or not during the doping and dedoping processes. The test was performed with four different scan rates and a linear graph in Figure 3.4. illustrates that the mass transfer is non-diffusion controlled.

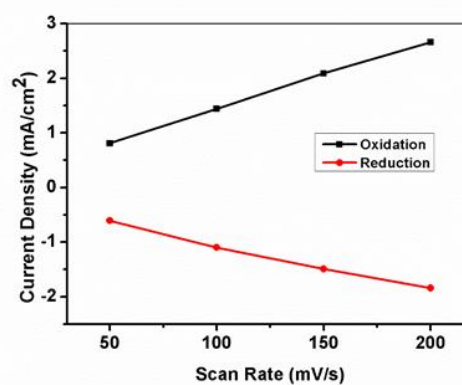
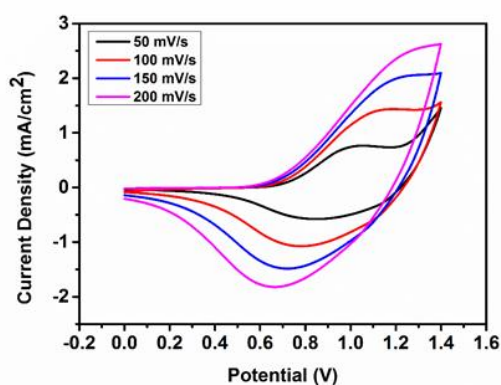


Figure 3. 4. Scan rate dependence of PSeQCz

Scan rate dependence test for PFiSeQ was performed in three different scan rates.

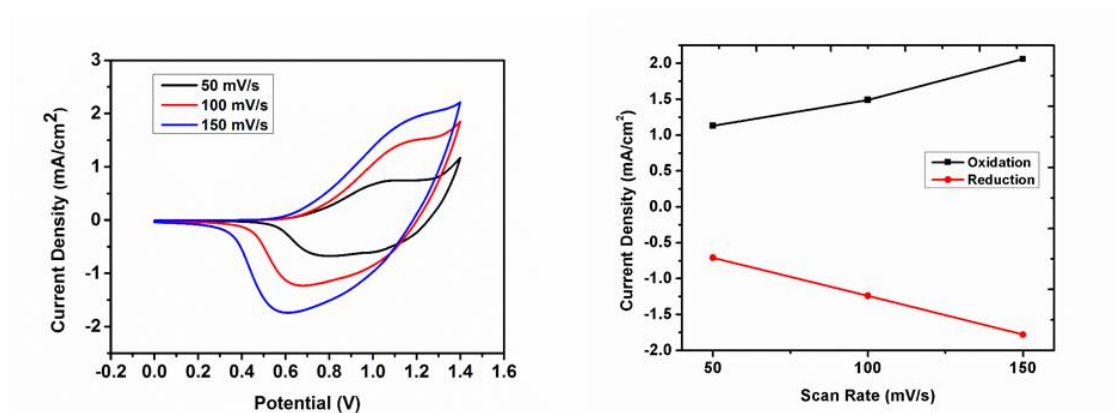


Figure 3. 5. Scan rate dependence of PFiSeQ

Scan rate dependence was performed via cyclic voltammetry and it showed that the mass transfer is non-diffusion controlled. The test was performed in six different scan rates as given by the linear graph in Figure 3.6.

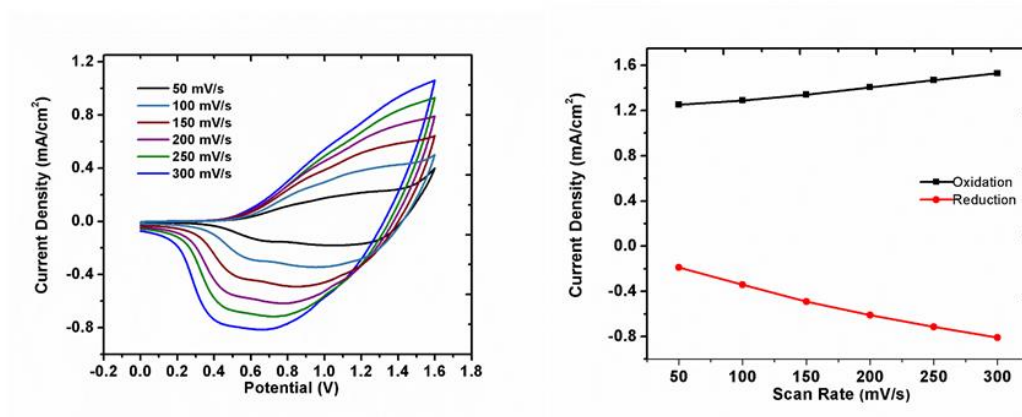


Figure 3. 2. Scan rate dependence of PBDTSeQ

Electrochemical properties of the polymers are represented in Table 1.

Table 1. Electrochemical properties of the polymers

	$E_{p-doping}$ (V)	$E_{p-dedoping}$ (V)	$E_{n-doping}$ (V)	$E_{n-dedoping}$ (V)	HOMO (eV)	LUMO (eV)	E_g^{ec} (eV)
PSeQCz	1.17	0.82	-1.78/-2.23	-1.37/-1.84	-5.45	-3.37	2.08
PFSeQ	1.20	0.69	-1.62/-2.0	-1.08/-1.57	-5.48	-3.55	1.93
PBDTSeQ	1.51	0.71	-1.36/-2.0	-1.32/-1.51	-5.24	-3.61	1.63

3.2. Spectroelectrochemical Characterizations

3.2.1. Spectroelectrochemical studies of the polymers

For the investigation of the optical and electronic changes of the polymer spectroelectrochemical tests were performed. To carry out the spectroelectrochemical studies, 3 mg polymer was dissolved in 1 mL of chloroform, and the solution was spray coated on a glass substrate coated with indium tin oxide (ITO). Obtained films were placed in a cell containing a solution of 0.1 M tetrabutylammonium hexafluorophosphate in acetonitrile (TBAPF₆/ACN), electrolyte/solvent system. In a monomer free system, the polymer film was doped step wise the applied potential.

Absorption changes were recorded as a function of wavelength. A potential range between 0 V and 1.2 V was applied. π - π^* corresponding λ_{max} values for PSeQCz were determined as 380 nm and 565 nm, respectively. The onset absorption values of the polymer, λ_{onset} , were 593 nm and 865nm, respectively.

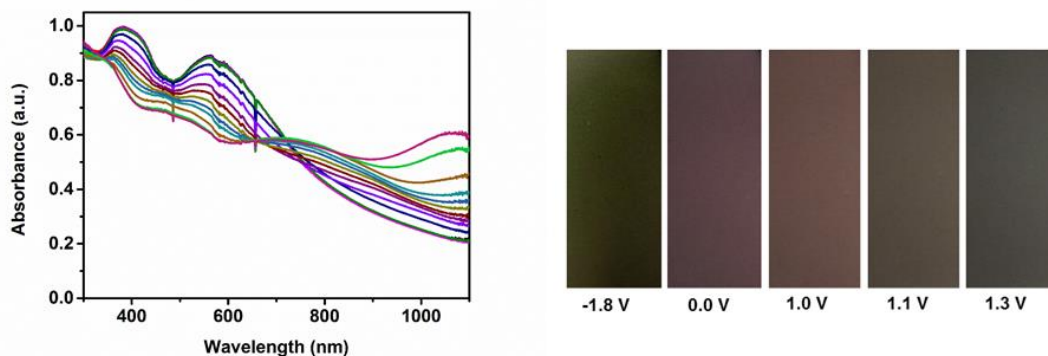
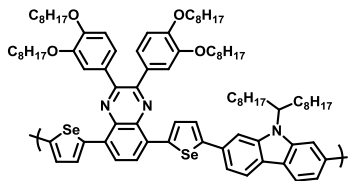


Figure 3.3. Electronic absorption spectra of PSeQCz in 0.1 M TBAPF₆/ACN solution and colors at different potentials

PSeQCz film presented multi chromic behavior. Under different applied potentials, the film exhibited a color range changing between dark green and grey. Table 2. illustrates the calorimetric values of the polymer film. L, a, and b values were defined by Commission Internationale de l'Eclairage (ICE). L stands for luminescence, a stands for red/green coordinate and b stands for yellow/blue coordinate.

Table 2. Colorimetric values of PSeQCz

	Potential (V)	L	a	b
	-1.8	18	-3	18
	0	31	12	3
	1.0	36	10	8
	1.1	35	3	9
	1.3	32	0	5

For PFISeQ, changes in absorption were monitored as a function of wavelength. Applied potential range was between 0 V and 1.2 V. π - π^* corresponding λ_{max} values for PFISeQ were determined as 422 nm and 685 nm, respectively. The onset absorption values of the polymer, λ_{onset} , were 797 nm and 825nm, respectively.

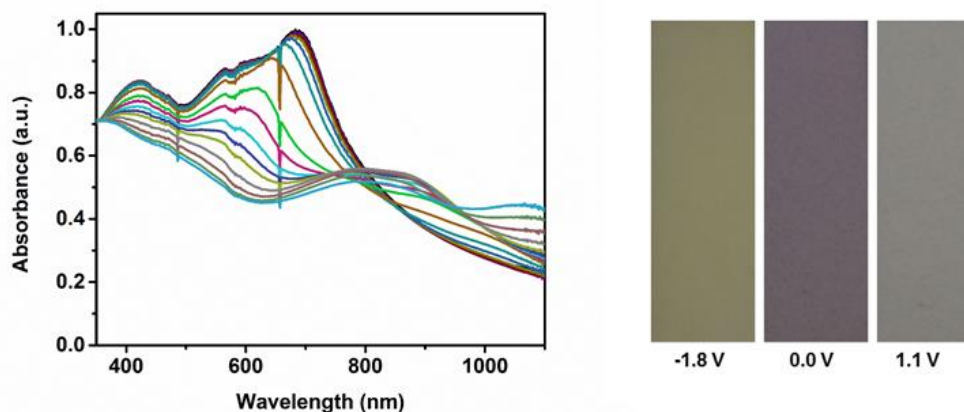
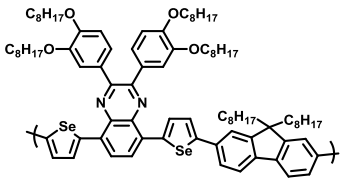


Figure 3. 4. Electronic absorption spectra of PFISeQ in 0.1 M TBAPF₆/ACN solution and colors at different potentials

PFISeQ film presented grey color under 1.1 V potential at oxidation state whereas became yellow/brown under -1.8 V potential at reduction state. Under different applied potentials varying between 0 and 1.2 V, the film possessed the L, a, and b values as illustrated in Table 3.

Table 3. Calorimetric values of PFiSeQ

	Potential (V)	L	a	b
	-1.8	53	-2	18
	0	42	6	-3
	1.1	55	0	3

For the collection of spectra of PBDTSeQ, a potential range was between 0 V and 1.2 V was applied. π - π^* corresponding λ_{\max} values for PBDTSeQ were determined as 445 nm and 615 nm, respectively. The onset absorption values of the polymer, λ_{onset} , were 598 nm and 775 nm, respectively.

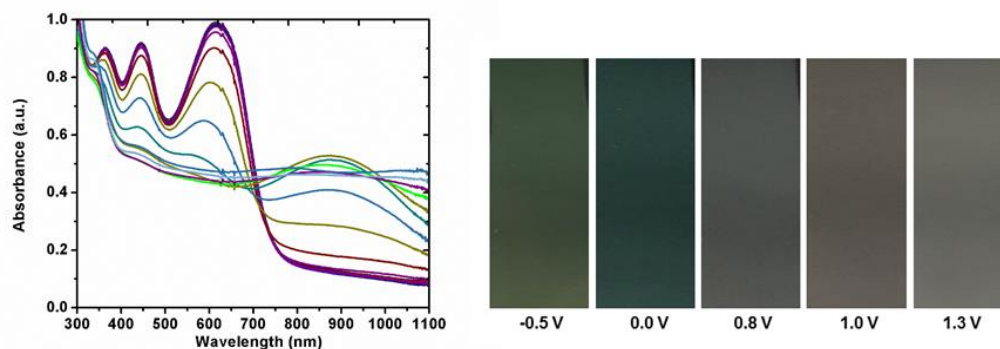
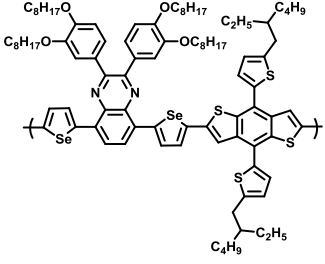


Figure 3. 5. Electronic absorption spectra of PBDTSeQ in 0.1 M TBAPF₆/ACN solution and colors at different potentials

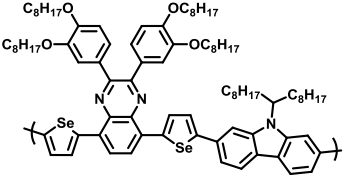
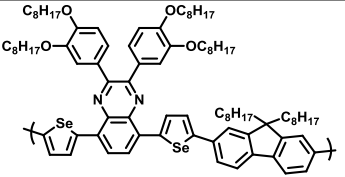
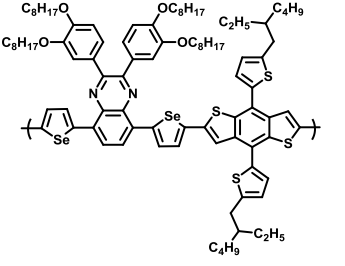
The polymer film showed greyish color under 0.8 V, grey/pink under 1.0 V, and light grey under 1.3 V potential at oxidation state whereas became greenish under -0.5 V potential at reduction state. Under different applied potentials varying between 0 and 1.2 V, the film possessed the L, a, and b values as illustrated in Table 4.

Table 4. Calorimetric values of PBDTSeQ

	Potential (V)	L	a	b
	-0.5	29	-9	8
	0	22	-9	-1
	0.8	33	-2	0
	1.0	34	1	4
	1.3	41	-1	5

The optical band gap of the polymer was calculated from the $E_g^{op} = \frac{hc}{\lambda_{onset}} = 1241/\lambda_{onset}$ formula which provides a result by means of Planck's constant in electron volts. Inserting the λ_{onset} value into the equation, the band gap for PSeQCz, PFISeQ and PBDTSeQ were calculated as 1.43 eV, 1.50 eV and 1.60 eV, respectively.

Table 5. Spectroelectrochemical properties of the polymers

	λ_{max} (nm)	λ_{onset} (nm)	E_g^{op} (eV)
	380/565	593/865	1.43
	422/685	797/825	1.50
	445/615	589/775	1.60

3.3. Kinetic Studies

Optical contrast and switching time of the conjugated polymers were obtained via kinetic studies. In order to conduct kinetic studies, 3 mg of the polymers were dissolved in chloroform and spray coated onto ITO coated glass substrate. The polymer films were placed in a cell which contains 0.1 M TBAPF₆/ACN electrolyte/solvent system. Neutral and fully oxidized state potentials were applied to the polymers in a certain time interval, 5 seconds. Potentials were applied at certain wavelengths specified at UV-Vis near IR spectra of the polymers. Investigation of optical contrast and switching time of the polymers was succeeded by a square wave potential step technique incorporated with UV-Vis spectrophotometer.

3.3.1. Kinetic Studies of the polymers

Percent optical contrast values for PSeQCz were recorded with respect to the specified wavelengths; 595 nm in visible region and 1075 nm in NIR region; respectively. During the potential switch from 0 V to 1.3 V in 5 seconds time interval, UV-Vis spectrophotometer was used to monitor the optical transmittance. Kinetic studies of PSeQCz showed at 595 nm, the percent transmittance change is 14 % with a switching time of 1.4 seconds whereas at 1075 nm it is 30 % with a switching time of 2.2 seconds. Optical transmittance changes at 595 nm and 1075 nm are depicted in Figure 3.10.

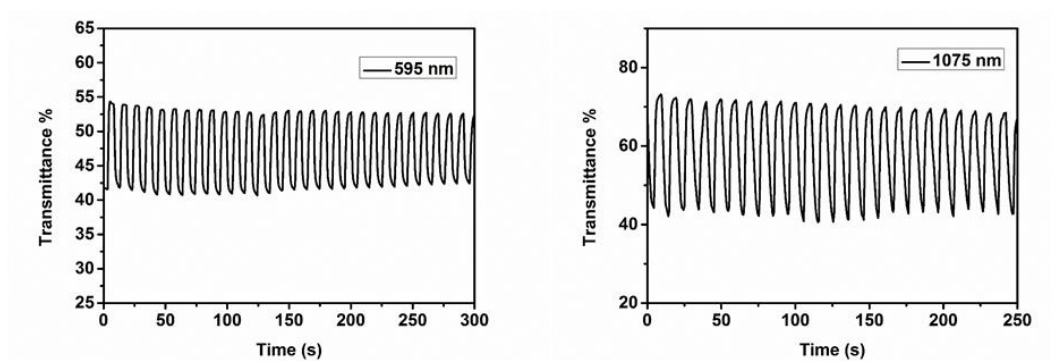


Figure 3. 6. Optical transmittance changes of PSeQCz at 595 nm and 1075 nm

Percent optical contrast values for PFISeQ were recorded at 680 nm in visible region. During the potential switch from 0 V to 1.3 V in 5 seconds time interval, UV-Vis spectrophotometer was used to monitor the optical transmittance. Kinetic studies of PFISeQ showed a percent transmittance change of 27 % with a switching time of 2.1 seconds.

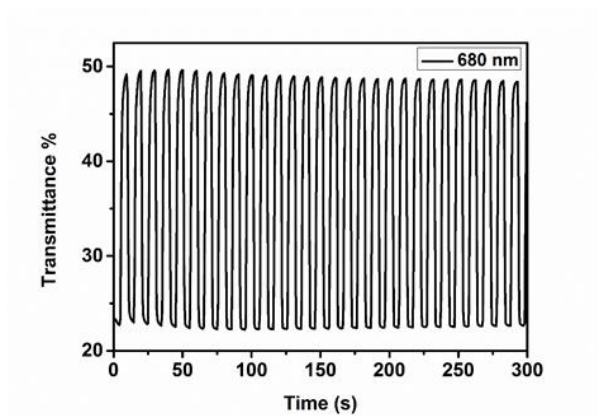


Figure 3. 7. Optical transmittance changes of PFISeQ at 680 nm

Percent optical contrast values of PBDTSeQ were recorded at 445 nm in visible region and 615 nm also in visible region, respectively. The potential switch was conducted from 0 V to 1.6 V in 5 seconds. Kinetic studies of PBDTSeQ revealed a percent transmittance change of 20 % with a switching time of 1.9 seconds at 445 nm while showing a 30 % with a switching time of 2.0 seconds at 615 nm.

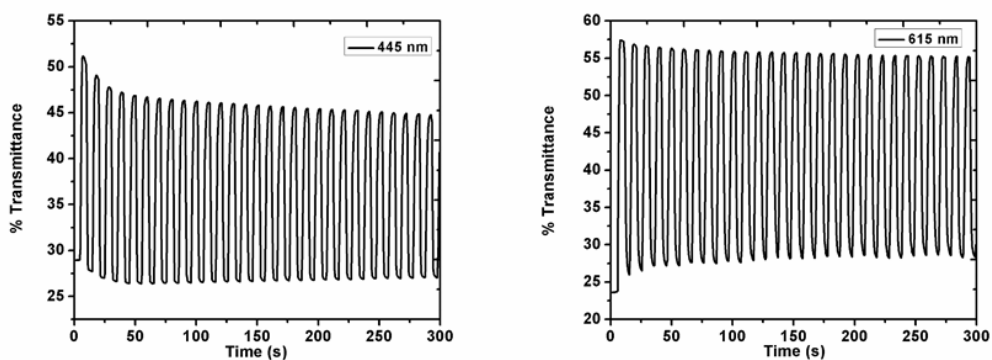


Figure 3. 8. Optical transmittance changes of PBDTSeQ at 445 nm and 615 nm

Summary of the kinetic studies of the polymers are depicted in Table 10.

Al were deposited on these layers as 0.6 nm and 100 nm, respectively. Since PC₇₀BM has a broad range of absorption, it was preferred as the acceptor in polymer:acceptor blend to improve the absorption.

Organic photovoltaics were designed based on the device stack; ITO/PEDOT:PSS/Polymer: PC₇₀BM/LiF/Al architecture. On each ITO coated substrate having a dimension of 2.45 inches, eight solar cells were placed. Characterization of devices was conducted under solar illumination in glove box. The device based on PBDTSeQ:PCBM blend demonstrated the best power conversion efficiency of among all, 4.05 % with a V_{OC} of 0.68 V, a J_{SC} of 13.96 mA/cm², and a FF of 43 %. PFiSeQ:PCBM based device demonstrated a power conversion efficiency of 0.7 % with a V_{OC} of 0.79 V, a J_{SC} of 2.8 mA/cm², and a FF of 32 %. PSeQCz:PCBM based device did not demonstrate any efficiency. This might be because of low molecular weight of the polymer.

Table 7. Photovoltaic properties of PBDTSeQ:PCBM-based OPV

Blend	V _{OC} (V)	J _{SC} (mA/cm ²)	FF (%)	PCE (%)
PBDTSeQ:PCBM (1:3)	0.68	13.96	43	4.05
PBDTSeQ:PCBM (1:3)	0.72	5.33	38	1.49

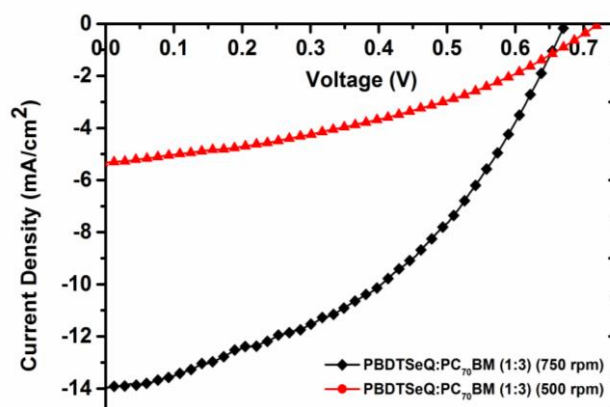


Figure 3.13. J-V curve of of PBDTSeQ:PCBM-based OPV

Table 8. Photovoltaic properties of PFiSeQ:PCBM-based OPV

Blend	V _{oc} (V)	J _{sc} (mA/cm ²)	FF (%)	PCE (%)
PFiSeQ:PCBM (1:2)	0.35	3.69	26	0.33
PFiSeQ:PCBM (1:1.5)	0.79	2.80	31	0.70

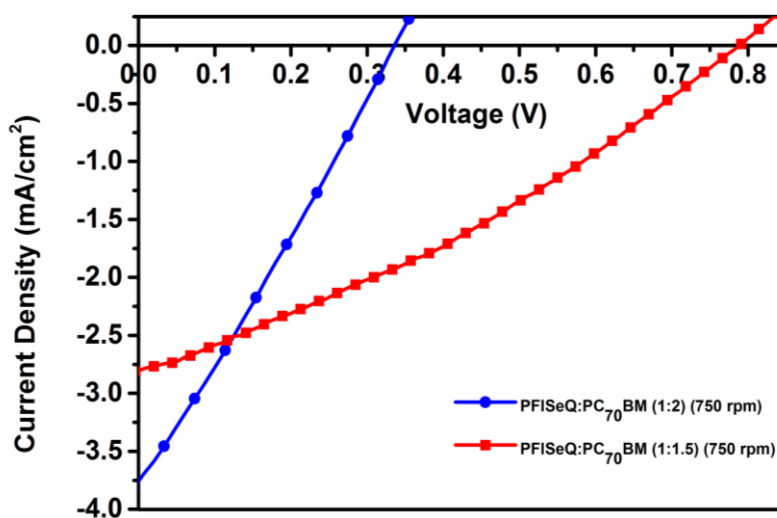


Figure 3.14. J-V curve of PFiSeQ:PCBM-based OPV

CHAPTER 4

CONCLUSIONS

Three novel polymers containing selenophene unit as π -bridge were designed and synthesized via Stille and Suzuki coupling polymerization methods. Selenophene was incorporated into the backbone in order to investigate the changes in optoelectronic properties of the polymers. The polymers were used as photoactive layers in organic photovoltaics following electrochemical, spectroelectrochemical, and kinetic studies.

Cyclic voltammetry studies showed that PSeQCz is ambipolar demonstrating both n and p-dopable characteristics. Electronic band gap of the polymer was determined as 2.08 eV calculated from the difference of HOMO and LUMO levels which are -5.45 eV and -3.37, respectively. Scan rate dependence test which was performed for four different scan rates which proved that the mass transfer is non-diffusion controlled. Cyclic voltammetry studies of PFlSeQ also proved that the polymer has ambipolar characteristics, as well. Electronic band gap was found as 1.93 eV and HOMO and LUMO levels are -5.48 eV and -3.55 eV, respectively. In order to conduct scan rate dependence test three different scan rates were performed and it was proven that the mass transfer is non-diffusion controlled same as the case for PSeQCz. It was figured out that PBDTSeQ is both n and p-dopable. Electronic band gap was determined as 1.63 eV from the difference of HOMO and LUMO levels which are -5.24 eV and -3.61 eV, respectively. Scan rate dependence was performed via six different scan rates and it was proven that the mass transfer is non-diffusion controlled.

In order to determine absorption maxima and optical band gaps of the polymers spectroelectrochemical studies were performed. Studies of PSeQCz depicted that the polymer is multichromic changing its color from neutral state to doped state with varying potential. Absorption maxima for the polymer were determined as 380 nm

and 565 nm, respectively whereas onset absorption values were 593 nm and 865 nm. The optical band gap was found to be 1.43 eV. Spectroelectrochemical studies of PFISeQ revealed that the polymer is multichromic, as well. Absorption maxima were 422 nm and 685 nm while onset values were found to be 797 nm and 825 nm. The optical band gap of the polymer is 1.50 eV. Absorption maxima of PBDTSeQ were 445 nm and 615 nm and the onset values were determined as 589 nm and 775 nm. The optical band gap of the polymer is 1.60 eV. Selenophene bridged polymer resulted in red-shift in the absorption and a lower band gap when compared its analogues bearing thiophene units as π -bridge and this shows consistency with the literature results.

Optical contrasts and switching times of the polymers were calculated via kinetic studies. PSeQCz has a percent transmittance of 14 % at 595 nm with a switching time of 1.4 seconds while having a percent transmittance of 30 % at 1075 nm with a switching time of 2.2 seconds. PFISeQ demonstrated 27 % optical transmittance at 680 nm with a switching time of 2.1 seconds. PBDTSeQ showed 20 % optical transmittance at 445 nm with a switching time of 1.9 seconds and 30 % optical transmittance at 615 nm with a switching time of 2.0 seconds. All polymers demonstrated low band gaps.

The best results were obtained with PBDTSeQ in photovoltaic studies. Polymer:PC₇₀BM with a ratio of 1:3 gave a PCE of 4.05 %, a V_{OC} of 0.68 V, a J_{SC} of 13.96 mA/cm², and a FF of 43 %. PFISeQ resulted in a power conversion efficiency of 0.7 %, a V_{OC} of 0.79 V, a J_{SC} of 2.8 mA/cm², and a FF of 32 % with Polymer:PC₇₀BM with a ratio of 1:1.15. PSeQCz did not result in any efficiency since carbazole bearing polymers generally have low molecular weights. One other reason might be the film morphology of the polymer blend. The relative lower power conversion efficiency of PFISeQ to PBDTSeQ might be a result of low molecular weight and the film morphology as well.

REFERENCES

- [1] Stejskal J, Trchová M, Bober P, Humpolíček P, Kašpárková V, Sapurina I, Shishov M A and Varga M 2015 *Conducting Polymers: Polyaniline*
- [2] Chiang J C and MacDiarmid A G 1986 “Polyaniline”: Protonic acid doping of the emeraldine form to the metallic regime *Synth. Met.* **13** 193–205
- [3] Walatka V V., Labes M M and Perlstein J H 1973 Polysulfur Nitride—a One-Dimensional Chain with a Metallic Ground State *Phys. Rev. Lett.* **31** 1139–42
- [4] Banister A J and Gorrell I B 1998 Poly(sulfur nitride): The First Polymeric Metal *Adv. Mater.* **10** 1415–29
- [5] Facchetti A 2011 π -Conjugated polymers for organic electronics and photovoltaic cell applications *Chem. Mater.* **23** 733–58
- [6] Chiang C K, Fincher C R, Park Y W, Heeger A J, Shirakawa H, Louis E J, Gau S C and MacDiarmid A G 1977 Electrical conductivity in doped polyacetylene *Phys. Rev. Lett.* **39** 1098–101
- [7] Brown A R, Bradley D D C, Burroughes J H, Friend R H, Greenham N C, Burn P L, Holmes A B and Kraft A M 1992 Light-emitting diodes based on conjugated polymers *Conduct. Polym. Their Appl. IEE Colloq.* **3472/1-2/4**
- [8] Kaur G, Adhikari R, Cass P, Bown M and Gunatillake P 2015 Electrically conductive polymers and composites for biomedical applications *RSC Adv.* **5** 37553–67
- [9] Reddinger J L and Reynolds J R 1999 Molecular Engineering of nonconjugated Polymers
- [10] Cheng Y J 2009 Synthesis of conjugated polymers for organic solar cell applications *Chem. Rev.* **109** 5868–923

- [11] Bundgaard E and Krebs F C 2007 Low band gap polymers for organic photovoltaics *Sol. Energy Mater. Sol. Cells* **91** 954–85
- [12] Havinga E E, ten Hoeve W and Wynberg H 1993 Alternate donor-acceptor small-band-gap semiconducting polymers; Polysquaraines and polycroconaines *Synth. Met.* **55** 299–306
- [13] Liu C, Wang K, Gong X and Heeger A J 2016 Low bandgap semiconducting polymers for polymeric photovoltaics *Chem. Soc. Rev.* **45** 4825–46
- [14] Skotheim T A and Reynolds J R 2007 *Handbook of Conducting Polymers: Conjugated Polymers Processing and Applications*
- [15] Novák P, Müller K, Santhanam K S V. and Haas O 1997 Electrochemically Active Polymers for Rechargeable Batteries *Chem. Rev.* **97** 207–82
- [16] Snook G A, Kao P and Best A S 2011 Conducting-polymer-based supercapacitor devices and electrodes *J. Power Sources* **196** 1–12
- [17] Muench S, Wild A, Friebe C, Huppler B, Janoschka T and Schubert U S 2016 Polymer-Based Organic Batteries *Chem. Rev.* **116** 9438–84
- [18] Song H K and Palmore G T R 2006 Redox-active polypyrrole: Toward polymer-based batteries *Adv. Mater.* **18** 1764–8
- [19] Mohammadi A 1985 Properties of Polypyrrole-Electrolyte-Polypyrrole Cells Filter paper humidified **133** 947–9
- [20] Pope M, Kallmann H P and Magnante P 1963 Electroluminescence in Organic Crystals *J. Chem. Phys.* **38** 2042–3
- [21] Tang C W and Vanslyke S A 1987 Organic electroluminescent diodes *Appl. Phys. Lett.* **51** 913–5
- [22] Mitschke U and Bäuerle P 2000 The electroluminescence of organic materials *J. Mater. Chem.* **10** 1471–507

- [23] Meerheim R, Lüssem B and Leo K 2009 Efficiency and stability of p-i-n type organic light emitting diodes for display and lighting applications *Proc. IEEE* **97** 1606–26
- [24] Bender V C, Marchesan T B and Alonso J M 2015 Solid-State Lighting: A Concise Review of the State of the Art on LED and OLED Modeling *IEEE Ind. Electron. Mag.* **9** 6–16
- [25] Tang C W 1986 Two-layer organic photovoltaic cell *Appl. Phys. Lett.* **48** 183–5
- [26] Tipnis R, Bernkopf J, Jia S, Krieg J, Li S, Storch M and Laird D 2009 Large-area organic photovoltaic module-Fabrication and performance *Sol. Energy Mater. Sol. Cells* **93** 442–6
- [27] Hu Z, Zhang J, Xiong S and Zhao Y 2012 Performance of polymer solar cells fabricated by dip coating process *Sol. Energy Mater. Sol. Cells* **99** 221–5
- [28] Galagan Y, Coenen E W C, Sabik S, Gorter H H, Barink M, Veenstra S C, Kroon J M, Andriessen R and Blom P W M 2012 Evaluation of ink-jet printed current collecting grids and busbars for ITO-free organic solar cells *Sol. Energy Mater. Sol. Cells* **104** 32–8
- [29] Yu G, Gao J, Hummelen J C, Wudl F and Heeger A J 1995 Polymer Photovoltaic Cells: Enhanced Efficiencies via a Network of Internal Donor-Acceptor Heterojunctions *Science (80-.)*. **270** 1789–91
- [30] Günes S, Neugebauer H and Sariciftci N S 2007 Conjugated polymer-based organic solar cells *Chem. Rev.* **107** 1324–38
- [31] Piliago C and Loi M A 2012 Charge transfer state in highly efficient polymer–fullerene bulk heterojunction solar cells *J. Mater. Chem.* **22** 4141
- [32] Sugiyama K, Ishii H, Ouchi Y and Seki K 2000 Dependence of indium–tin–oxide work function on surface cleaning method as studied by ultraviolet and

- x-ray photoemission spectroscopies *J. Appl. Phys.* **87** 295–8
- [33] Qi B and Wang J 2013 Fill factor in organic solar cells *Phys. Chem. Chem. Phys.* **15** 8972
- [34] Koch N 2007 Organic electronic devices and their functional interfaces *ChemPhysChem* **8** 1438–55
- [35] Koizumi Y, Shida N, Ohira M, Nishiyama H, Tomita I and Inagi S 2016 Electropolymerization on wireless electrodes towards conducting polymer microfibre networks *Nat. Commun.* **7** 10404
- [36] Inagi S and Fuchigami T 2014 Electrochemical post-functionalization of conducting polymers *Macromol. Rapid Commun.* **35** 854–67
- [37] Inagaki T, Hunter M, Yang X Q, Skotheim T A, Lee H S and Okamoto Y 1988 Electrochemical Polymerization of Pyrrole Derivatives *Mol. Cryst. Liq. Cryst. Inc. Nonlinear Opt.* **160** 79–88
- [38] Kanazawa K K, Diaz A F, Geiss R H, Gill W D, Kwak J F, Logan J A, Rabolt J F and Street G B 1979 “Organic metals”: polypyrrole, a stable synthetic “metallic” polymer *J. Chem. Soc., Chem. Commun.* 854–5
- [39] Heinze J 1990 Electronically conducting polymers *Electrochem. IV* **152** 1–47
- [40] Walton D J 1990 Electrically conducting polymers *Mater. Des.* **11** 142–52
- [41] Bott R 2014 *Conducting polymers book*
- [42] Vorotyntsev M A, Zinovyeva V A and Konev D V. 2010 Mechanisms of Electropolymerization and Redox Activity: Fundamental Aspects *Electropolymerization Concepts, Mater. Appl.* 27–50
- [43] Myers R E 1986 Chemical oxidative polymerization as a synthetic route to electrically conducting polypyrroles *J. Electron. Mater.* **15** 61–9
- [44] Abu-Thabit N Y 2016 Chemical Oxidative Polymerization of Polyaniline: A

Practical Approach for Preparation of Smart Conductive Textiles *J. Chem. Educ.* **93** 1606–11

- [45] Stille J K 1986 The Palladium-Catalyzed Cross-Coupling Reactions of Organotin Reagents with Organic Electrophiles *Angew. Chemie Int. Ed.* **25** 508–24
- [46] Carsten B, He F, Son H J, Xu T and Yu L 2011 Stille polycondensation for synthesis of functional materials *Chem. Rev.* **111** 1493–528
- [47] Miyaura N and Yamada K 1979 Our Continuous Discovered *Tet. Lett.* 3437–40
- [48] Akihiro Yokoyama †, Hirofumi Suzuki †, Yasuhiro Kubota ‡, Kazuei Ohuchi ‡, Hideyuki Higashimura *,‡ and and Tsutomu Yokozawa* † 2007 Chain-Growth Polymerization for the Synthesis of Polyfluorene via Suzuki–Miyaura Coupling Reaction from an Externally Added Initiator Unit 7236–7
- [49] Lennox A J J and Lloyd-Jones G C 2014 Selection of boron reagents for Suzuki–Miyaura coupling *Chem. Soc. Rev.* **43** 412–43
- [50] Sonogashira K, Tohda Y and Hagihara N 1975 A convenient synthesis of acetylenes: Catalytic substitutions of acetylenic hydrogen with bromoalkenes, iodoarenes, and bromopyridines *Tetrahedron Lett.* **16** 4467–70
- [51] Melchor M G 2013 *A Theoretical Study of Pd-Catalyzed C – C Cross-Coupling Reactions*
- [52] Wang D and Gao S 2014 Sonogashira coupling in natural product synthesis *Org. Chem. Front.* **1** 556
- [53] Mizoroki T, Mori K and Ozaki A 1971 Arylation of Olefin with Aryl Iodide Catalyzed by Palladium *Bull. Chem. Soc. Jpn.* **44** 581–581
- [54] Heck R F and Nolley J P 1972 Palladium-catalyzed vinylic hydrogen

- substitution reactions with aryl, benzyl, and styryl halides *J. Org. Chem.* **37** 2320–2
- [55] Beletskaya I P and Cheprakov A V. 2000 Heck reaction as a sharpening stone of palladium catalysis *Chem. Rev.* **100** 3009–66
- [56] Forrest S R 2004 The path to ubiquitous and low-cost organic electronic appliances on plastic *Nature* **428** 911–8
- [57] Brandt R G, Yue W, Andersen T R, Larsen-Olsen T T, Hinge M, Bundgaard E, Krebs F C and Yu D 2015 An isoindigo containing donor–acceptor polymer: synthesis and photovoltaic properties of all-solution-processed ITO- and vacuum-free large area roll-coated single junction and tandem solar cells *J. Mater. Chem. C* **3** 1633–9
- [58] Dou L, Liu Y, Hong Z, Li G and Yang Y 2015 Low-Bandgap Near-IR Conjugated Polymers/Molecules for Organic Electronics *Chem. Rev.* **115** 12633–65
- [59] Huo L and Hou J 2011 Benzo[1,2-b:4,5-b']dithiophene-based conjugated polymers: band gap and energy level control and their application in polymer solar cells *Polym. Chem.* **2** 2453
- [60] Boborodea A and Brookes A 2017 Gel permeation chromatography – Atmospheric pressure chemical ionization – Mass spectrometry for characterization of polymer additives *Int. J. Polym. Anal. Charact.* **22** 210–4
- [61] Heeney M, Zhang W, Crouch D J, Chabinye M L, Gordeyev S, Hamilton R, Higgins S J, McCulloch I, Skabara P J, Sparrowe D and Tierney S 2007 Regioregular poly(3-hexyl)selenophene: a low band gap organic hole transporting polymer. *Chem. Commun. (Camb)*. 5061–3
- [62] Kronemeijer A J, Gili E, Shahid M, Rivnay J, Salleo A, Heeney M and Sirringhaus H 2012 A selenophene-based low-bandgap donor-acceptor

- polymer leading to fast ambipolar logic *Adv. Mater.* **24** 1558–65
- [63] Kang I, An T K, Hong J A, Yun H J, Kim R, Chung D S, Park C E, Kim Y H and Kwon S K 2013 Effect of selenophene in a DPP copolymer incorporating a vinyl group for high-performance organic field-effect transistors *Adv. Mater.* **25** 524–8
- [64] Shahid M, McCarthy-Ward T, Labram J, Rossbauer S, Domingo E B, Watkins S E, Stingelin N, Anthopoulos T D and Heeney M 2012 Low band gap selenophene–diketopyrrolopyrrole polymers exhibiting high and balanced ambipolar performance in bottom-gate transistors *Chem. Sci.* **3** 181
- [65] Saadeh H a, Lu L, He F, Bullock J E, Wang W, Carsten B and Yu L 2012 Polyselenopheno 3,4-b selenophene for Highly Efficient Bulk Heterojunction Solar Cells *ACS Macro Lett.* **1** 361–5
- [66] Fei Z, Han Y, Gann E, Hodsdon T, Chesman A S R, McNeill C R, Anthopoulos T D and Heeney M 2017 Alkylated Selenophene-Based Ladder-Type Monomers via a Facile Route for High-Performance Thin-Film Transistor Applications *J. Am. Chem. Soc.* **139** 8552–61
- [67] Liao S H, Jhuo H J, Cheng Y S and Chen S A 2013 Fullerene derivative-doped zinc oxide nanofilm as the cathode of inverted polymer solar cells with low-bandgap polymer (PTB7-Th) for high performance *Adv. Mater.* **25** 4766–71
- [68] Pan H, Li Y, Wu Y, Liu P, Ong S, Zhu S and Xu G 2007 Polymer Semiconductors for Thin-Film Transistors *Semiconductors* 4112–3
- [69] Wang H, Shi Q, Lin Y, Fan H, Cheng P, Zhan X, Li Y and Zhu D 2011 Conjugated Polymers Based on a New Building Block: Dithienophthalimide *Macromol. (Washington, DC, U. S.)* **44** 4213–21
- [70] Hou J, Park M, Zhang S, Yao Y, Chen L, Li J and Yang Y 2008 Bandgap and

- Molecular Energy Level Control of Conjugated Polymer Photovoltaic Materials Based on Benzo [1 , 2-b : 4 , 5-b '] dithiophene *Society* 6012–8
- [71] Chuang H-Y, Hsu S-C, Lee P-I, Lee J-F, Huang S-Y, Lin S-W and Lin P-Y 2014 Synthesis and properties of a new conjugated polymer containing benzodithiophene for polymer solar cells *Polym. Bull.* **71** 1117–30
- [72] Ye L, Zhang S Q, Huo L J, Zhang M J and Hou J H 2014 Molecular Design toward Highly Efficient Photovoltaic Polymers Based on Two-Dimensional Conjugated Benzodithiophene *Acc. Chem. Res.* **47** 1595–603
- [73] Hu T, Han L, Xiao M, Bao X, Wang T, Sun M and Yang R 2014 Enhancement of photovoltaic performance by increasing conjugation of the acceptor unit in benzodithiophene and quinoxaline copolymers † *J. Mater. Chem. C Mater. Opt. Electron. devices* **0** 1–7
- [74] Song K W, Lee T H, Ko E J, Back K H and Moon D K 2014 Polymer solar cells based on quinoxaline and dialkylthienyl substituted benzodithiophene with enhanced open circuit voltage *J. Polym. Sci. Part A Polym. Chem.* **52** 1028–36
- [75] Kitazawa D, Watanabe N, Yamamoto S and Tsukamoto J 2009 Quinoxaline-based ??-conjugated donor polymer for highly efficient organic thin-film solar cells *Appl. Phys. Lett.* **95** 5–8
- [76] Kitazawa D, Watanabe N, Yamamoto S and Tsukamoto J 2012 Conjugated polymers based on quinoxaline for polymer solar cells *Sol. Energy Mater. Sol. Cells* **98** 203–7
- [77] Zhou E, Cong J, Tajima K and Hashimoto K 2010 Synthesis and photovoltaic properties of donor-acceptor copolymers based on 5,8-dithien-2-yl-2,3-diphenylquinoxaline *Chem. Mater.* **22** 4890–5
- [78] Lee S K, Lee W H, Cho J M, Park S J, Park J U, Shin W S, Lee J C, Kang I N

- and Moon S J 2011 Synthesis and photovoltaic properties of quinoxaline-based alternating copolymers for high-efficiency bulk-heterojunction polymer solar cells *Macromolecules* **44** 5994–6001
- [79] Kutkan S, Goker S, Hacıoglu S O and Toppare L 2016 Syntheses, electrochemical and spectroelectrochemical characterization of benzothiadiazole and benzoselenadiazole based random copolymers *J. Macromol. Sci. Part A* **53** 475–83
- [80] Li Y, Ko S-J, Park S Y, Choi H, Nguyen T L, Uddin M A, Kim T, Hwang S, Kim J Y and Woo H Y 2016 Quinoxaline–thiophene based thick photovoltaic devices with an efficiency of ~8% *J. Mater. Chem. A* **4** 9967–76
- [81] Durmus A, Gunbas G E and Toppare L 2007 New, Highly Stable Electrochromic Polymers from 3,4-Ethylenedioxythiophene−Bis-Substituted Quinoxalines toward Green Polymeric Materials *Chem. Mater.* **19** 6247–51
- [82] Istanbuluoglu C, Göker S, Hizalan G, Hacıoglu S O, Udum Y A, Yildiz E D, Cirpan A and Toppare L 2015 Synthesis of a benzotriazole bearing alternating copolymer for organic photovoltaic applications *New J. Chem.* **39** 6623–30
- [83] Zhang J, Cai W, Huang F, Wang E, Zhong C, Liu S, Wang M, Duan C, Yang T and Cao Y 2011 Synthesis of quinoxaline-based donor-acceptor narrow-band-gap polymers and their cyclized derivatives for bulk-heterojunction polymer solar cell applications *Macromolecules* **44** 894–901
- [84] Goker S, Hizalan G, Kutkan S, Arslan Udum Y, Cirpan A and Toppare L 2016 Incorporation of different conjugated linkers into low band gap polymers based on 5,6-Bis(octyloxy)-2,1,3 benzooxadiazole for tuning optoelectronic properties *J. Polym. Sci. Part A Polym. Chem.* **54** 2459–67
- [85] Grubisic Z, Rempp P and Benoit H 1969 A Universal Calibration for Gel Permeation Chromatography *Rubber Chem. Technol.* **42** 636–40

- [86] Moore J C 1964 Gel permeation chromatography. I. A new method for molecular weight distribution of high polymers *J. Polym. Sci. Part A Gen. Pap.* **2** 835–43
- [87] Bocarsly A B 2012 Cyclic Voltammetry *Charact. Mater.* 702–6

APPENDIX
NMR SPECTRA

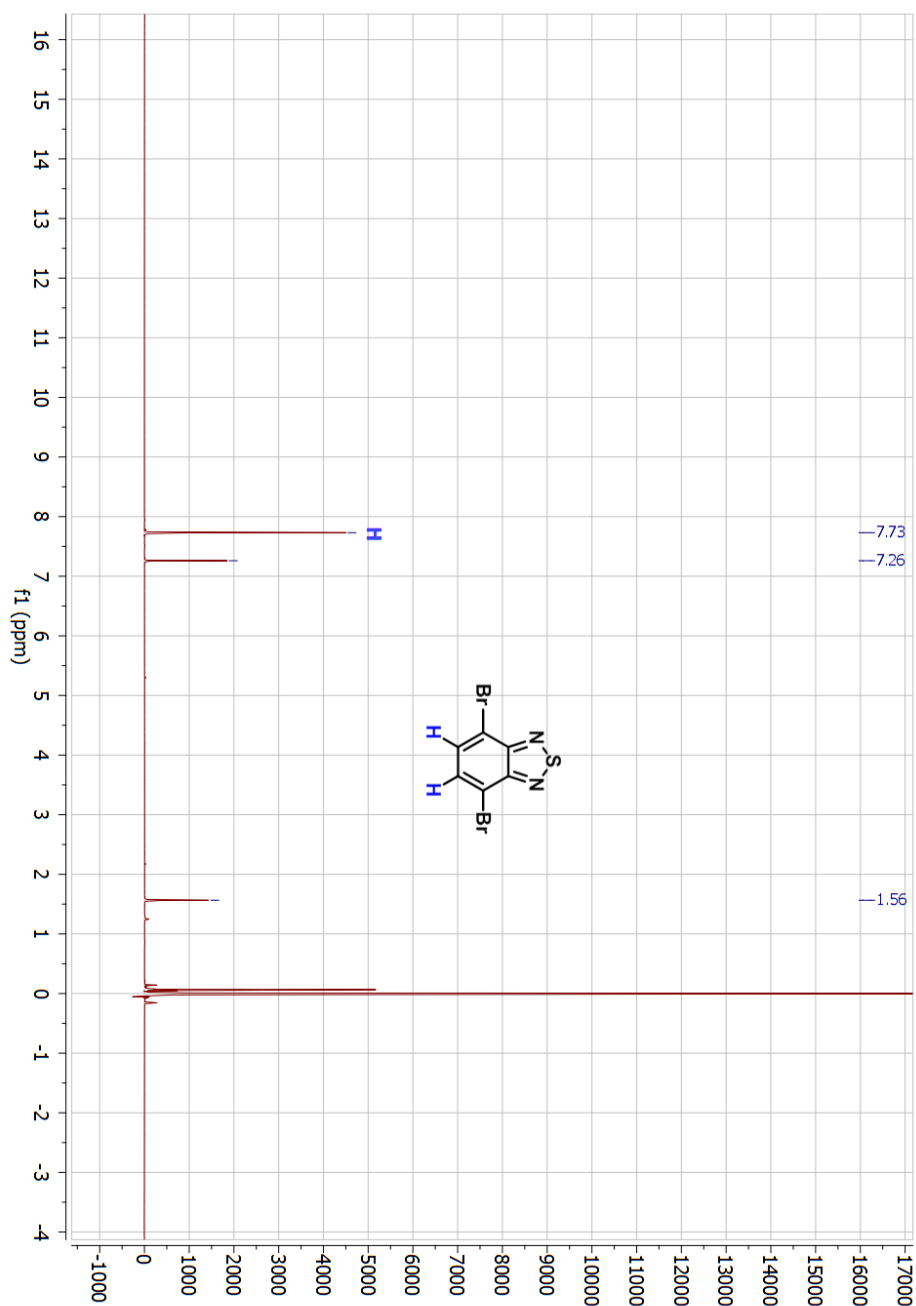


Figure A 1. ¹H-NMR spectrum of 4,7- dibromobenzo[c][1,2,5]thiadiazole

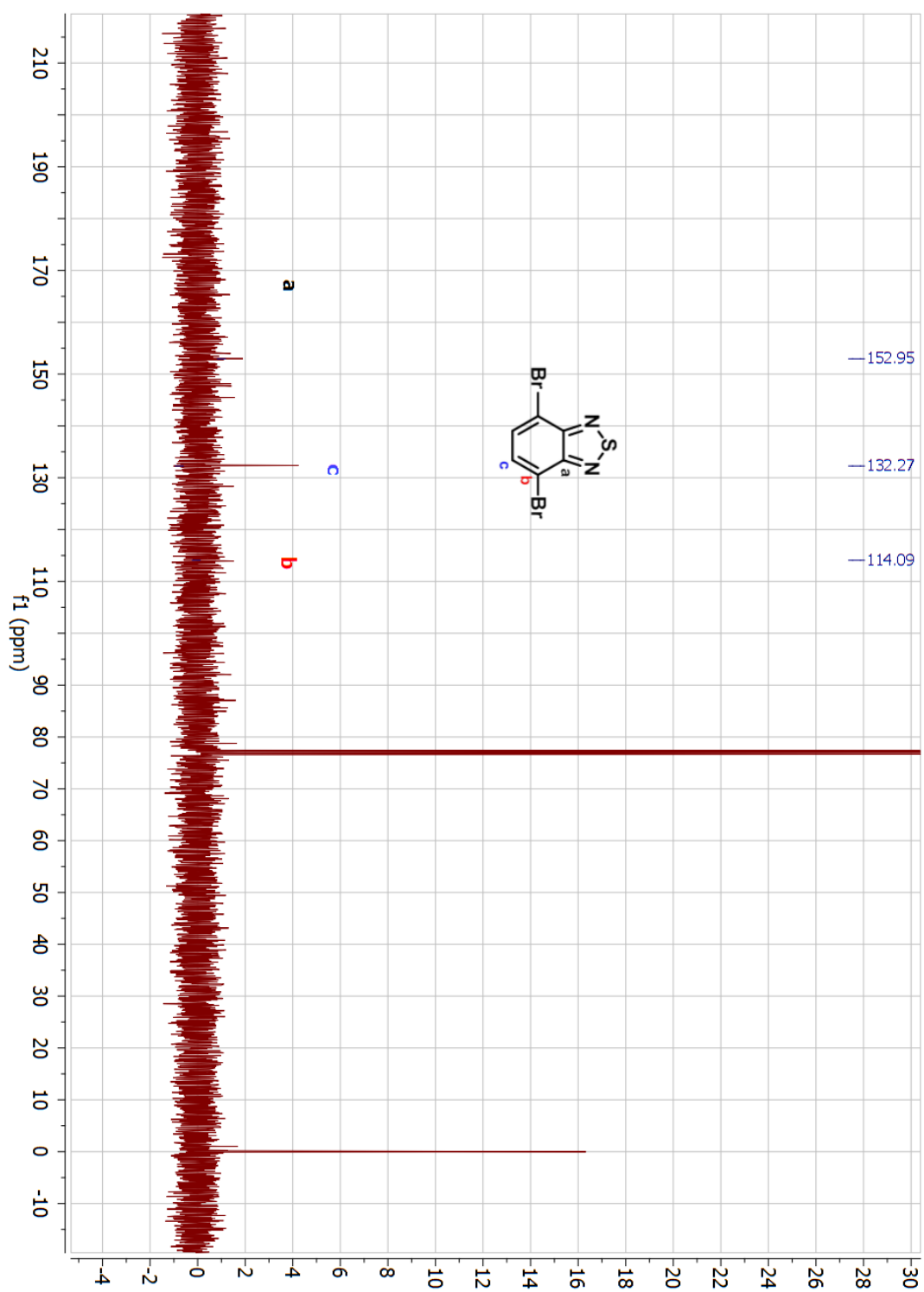


Figure A 2. ^{13}C -NMR spectrum of 4,7- dibromobenzo[c][1,2,5]thiadiazole

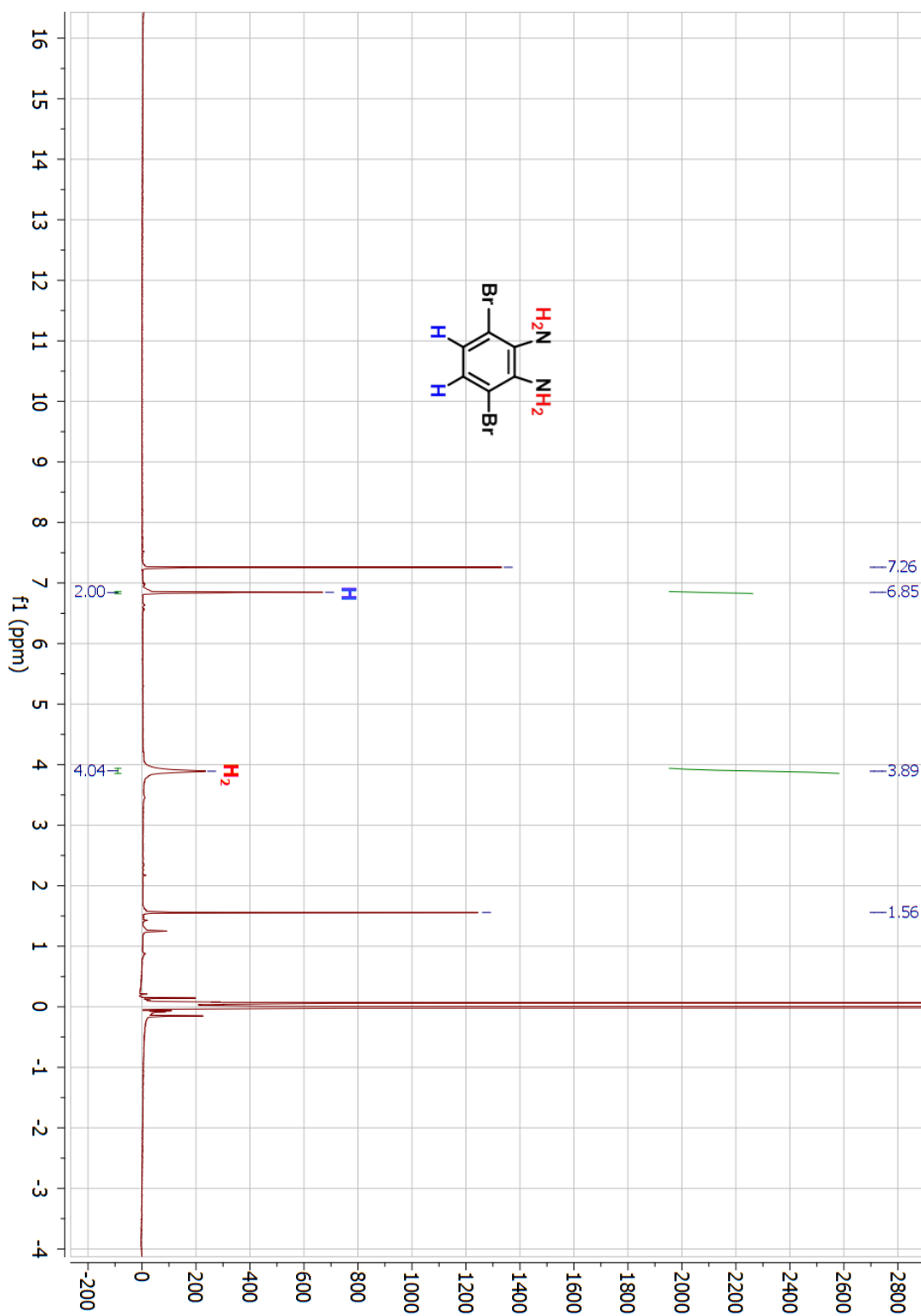


Figure A 3. $^1\text{H-NMR}$ spectrum of 3,6-dibromobenzene-1,2-diamine

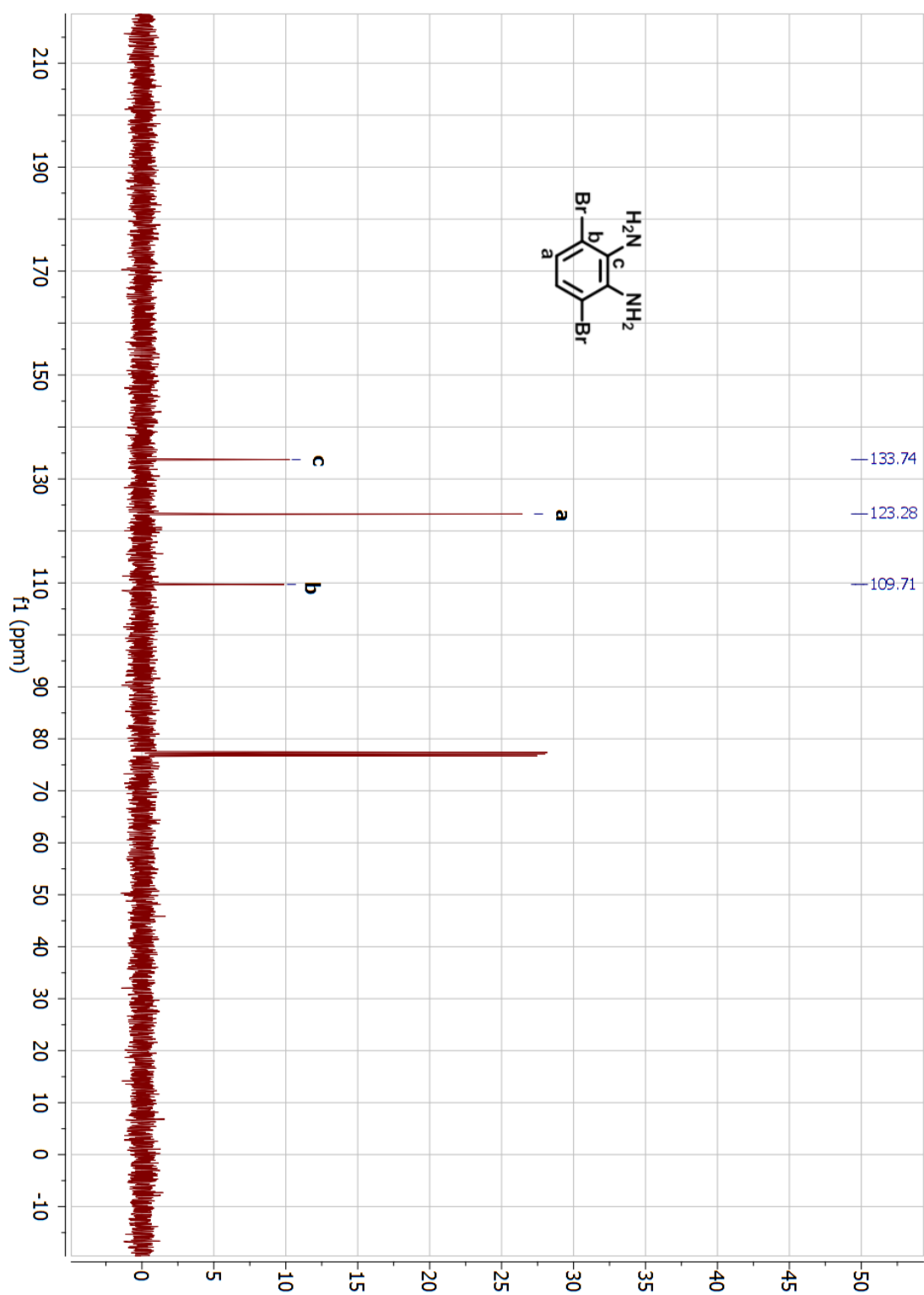


Figure A 4. ^{13}C -NMR spectrum of 3,6-dibromobenzene-1,2-diamine

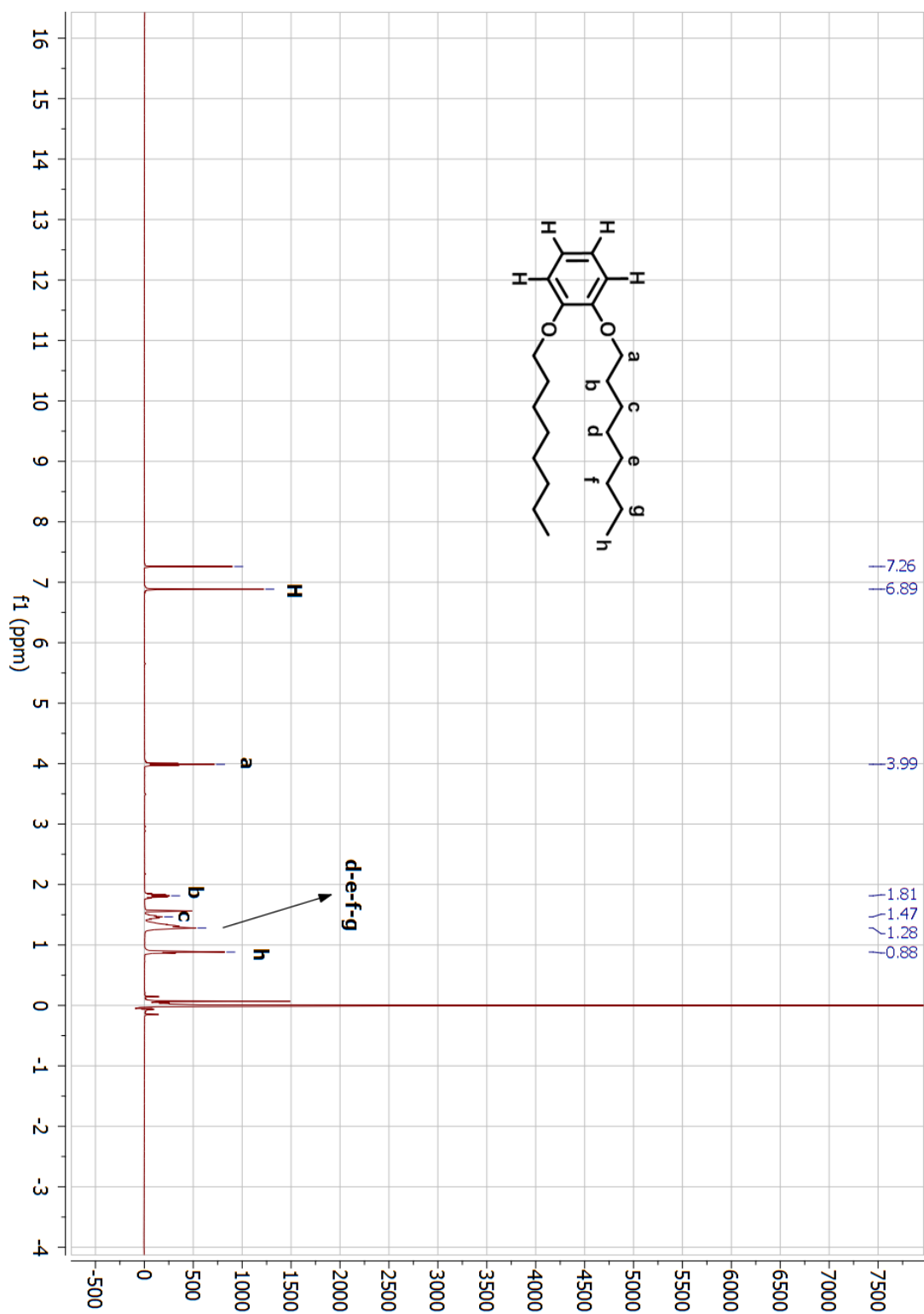


Figure A 5. $^1\text{H-NMR}$ spectrum of 1,2-bis(octyloxy)benzene

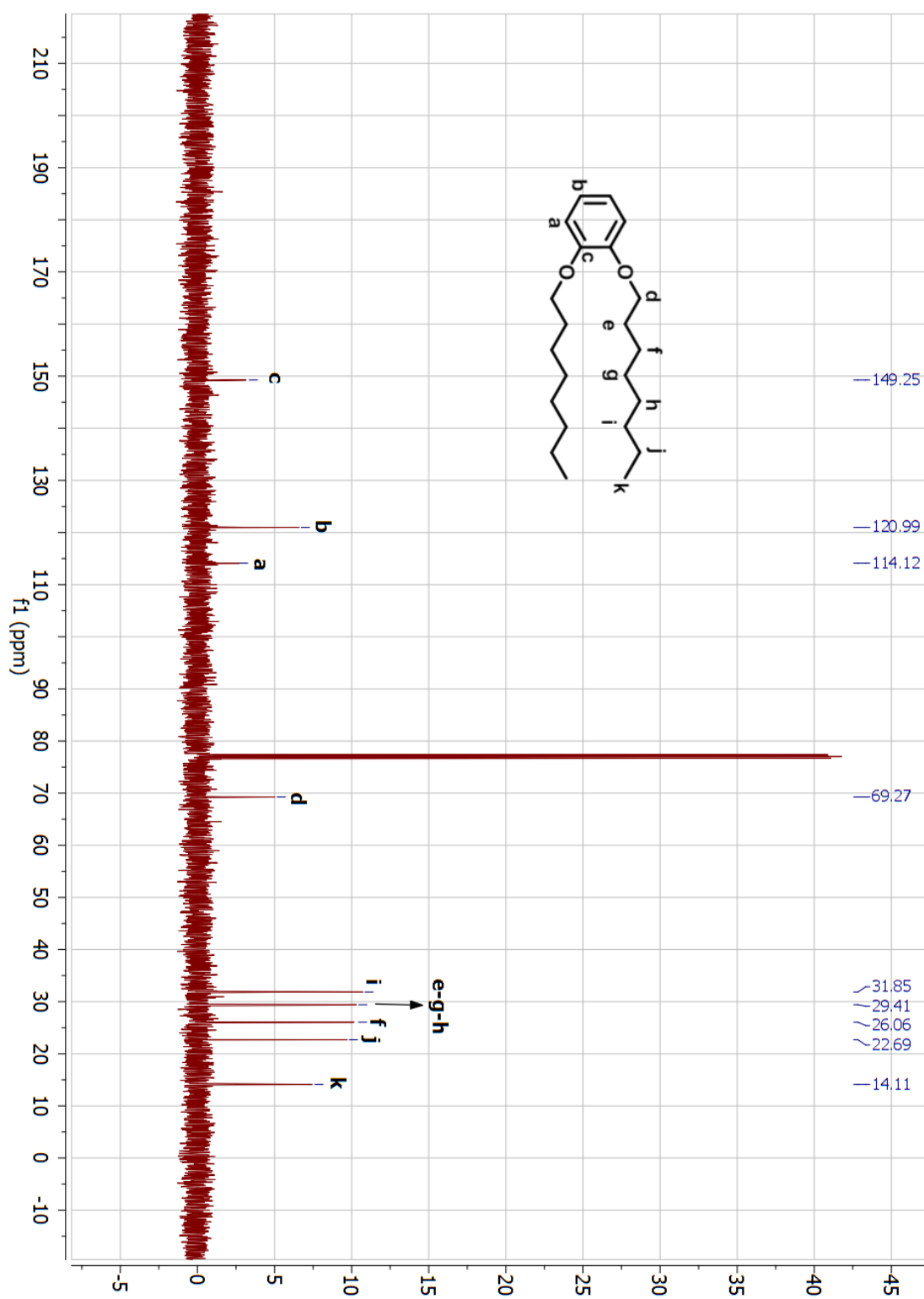


Figure A 6. ¹³C-NMR spectrum of 1,2-bis(octyloxy)benzene

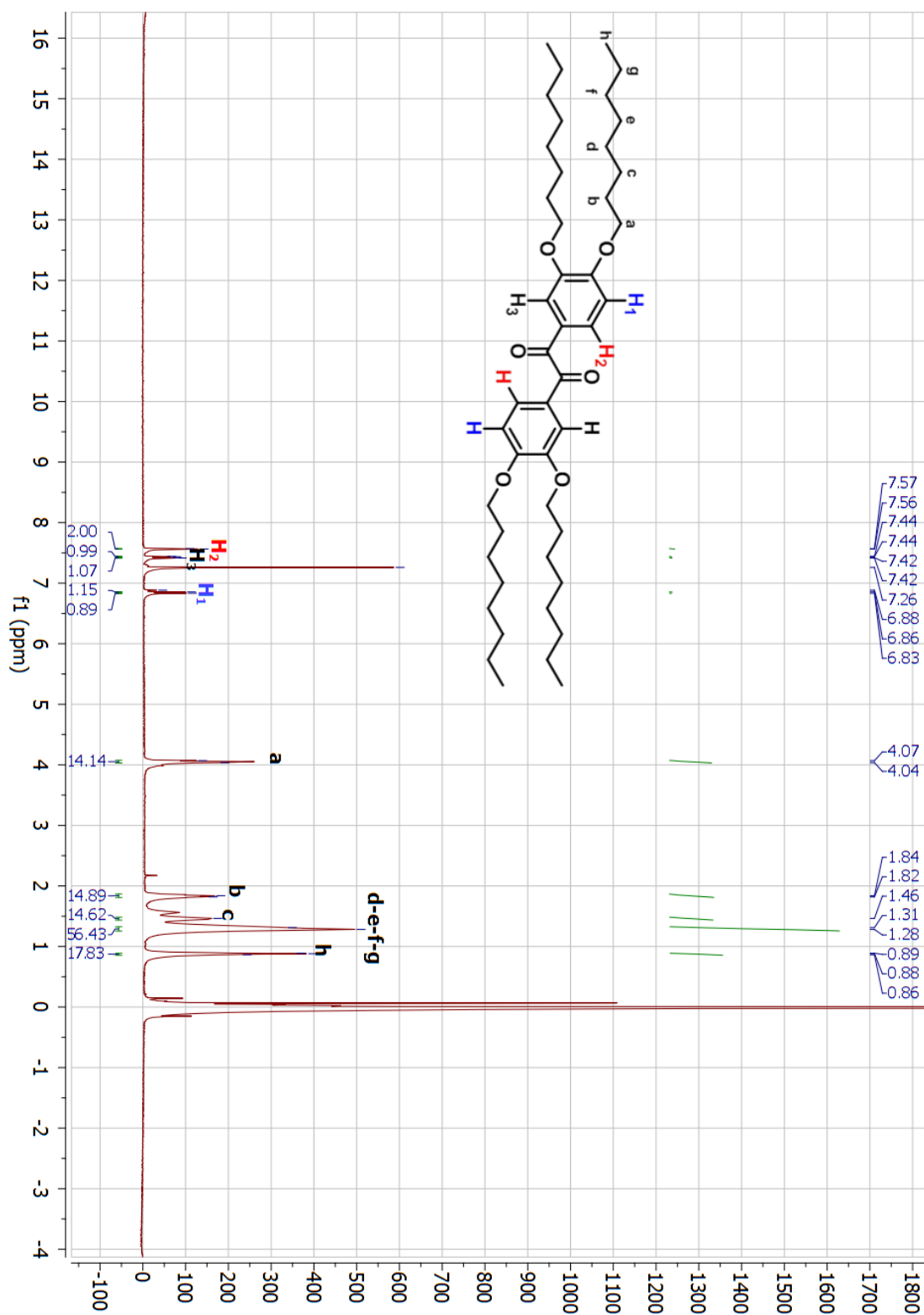


Figure A 7. $^1\text{H-NMR}$ spectrum of 1,2-bis(3,4-bis(octyloxy)phenyl)ethane-1,2-dione

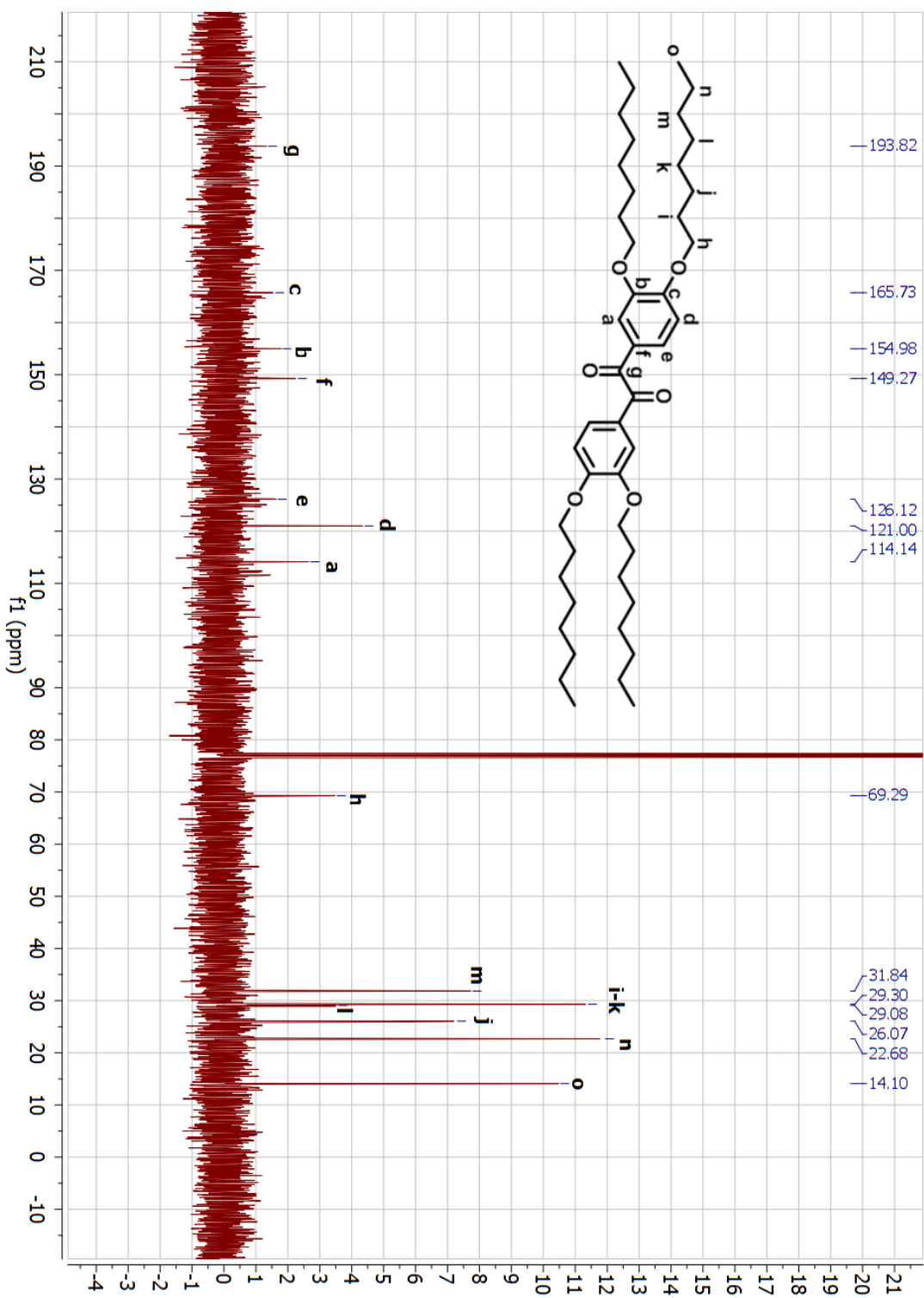


Figure A 8. ^{13}C -NMR spectrum of 1,2-bis(3,4-bis(octyloxy)phenyl)ethane-1,2-dione

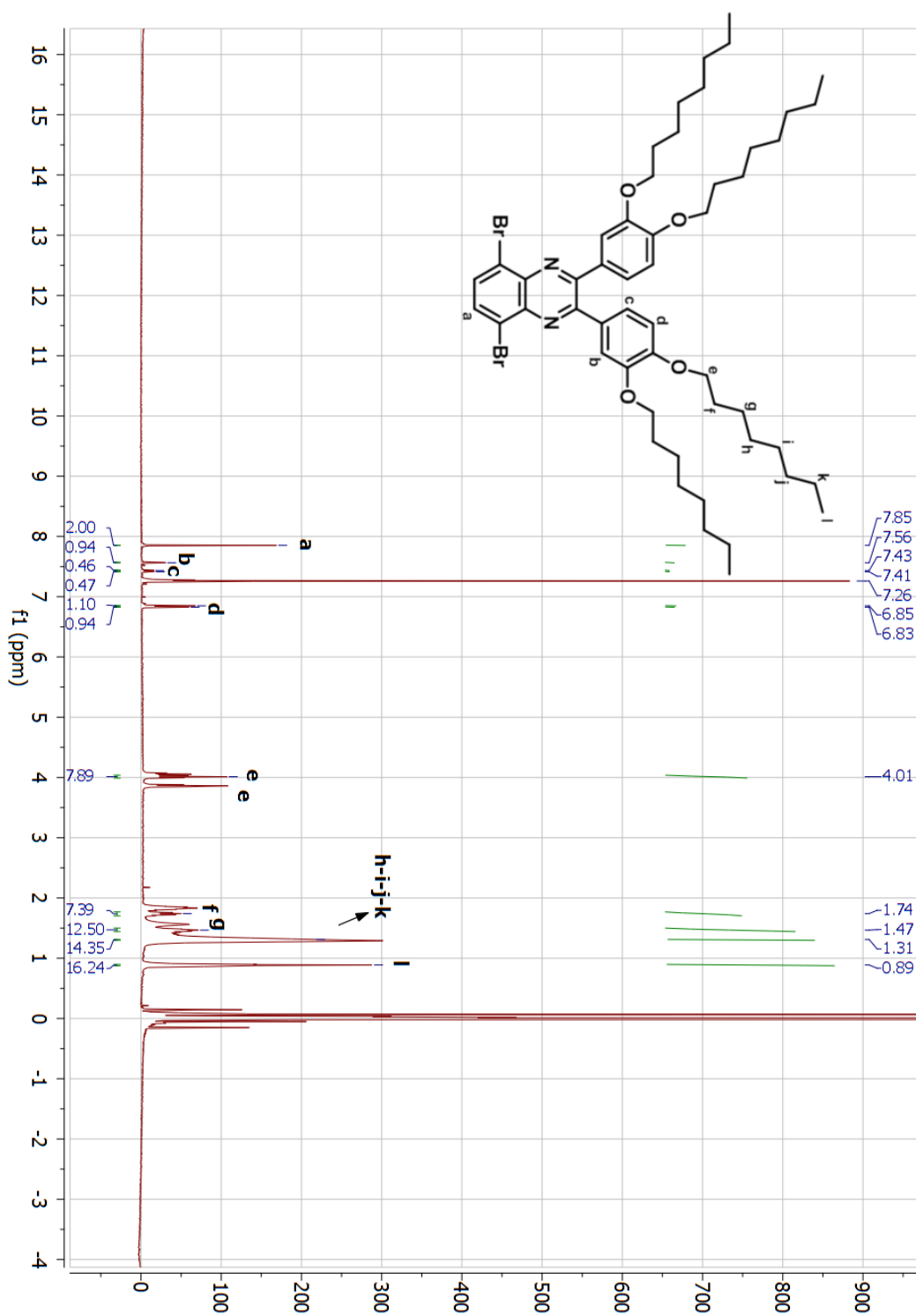


Figure A 9. ¹H-NMR spectrum of 2,3-bis(3,4-bis(octyloxy)phenyl)-5,8-dibromoquinoxaline

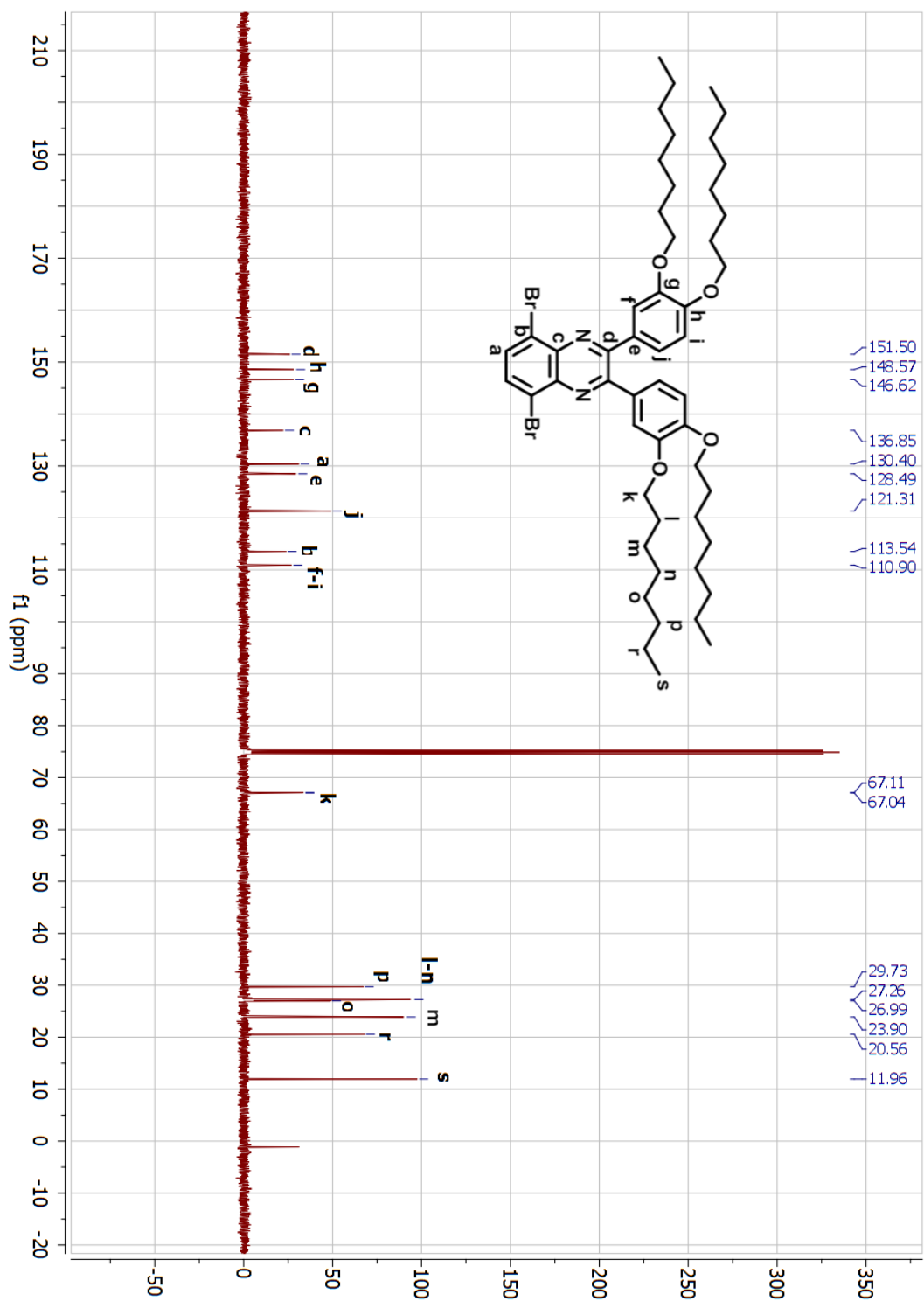


Figure A 10. ^{13}C -NMR spectrum of 2,3-bis(3,4-bis(octyloxy)phenyl)-5,8-dibromoquinoxaline

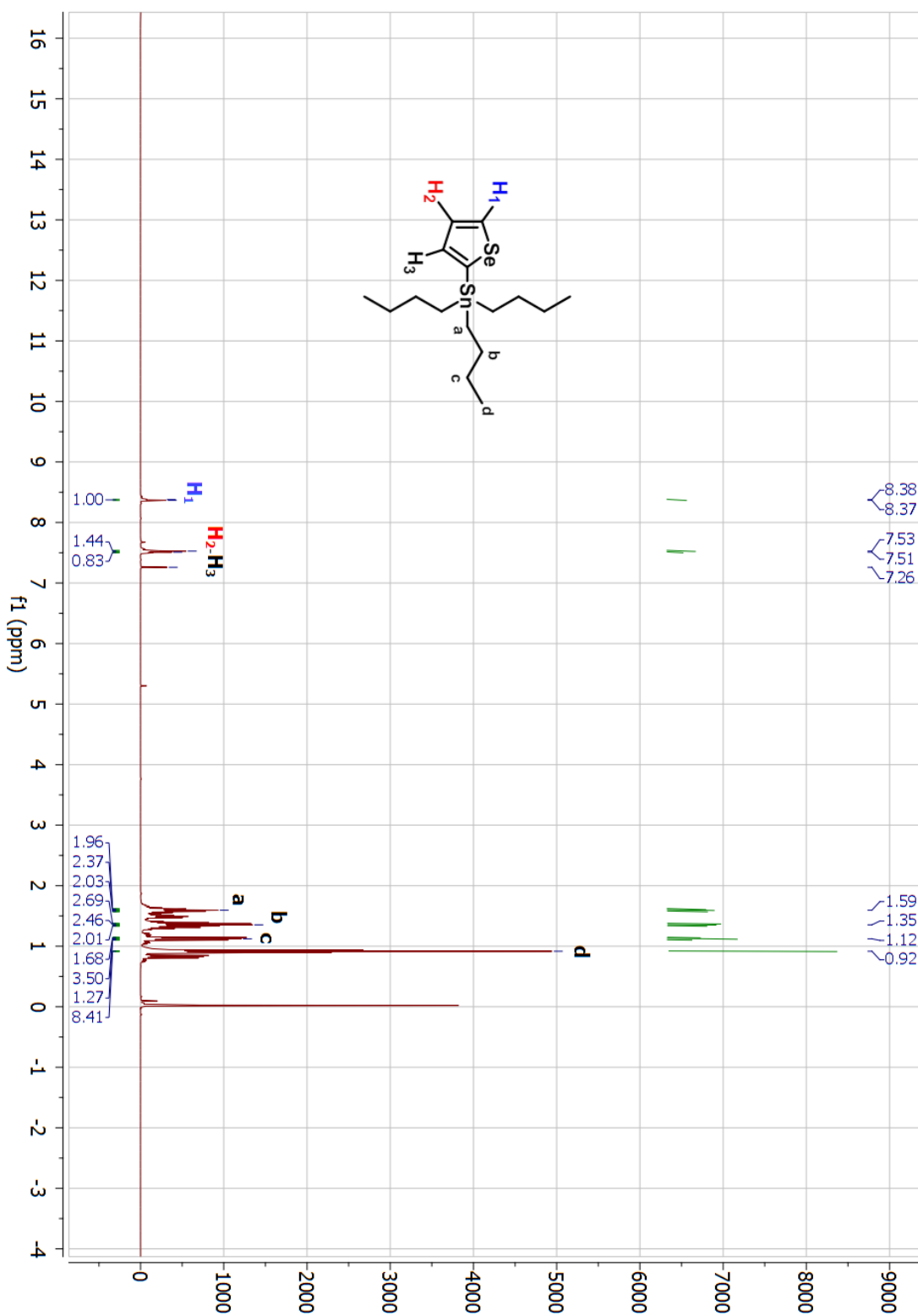


Figure A 11. $^1\text{H-NMR}$ spectrum of tributyl(selenophen-2-yl)stannane

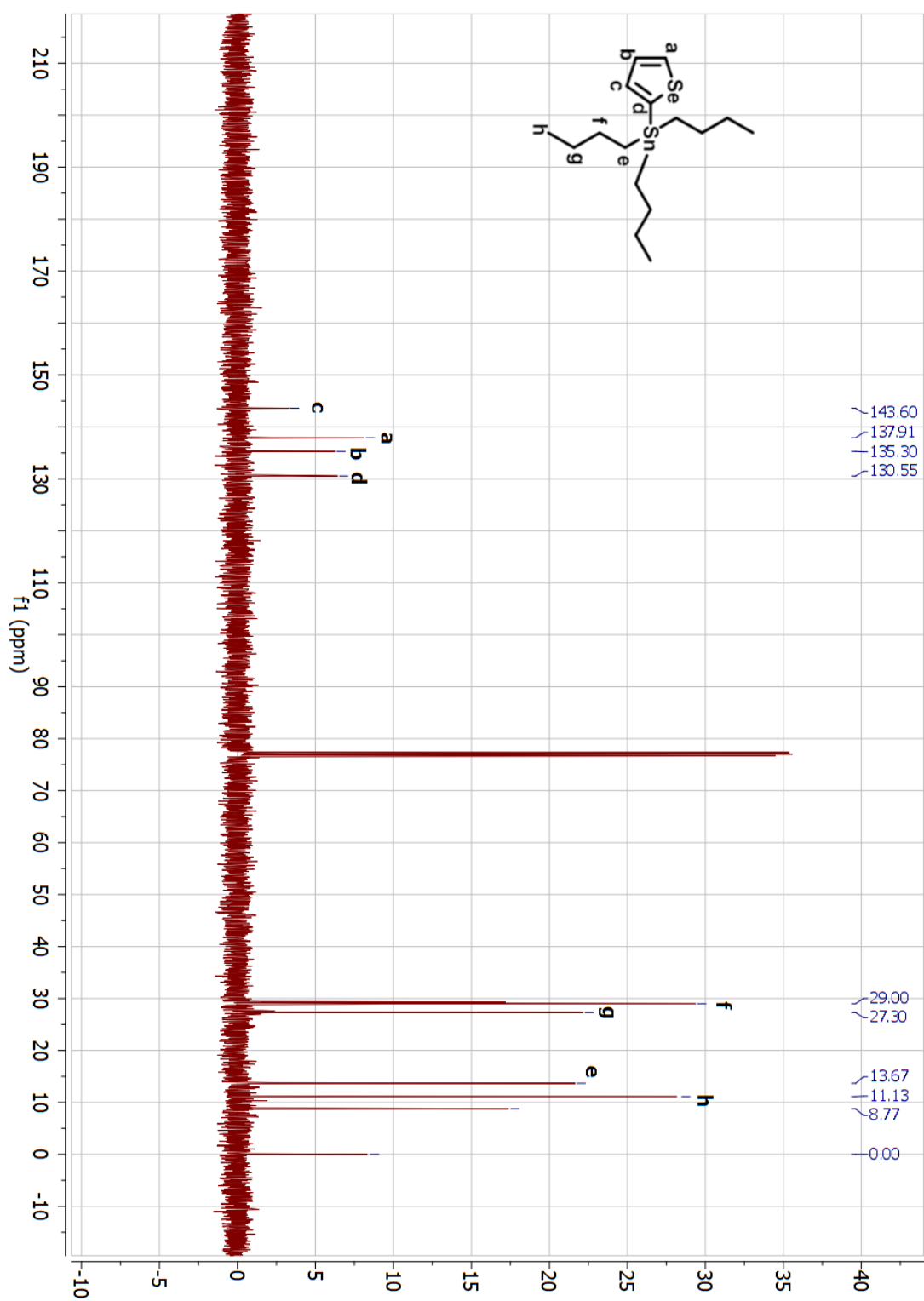


Figure A 12. ^{13}C -NMR spectrum of tributyl(selenophen-2-yl)stannane

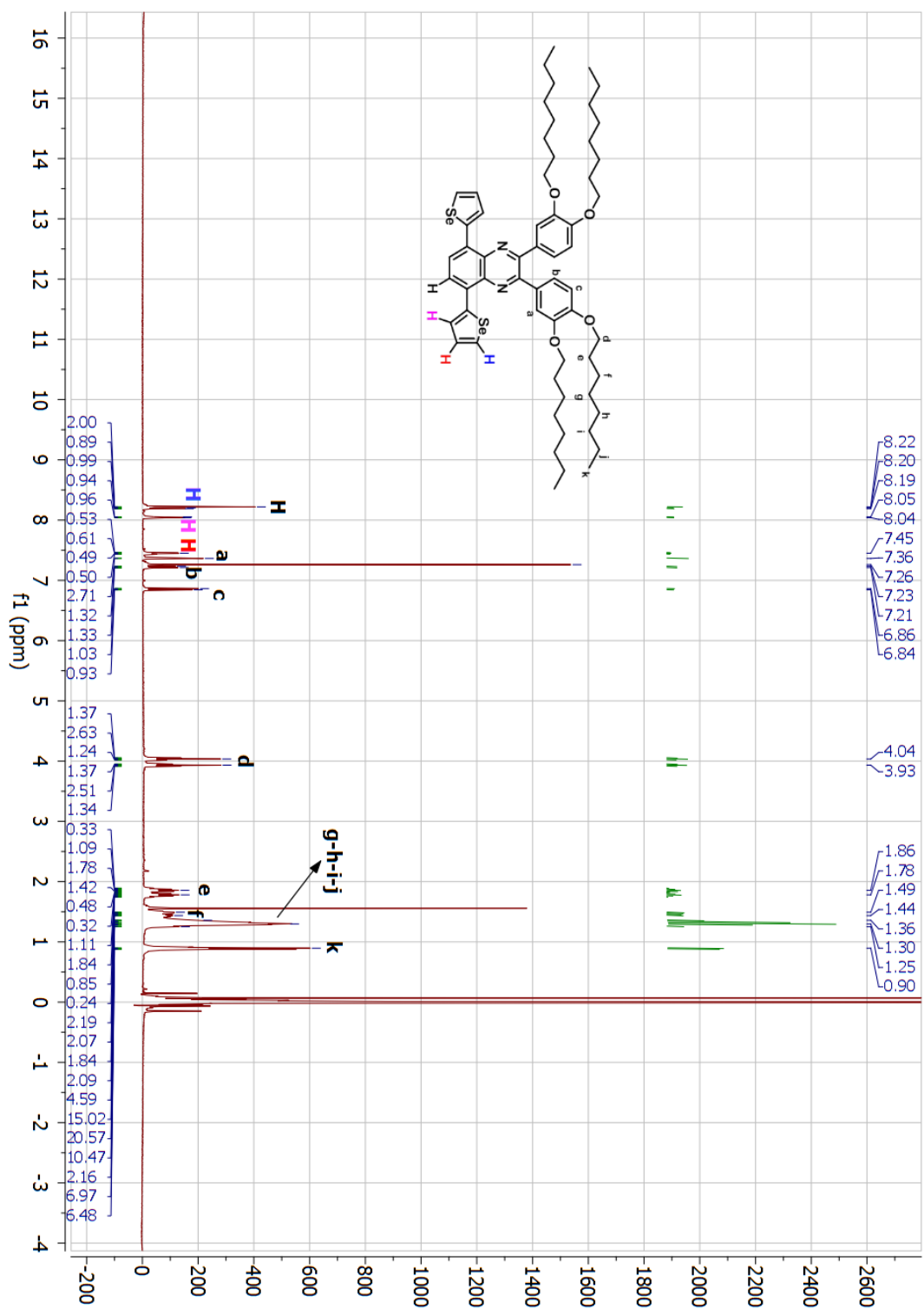


Figure A 13. ¹H-NMR spectrum of 2,3-bis(3,4-bis(octyloxy)phenyl)-5,8-di(selenophen-2-yl)quinoxaline

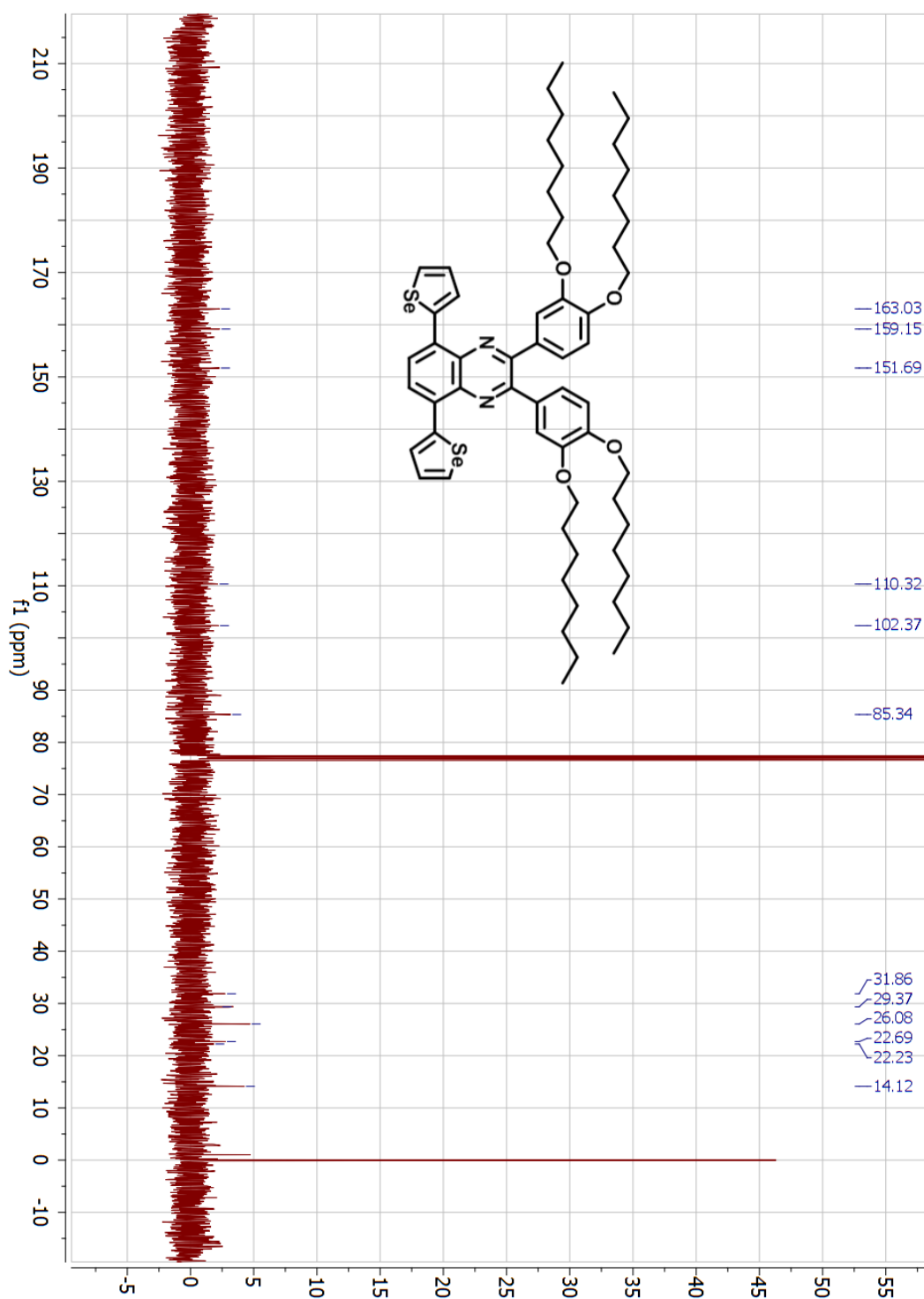


Figure A 14. ^{13}C -NMR spectrum of 2,3-bis(3,4-bis(octyloxy)phenyl)-5,8-di(selenophen-2-yl)quinoxaline

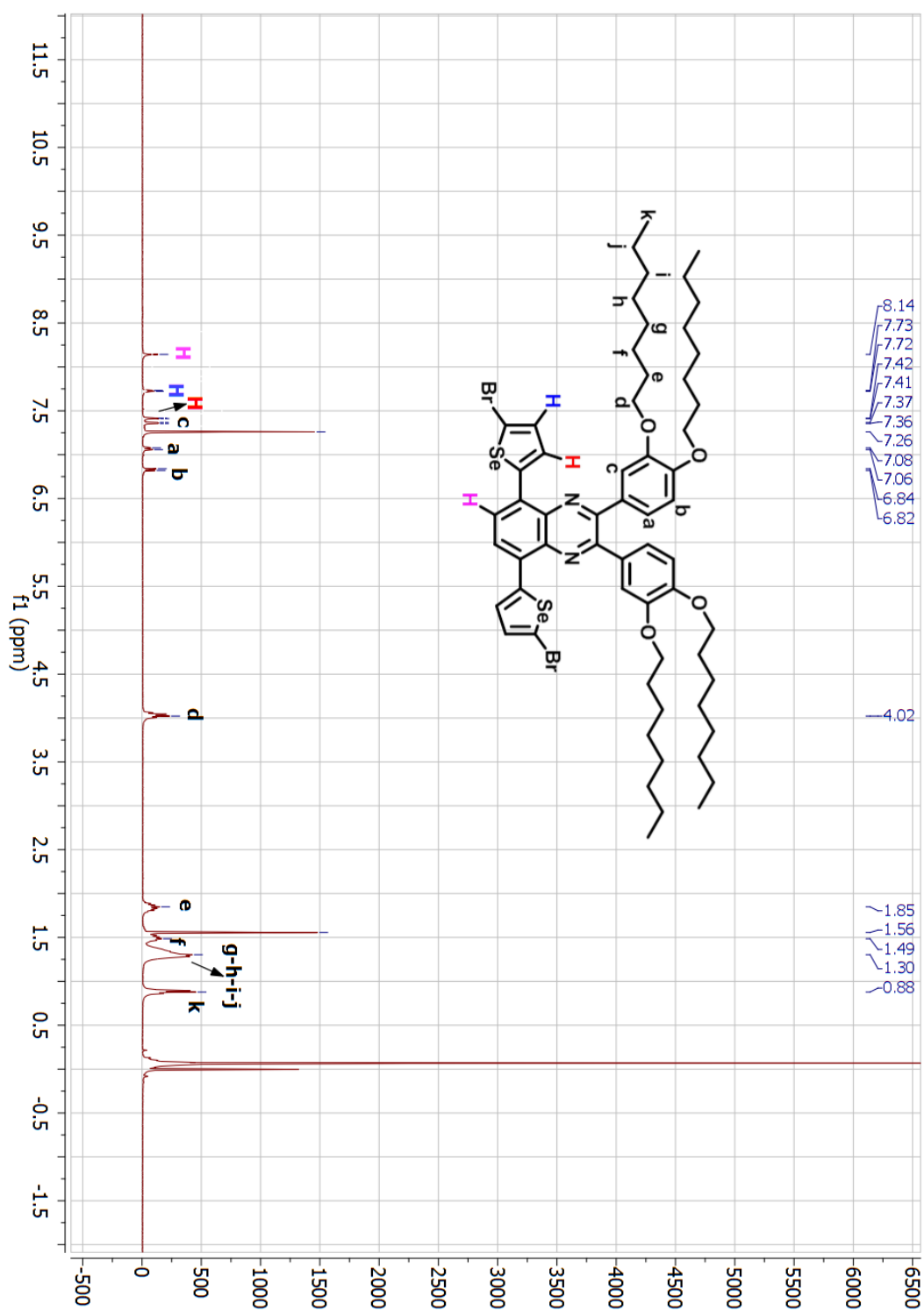


Figure A 15. ¹H-NMR spectrum of 2,3-bis(3,4-bis(octyloxy)phenyl)-5,8-bis(5-bromoselenophen-2-yl) quinoxaline

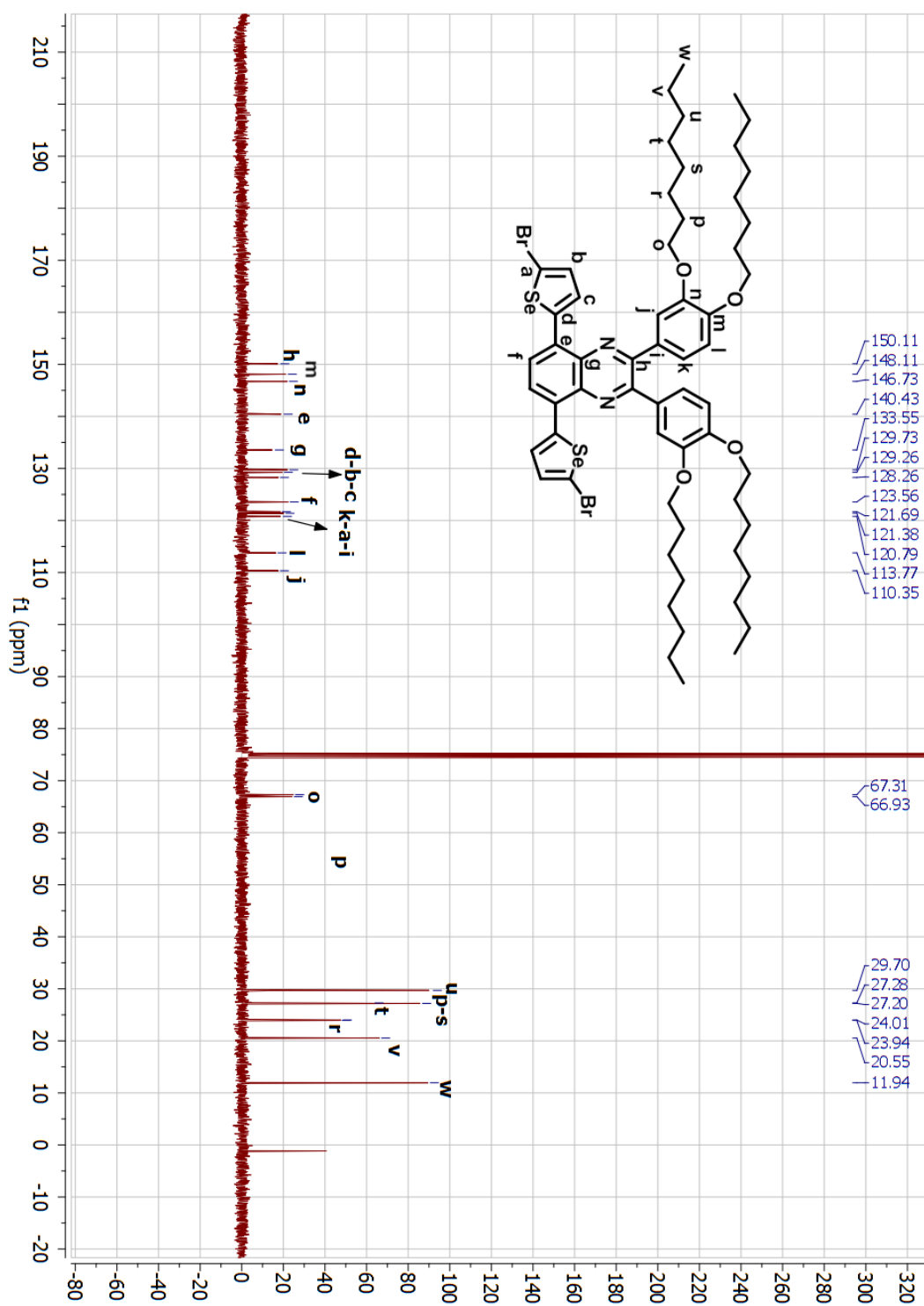


Figure A 16. ^{13}C -NMR spectrum of 2,3-bis(3,4-bis(octyloxy)phenyl)-5,8-bis(5-bromoselenophen-2-yl) quinoxaline